Neural control of optic flow-based navigation in *Drosophila melanogaster*

by

Victoria Pokusaeva

April, 2023

A thesis submitted to the
Graduate School
of the
Institute of Science and Technology Austria
in partial fulfillment of the requirements
for the degree of
Doctor of Philosophy

Committee in charge:
Mario de Bono, Chair
Daria Siekhaus
Eugenia Chiappe
Maximilian Jösch

"An animal's eyes have the power to speak a great language."

Martin Buber

The thesis of Victoria Pokusaeva titled *Neural control of optic flow-based navigation in Drosophila melanogaster* is approved by:

Supervisor: Maximilian Jösch, ISTA, Klosterneuburg, Austria

Signature: _____

Committee Member: Daria Siekhaus, ISTA, Klosterneuburg, Austria

Signature: _____

Committee Member: Eugenia Chiappe, Champalimaud Foundation, Lisbon, Portugal

Signature: _____

Defense Chair: Mario de Bono, ISTA, Klosterneuburg, Austria

Signature: _____

Signed page is on file

ISTA Thesis, ISSN: 2663-337X

I hereby declare that this thesis is my own work and that it does not contain other people's work without this being so stated; this thesis does not contain my previous work without this being stated, and the bibliography contains all the literature that I used in writing the dissertation.

I declare that this is a true copy of my thesis, including any final revisions, as approved by my thesis committee, and that this thesis has not been submitted for a higher degree to any other university or institution.

I certify that any republication of materials presented in this thesis has been approved by the relevant publishers and co-authors.

Signature: _____

Victoria Pokusaeva

April, 2023

Signed page is on file

Abstract

During navigation, animals can infer the structure of the environment by computing the optic flow cues elicited by their own movements, and subsequently use this information to instruct proper locomotor actions. These computations require a panoramic assessment of the visual environment in order to disambiguate similar sensory experiences that may require distinct behavioral responses. The estimation of the global motion patterns is therefore essential for successful navigation. Yet, our understanding of the algorithms and implementations that enable coherent panoramic visual perception remains scarce. Here I pursue this problem by dissecting the functional aspects of interneuronal communication in the lobula plate tangential cell network in *Drosophila melanogaster*. The results presented in the thesis demonstrate that the basis for effective interpretation of the optic flow in this circuit are stereotyped synaptic connections that mediate the formation of distinct subnetworks, each extracting a particular pattern of global motion.

Firstly, I show that gap junctions are essential for a correct interpretation of binocular motion cues by horizontal motion-sensitive cells. HS cells form electrical synapses with contralateral H2 neurons that are involved in detecting yaw rotation and translation. I developed an FlpStop-mediated mutant of a gap junction protein ShakB that disrupts these electrical synapses. While the loss of electrical synapses does not affect the tuning of the direction selectivity in HS neurons, it severely alters their sensitivity to horizontal motion in the contralateral side. These physiological changes result in an inappropriate integration of binocular motion cues in walking animals. While wild-type flies form a binocular perception of visual motion by non-linear integration of monocular optic flow cues, the mutant flies sum the monocular inputs linearly. These results indicate that rather than averaging signals in neighboring neurons, gap-junctions operate in conjunction with chemical synapses to mediate complex non-linear optic flow computations.

Secondly, I show that stochastic manipulation of neuronal activity in the lobula plate tangential cell network is a powerful approach to study the neuronal implementation of optic flow-based navigation in flies. Tangential neurons form multiple subnetworks, each mediating course-stabilizing response to a particular global pattern of visual motion. Application of genetic mosaic techniques can provide sparse optogenetic activation of HS cells in numerous combinations. These distinct combinations of activated neurons drive an array of distinct behavioral responses, providing important insights into how visuomotor transformation is performed in the lobula plate tangential cell network. This approach can be complemented by stochastic silencing of tangential neurons, enabling direct assessment of the functional role of individual tangential neurons in the processing of specific visual motion patterns.

Taken together, the findings presented in this thesis suggest that establishing specific activity patterns of tangential cells via stereotyped synaptic connectivity is a key to efficient optic flow-based navigation in *Drosophila melanogaster*.

Acknowledgments

I am thankful for everyone who contributed to my scientific and personal development during my studies and research work, and without whom an accomplishment of this thesis would not be possible. I express special gratitude to Prof. Olga Ozoline and her research group for introducing me to experimental sciences and academic life, particularly to Dr. Maria Tutukina and Dr. Sergei Antipov for their overwhelming support throughout my graduate studies. I am immensely grateful to Prof. Fyodor Kondrashov who for a long time remained my mentor and friend, and for his team who became my second family. I am beholden to the researchers and stuff in Center for Genomic Regulation in Barcelona, and specifically to groups of Dr. Guillaume Filion and Dr. Lucas Carey for their assistance to my technical and scientific training. I am very thankful for all the support I received in the past 6 years from ISTA and the Graduate School. I am especially grateful to my supervisor Prof. Maximilian Jösch and the whole Neuroethology group that provided me with an opportunity to discover the field of neuroscience. Special thanks go to Roshan Satapathy and Olga Symonova, without whom the accomplishment of the experiments presented in the thesis would not be possible.

I am very appreciative of the scientific assistance that I received from Scientific Service Units at ISTA, and specifically Imaging and Optics Facility and Lab Support Facility. I am also grateful for the funding provided by European Union's Horizon 2020 research and innovation program under the Marie Skłodowska-Curie programme (665385) and The German Research Foundation grant DFG (SPP2205) "Evolutionary optimization of neuronal processing".

I am immensely thankful to my family, and especially to my husband, for their unconditional support that kept me going during my PhD years.

About the Author

Victoria Pokusaeva completed an MSc in Biophysics at Voronezh State University in 2013. She performed scientific part of her master thesis at the Institute of Cell Biophysics RAS where she investigated potential applications of ferritin proteins for bioengineering. In 2013 Victoria joined the Center for Genomic Regulation in Barcelona, where she studied evolutionary and molecular genomics. In September 2016 Victoria started PhD at ISTA and joined Neuroethology group. There, under the supervision of professor Maximilian Jösch, she investigated the neural mechanisms of visually-guided course control in flies. Victoria's research interests include animal behavior, physiology and evolutionary history.

List of Collaborators

Roshan Satapathy
Performed the behavioral experiments, analysis of behavioral data, and assisted with the preparation of the final figures presented in the thesis.

Dr. Olga Symonova
Developed visual stimuli used for physiological analysis, provided the technical assistance for the patch-clamp set-up, performed the analysis of physiological data, and contributed to the development of final figures presented in the thesis.

Mia Juračić (group of Prof. Fyodor Kondrashov, ISTA)
Assisted in the development of the western blot analysis.

Lisa Hofer
Developed the pipeline for analysis of neuronal morphology.

Dr. Armel Nicolas
Performed the mass-spectrometry analysis.

Dr. Jesse Isaacman-Beck (group of Prof. Thomas R Clandinin, Stanford University)
Provided the vectors for the development of new mosaic genetic tools presented in Chapter 3.

Ece Sönmez
Performed the fly crosses and brain imaging presented in Chapter 3.3.2.

Table of Contents

List of Figures

List of Abbreviations

AD ..... Transcription activation domain
C3 ..... Centrifugal cell 3
CH ..... Centrifugal Horizontal
CNMN ..... Cervical nerve motor neuron
CT ..... Complex tangential neuron
DBD ..... DNA-binding domain
DN ..... Descending neuron
EMD ..... Elementary motion detector
FD ..... Figure detecting
FLP ..... Flippase
GECIs ..... Genetically encoded calcium indicators
GEVIs ..... Genetically encoded voltage indicators
GRASP ..... GFP Reconstitution Across Synaptic Partners
H1 ..... Horizontal 1
H2 ..... Horizontal 2
HS ..... Horizontal system equatorial
HSE ..... Horizontal system Southern
HSN ..... Horizontal system Northern
HSS ..... Horizontal system
inx ..... Innexin
IR ..... Infra-Red
L1 ..... Lamina neuron 1
L2 ..... Lamina neuron 2
LIP ..... Lateral intraparietal area
LM ..... Lateromedial area
LPTC ..... Lobula plate tangential cell
MARCM ..... Mosaic analysis with a repressible cell marker
Mi ..... Medulla intrinsic neuron
MiMIC ..... Minos-mediated integration cassette
MSTd ..... Dorsal medial superior temporal area
nBOR ..... Nucleus of the basal optic root
ND ..... Null-direction
OKR ..... Optokinetic response
OMR ..... Optomotor response
PD ..... Preferred direction
RFOF ..... Receptive field optic flow
RNAi ..... RNA interference
SPARC ..... Sparse Predictive Activity through Recombinase Competition
Tm ..... Transmedullary neuron
TNT-LC ..... Tetanus toxin light chain
V1 ..... Vertical 1
VOR ..... Vestibular-ocular reflex
VS ..... Vertical system

Chapter 1
Introduction

1.1 Optic flow and the control of animal locomotion

While moving in the environment, humans and animals detect a coherent shift of the visual image that reflects their ego motion. This global pattern of the motion, known as optic flow (Gibson, 1950), can be defined as the vector field resulting from apparent displacement of local objects. The structure of the vector field depends on animal ego motion and is often described as a sum of its rotational and translational components. Optic flow is a rich source of visual information that is masterfully exploited by animals for successful navigation in a complex environment (Egelhaaf et al., 1988; Srinivasan et al., 1996; Warren, 1998, 2021). Recent progress in our understanding of optic-flow-based navigation in animals is successfully used in modern computer vision algorithms and robotics (Capito et al., 2020; Efros et al., 2003; Pan et al., 2011; Serres & Ruffier, 2016).

1.1.1 Optic flow-based perception of ego-motion

Each movement of an animal in the environment is associated with a certain structure of the optic flow. This way the animal constantly uses visual information to decode its self-motion during navigation. In a largely variable natural environment this decoding is possible only because rotational and translational components of optic flow change stereotypically with each movement of the animal along its body axes (Koenderink, 1986) (Figure 1). Rotation is mostly uniform throughout the visual scene, while translational vectors depend on the distance of objects and the direction of heading.

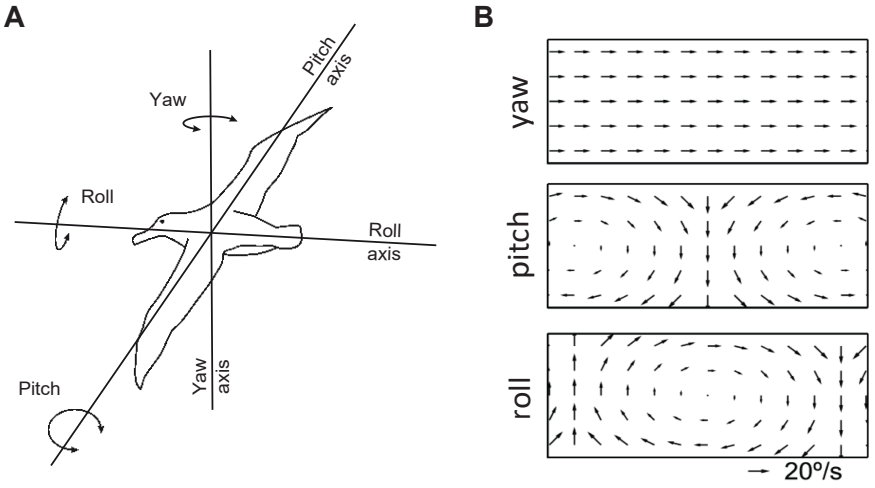

Figure 1. Animal self-motion produces stereotyped patterns of optic flow fields. A) Three main axes of animal-centered rotation around the pitch, roll and yaw. B) Vector fields representing local motion associated with yaw, pitch, and roll self-motion.

The statistics of optic flow is defined, to a great degree, by the ecology of an animal. For example, walking animals, in contrast to flying insects and birds, are mostly stable around the roll and the pitch axes and rarely experience high velocity vertical vectors of motion (Eckert & Zeil, 2001). Therefore, it is not surprising that neural implementation of optic flow analysis in different

animals evolved in accordance with their type of movement (Buschbeck & Strausfeld, 1997; Orlandi, 2013).

Even though visual cues carry a rich source of information, an efficient decoding of animal ego motion requires their integration with other sensory modalities, such as vestibular inputs and proprioception. In primates, neurons in two cortical areas implicated in self-motion perception, MSTd and LIP, show both visual and vestibular selectivity (Gu et al., 2006, 2008; Hou et al., 2019). In birds, optic-flow-sensitive neurons in two retinal-recipient nuclei, LM and nBOR, form direct and mediated projections onto oculomotor- and vestibulocerebellum to control the flight (Wylie et al., 2018). In flying insects, mechanosensory inputs from halters and proprioception regulate fast (in the range of 10-20 ms) posture stabilization during locomotion (Dickinson & Muijres, 2016), but also provide feedback from the body to the brain to control visually guided navigation (Bartussek & Lehmann, 2016; Fujiwara et al., 2022; Kathman & Fox, 2019).

1.1.2 Heading and gaze stabilization

For survival, animals have to extract critical visual features fast and efficiently. During locomotion however, this process can be largely compromised due to the motion-induced image blur (Land, 1999). Without efficient motion compensation, the visual system would lose its resolution as well as its ability to estimate the heading and the distance during active locomotion. That is why animals and humans navigate through the visual environment by alternating stable eye fixations with rapid eye saccades (Yarbus, 2013). The first provides the extended periods of stable gaze, and the second, a shift of gaze direction with a transient decrease of visual sensitivity. This way the visual system minimizes the experience of blurry low-informative images. In some animals this compensatory eye movement is accompanied or replaced by head and body movement, depending on body anatomy (Blaj & van Hateren, 2004; Pratt, 1982).

Smooth gaze stabilization is achieved by reflex-like responses to vestibular and visual signals, and are known as the vestibular–ocular reflex (VOR), the optokinetic response (OKR) and the optomotor response (OMR). VOR is a compensatory eye movement opposite to the direction of head movement that is triggered by the vestibular system in both vertebrate and invertebrate animals (Raphan et al., 1983; Rovainen, 1976; Sandeman & Okajima, 1973). In contrast, OKR occurs in response to visual motion when the head is stationary, and is characterized by slow eye movement in the direction of visual motion and rapid counter-movement that "resets" the gaze back to the starting point (Fritsches & Marshall, 2002; Komatsuzaki et al., 1969; Land, 2015; Tauber & Atkin, 1967). OMR, similar to OKR, is mediated by the visual system, but involves movement of the entire body and not just the eyes (McCann & MacGinitie, 1965; Portugues & Engert, 2009).

The compensatory mechanisms for gaze stabilization help animals to detect exafferent (externally generated) stimuli and adjust the locomotion accordingly. However, these mechanisms are largely incompatible with voluntary movements that produce reafferent (internally generated) stimuli. This incongruity gave rise to an idea of efference-copy, an internal duplicate of motor command that suppresses sensory consequences during voluntary movements (Brooks & Cullen, 2019; von Holst & Mittelstaedt, 1950). Several neuronal implementations of efference-copy were discovered in both vertebrate and invertebrate visual systems (Erickson & Thier, 1991; Kim et al., 2015; Zhang et al., 2004).

1.1.3 Depth perception using optic flow cues

For successful navigation, apart from the information about the self-motion, animals require visual information to specify the distance of surrounding surfaces and objects. This information can be acquired through depth cues. During quiescence animals use binocular disparity as the main depth cue (Nityananda & Read, 2017; Wheatstone, 1838), whereas moving

animals largely rely on optic flow (Davies & Green, 1990; Lee & Reddish, 1981; Lehrer et al., 1988).

Depth perception in moving animals requires constant gaze control that maximizes translational and limit rotational cues. This way the distance of an object can be estimated as a rate of increase of the angle from the direction of heading to the object (Kaiser & Mowafy, 1993). This strategy is thought to be employed during landing of some birds, diving of gannets, and even striding and jumping in humans (Davies & Green, 1990; Lee & Reddish, 1981). Smooth landing of flying insects is also controlled using optic flow cues. For example, honey bees perform grazing landing on a horizontal surface by keeping constant the magnitude of optic flow in the ventral area (Srinivasan et al., 2000, 2001). Since translational optic flow varies with the inverse of distance this strategy allows smooth deceleration. Similarly, balancing the magnitude of optic flow cues in the lateral visual field of each eye allows flying insects to avoid collisions (Srinivasan et al., 1991). Importantly, these strategies do not require direct computation of the distance or the animal speed, and remain computationally economical.

Depth perception using motion cues demonstrates that exploiting variables in the optic flow field can provide simple solutions for rather complex orientation tasks. Still, the exact neuronal implementations of these computations are poorly understood. Nevertheless, application of optic flow in animal depth perception served as inspiration for computer vision algorithms used in autonomous vehicles, robotics and spacecraft navigation systems (Milde et al., 2015; Ohradzansky et al., 2018; Serres & Viollet, 2018; Valette et al., 2010). Perhaps, the advances in algorithms for optic flow processing will one day be translated into the discovery of neural circuits that perform those functions in animal brains.

1.2 Drosophila melanogaster as a model to study neural circuits for optic flow-based navigation

Drosophila melanogaster is a popular model organism across various fields of biological sciences due to its genetic tractability, rapid generation time and low cost. Despite the small size of their nervous system, fruit flies present complex and at the same time very robust visually-guided behaviors. Due to the efficient reproduction of *Drosophila* in laboratory conditions and its small size, the analysis of fly behavioral responses can be performed at an unprecedented scale. In combination with functional recording techniques and sophisticated tools for targeted manipulations of neural circuits, unravelling neural substrates of visually guided behaviors in fruit flies reaches exceptional precision. These insights have significant implications not only for invertebrate neurobiology, but also more generally for functional studies of the nervous system in normal and pathological conditions.

1.2.1 Ecology of motion vision in *Drosophila*

Drosophila melanogaster (fruit fly) is a small fly with a rapid life cycle (approximately 10 days at 25 °C) that feeds and mates on ripe fruits. Despite its miniature body size and tiny brain, *Drosophila* can survive in almost every corner of the world. The extreme adaptability of this species suggests a very efficient neural control of behavior, that can provide both robustness and flexibility of responses. How does the tiny brain of *Drosophila* achieve it so masterfully? The answer may lie in the natural history and ecology of this species.

Fruit flies largely depend on their sense of sight to control navigation, reproduction and survival. As other "visual" animals, flies use different properties of light, such as color, intensity and polarization, to obtain key information about the surrounding environment. The environment, however, is rarely static, and animals are constantly presented with various visual motion cues. These cues are particularly complex for actively navigating animals, such as flying insects. Fruit flies with their light body weight and large wing size experience perturbations even in relatively still air. Nevertheless, flies possess remarkable aerial control of the body. *Drosophila* initiates evasive flight behavior within 5 milliseconds, which is among the fastest correction reflexes observed in animals (Beatus et al., 2015). This superb motion control is a result of coevolution of animal lifestyle and its sensory processing circuits. Considering the rather modest computational capacity of *Drosophila* nervous system, studies of visual adaptations in this species can teach us how nature finds simple solutions for seemingly complex tasks.

Drosophila has compound eyes with 750 individual modules, or ommatidia, that cover wide visual field of 330° in azimuth and 180° in elevation (Hardie, 1985). Each ommatidium is slightly offset from its neighbors, allowing the animal to collect the information from each point in the visual space. This information acquired by photoreceptors runs in parallel in isolated visual columns that preserve retinotopic structure. Even though the visual acuity of compound eyes is low due to the wide spacing between photoreceptors, the parallel processing provides efficient extraction of motion information. This sacrifice is due to the extreme importance of motion vision for fly survival. *Drosophila* often navigates through cluttered environments, and have to react and readjust their course in response to external objects within milliseconds. This maneuverability can be guaranteed only by swift extraction of visual motion cues and their immediate employment in sensory-motor coordination. It was demonstrated that retina and motion circuits in the fly eye are adapted to reliably detect moving objects and evaluate their direction and speed even in noisy and non-homogeneous visual environments (Drews et al., 2020; Fenk et al., 2022; Juusola et al., 2017; Maimon et al., 2010). These adaptations guarantee robust and fast motion-induced responses across variable and complex natural scenes.

Almost every visual stimulus can be interpreted by an animal in multiple ways, and evoke distinct responses depending on the context. For example, looming stimuli elicit landing responses

in flying *Drosophila*, but escape in perched ones. Both escape and landing can be executed with extreme speed and precision by optimally tuned visual circuits, however the choice of response is a key. That is why sensory-motor transformation evolved not to be a feedforward process that solely depends on stimulus presented to an animal. The behavioral state was shown to largely influence visual processing. For example, the state of active locomotion modulates gain and speed sensitivity of neurons that comprise motion vision circuits in *Drosophila* (Chiappe et al., 2010; Maimon et al., 2010; Suver et al., 2012; Tuthill et al., 2014). In addition, target-oriented or voluntary behavior diminishes responses to behaviorally irrelevant stimuli. For example, voluntary turns and escape maneuvers are known to suppress stabilization reflexes that are otherwise extremely robust (Fischer & Schnell, 2022; Kim et al., 2015). The internal state of the animal also largely affects the performance of the visual system. For instance, energy limitations induced by hunger modulate activity of wide-field motion-sensitive neurons and reduce the strength of compensatory optomotor responses (Longden et al., 2014). Context-dependent flexibility of visually-guided responses is achieved via neuromodulation, and enables optimal behavioral performance of the fly in a given environmental context.

Complex and highly variable natural environments present sensory challenges for animals. Tiny brains of *Drosophila* evolved to provide fast contextual choice and superb execution of visually-induced behaviors combining highly conserved morphology and wiring of neurons with flexibility in their responses. Such unexpected complexity of visual circuits in flies creates challenges for their studies in experimental conditions.

1.2.2 Paradigms of visual behavior in *Drosophila*

Molecular and physiological adaptations typically reveal themselves in changes of animal behavior. Therefore, behavior can be considered as an "ultimate" phenotype, that is a key substrate for selection. Just observing animal behavior in the natural environment allows us to make predictions about the underlying neuronal control. That was brilliantly done by the pioneer of ethology Nikolaas Tinbergen in his classic work The Study of Instinct (1951). Even though the natural habitat of an animal is the only setting in which a behavior adequately manifests itself, field experiments are not always the best choice for behavioral studies. That is related to uncontrolled experimental conditions that make interpretations rather challenging. This is why behavioral responses are often tested individually by presenting animals only with relevant stimuli. This reductionist, one-thing-at-a-time, approach has proven to be very powerful in mapping neural substrates of defined animal actions. It also provides reproducibility, and promotes the development of sophisticated technologies for the generation of sensory stimuli as well as for the detection and analysis of animal responses. Despite these technical advances, the choice of exact settings for behavioral tests remains challenging.

Drosophila, as a model for behavioral studies in laboratory settings, offers numerous advantages, among which are genetic tractability, small size, and ability to use numerous individuals. In addition, fruit flies offer multiple well-developed behavioral paradigms, a lot of which are based on visual responses such as phototaxis, escape, fixation and optomotor reflex (Götz, 1968, 1980; Hammond & O'Shea, 2007; McEwen, 1918). Traditionally, behavioral studies involved tests of fly populations, where multiple individuals are subjected to a visual stimulus and the average response is analyzed. This approach was applied for phenotyping mutant strains, and led to discoveries of genes that are involved in insect vision. For example, mutations in *norp* (no receptor potential) caused the loss of phototaxis (Pak et al., 1969), and mutations in *omb* (optomotor blind) the loss of motion-induced responses (Heisenberg, 1972; Pflugfelder et al., 1992). The relative simplicity of the population tests makes them handy for fast assessment of animal performance.

The traditional population paradigms, however, provide only limited information about stimulus-induced responses, that is often not sufficient to study underlying neural circuits.

Understanding the neuronal substrate of a behavior would require tracking detailed dynamics of animal activity in responses to well-controlled stimuli. This can be achieved by using individual fly assays, where each individual is studied separately. There are two types of individual fly paradigms: freely behaving and tethered, each offering advantages and frequently used to complement each other. Freely walking or flying paradigms are very attractive, because they allow studies of fly responses in the context of its habitual locomotion state. That is why they are frequently employed for visual discrimination or choice tasks, as well as for visual fixation and navigation (Cruz et al., 2021; Maimon et al., 2008; Mimura, 1982; Strauss, 2002; Wehner, 1972).

It was observed, however, that the performance of animals would depend on the exact settings at which an interaction with the visual stimulus or an object occurs. In other words, parameters such as the angle of approach, the speed of locomotion, and the preceding trajectory can substantially influence visual responses. That increases the variability, and makes it difficult to disentangle stimulus-induced responses from the contextual aspects. In addition, recording of freely behaving animals is not technically simple and often imposes limitations on temporal and spatial resolution of acquired data. These limitations become critical when responses happen very fast, or when tracking some body parts is necessary. The paradigms for tethered flying and walking flies were developed in order to avoid technical challenges of video recordings and limit the influence of self-motion on stimulus perception. In the walking paradigm, the animal is fixed in front of a screen and turns a spherical treadmill. This way the trajectory of fly locomotion can be inferred from infra-red (IR) sensors or cameras that track optic flow fields, which originate from the moving ball. In the flying paradigm, the animal is placed in front of the screen or in the center of the flight simulator, and attached to a tungsten wire, a torque meter or, in more recent setups, to a steel pin placed within a magnetic field (Figure 2B). The intended flying maneuvers of the animal can be estimated with a torque meter that directly measures left–right thrusts of the animal, or with an IR wingbeat analyzer that measures differences in wingbeat amplitudes.

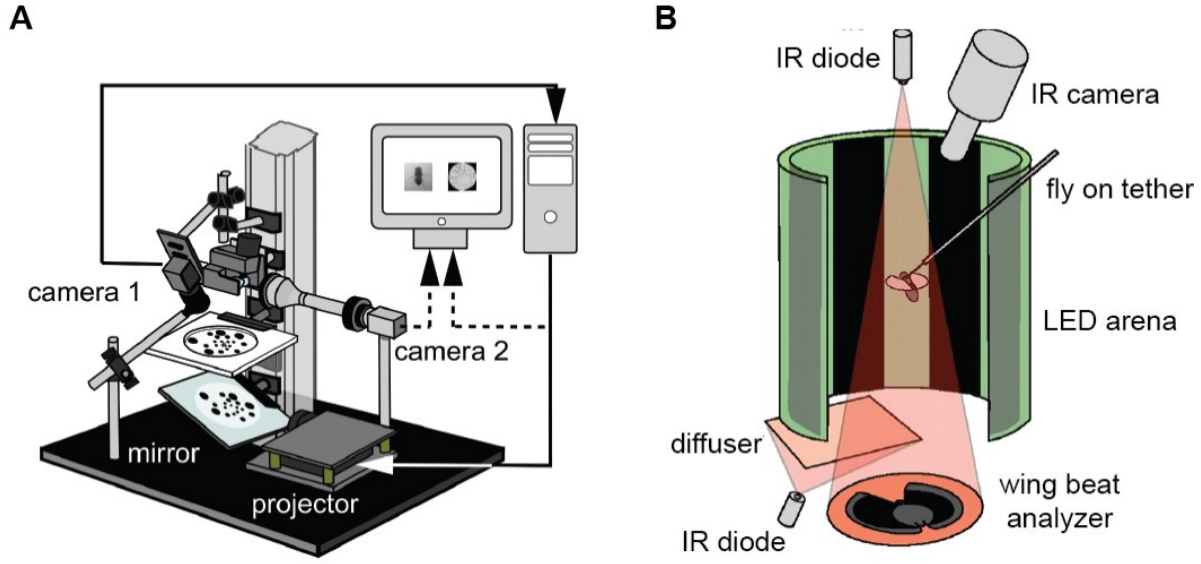

Figure 2. Examples of visual behavioral in *Drosophila melanogaster*. A) Freely-walking animal set-up to study visually-induced posture control (Cruz et al., 2021). B) Tethered flying animal set-up to antennal movement during visually-guided steering (Mamiya et al., 2011).

An obvious disadvantage of using tethered animals is the decoupling between locomotion and changes in the visual scene. As a result, the animal does not get expected self-motion-induced sensory cues, and therefore can exhibit altered behavioral responses. This problem was overcome by generating a so-called closed loop between the fly's behavior and the movement of the presented stimulus (Heisenberg & Wolf, 1979). For that, the information about the animal motion

is analyzed (via a torque meter, or a detector) and immediately used to change the position of the stimulus accordingly. This advancement became critical for the further adaptation of the tethered fly paradigm for studies of various visual responses, including visual tracking and pursuit, visually-guided control of locomotion and visual discrimination (Brembs & Heisenberg, 2001; Green et al., 2019; Hindmarsh Sten et al., 2021; Tammero et al., 2004). Importantly, tethered fly paradigms can be combined with neuronal recordings to acquire data of animal behavior and neuronal activity simultaneously, which enables more efficient mapping of neuronal substrates of behaviors (Ache et al., 2019; S. S. Kim et al., 2017; Seelig et al., 2010). Tethered paradigms as well made it possible to study in detail how the active state of the fly affects response properties of neurons involved in visuomotor transformations (Chiappe et al., 2010; Maimon et al., 2010; Strother et al., 2018).

Recent advancements in virtual reality (VR) technologies make it possible to achieve almost full immersion of an animal into the visual environment (Stowers et al., 2017). These technologies are being actively applied in both tethered and freely-moving animals, and provide full control of the visual environment of flies as well as their full engagement with visual stimuli (Figure 2A). Due to their versatility VR technologies can be adapted to study the effect of any visual features on behavioral responses in *Drosophila*. This technique helps to reach in laboratory conditions the level of interaction of animals with the visual environment similar to those occurring in nature.

Individual fly paradigms are proven to be extremely effective to study visuomotor transformation in the fly brain. Nevertheless, it is important to remember that animal responses can be largely affected by the presence of conspecifics in the surrounding (Ferreira & Moita, 2020; Klibaite & Shaevitz, 2020; Ramdya et al., 2015; Rooke et al., 2020). Active research of collective behavior in *Drosophila* began only recently, but it is evident that visual responses of solitary flies can differ from those in a group. In addition, behavioral variabilities that are observed in population paradigms do not always originate from experimental conditions, they can be biologically meaningful (Honegger & de Bivort, 2018; Mollá-Albaladejo & Sánchez-Alcañiz, 2021). In other words, flies can express behavioral variability that originates from small developmental and genetic differences. This phenomenon is of high interest since it provides insights on molecular processes that control neural circuit formation. Therefore, the choice of the behavioral paradigm has to always reconcile with the specific goals of a study, considering all the potential advantages and drawbacks.

1.2.3 Measuring neuronal activity

The ability to reliably measure neuronal activity defines the success of experimental studies in neuroscience. A long history of development of highly technical methods made it possible to study neuronal activity at any scale, from a single membrane channel to the whole brain. The choice of the method is made based on the goals of the study and the used model system. In *Drosophila*, changes in the activity of neurons are assessed by deploying two types of techniques — electrophysiological recordings and optical imaging. Electrophysiological techniques are employed on a single-cell level, and provide information about the currents flowing across the membrane. Optical imaging, on the other hand, enables the access to the activity of cell populations, and is more applicable to study neuronal interactions and large-scale brain dynamics. Both of these techniques are suitable for *in vivo* analysis, allowing direct assessment of neuronal substrates of sensory processing and motor control.

Electrophysiological techniques

From the moment when "animal electricity" was discovered by Galvani it became evident that all fundamental physiological processes are subjected to basic principles of physics and chemistry. That shifted biology into the realm of mechanical science and stimulated the development of experimental techniques to study biological processes. Two centuries later, due to

the establishment of electrophysiological methods, our knowledge about "animal electricity" is growing day by day.

Electrophysiological approaches in neuroscience can be broadly separated into extracellular and intracellular recording techniques. Both of them rely on the use of fine electrodes to measure electric currents that result from the constant ion flow across the membrane of excitable cells. Due to the low amplitude of these biological currents the recorded signal is further subjected to amplification and digitization.

Extracellular recording is one of the oldest and most common techniques for recording electrical activity across neurons in awake animals. These measurements are usually performed in the extracellular fluid in the vicinity of cells of interest. The activity of a single cell or population of cells produces local currents, or extracellular field potentials. The flux of positive ions into a cell leaves behind a net negative charge, while the flux of positive ions out of a cell generates a net positive charge outside the cell. These local extracellular potentials can be recorded and be used to infer the activity of neurons. In *Drosophila*, extracellular recording is the method of choice to study the peripheral nervous system. Being relatively simple to perform and minimally invasive, this technique allows measuring stimuli-induced responses in sensory organs in almost intact animals. For example, single-sensillum recordings are routinely used to measure the activity of olfactory sensory neurons in response to odors (de Bruyne et al., 1999), and electroretinogram — to study phototransduction in photoreceptors (Hotta & Benzer, 1969). These techniques allow a robust assessment of responses in sensory organs, and can be used to study sensory impairments in mutant animals.

Although extracellular recording provides information about the voltage changes across the tissue, it reveals very little about the changes in membrane properties and activity of ion channels. Detailed analysis of the changes in cell membrane potential requires direct intracellular access which is possible using sharp electrode techniques or patch-clamp recordings. Sharp microelectrode studies are performed by penetrating a cell with a fine-tipped glass electrode with a high resistance (tens or hundreds of MΩ). This technique works best with large cells, and in fruit flies is often used to study neuromuscular junctions (Jan & Jan, 1976). Sharp electrodes, however, induce a rupture in the cell membrane that limits the duration of a stable recording, especially in neurons of small size. Whole-cell patch clamp recording is a gentle alternative to using sharp microelectrodes. Patch clamp is performed using a microelectrode with a bigger tip diameter that is brought into contact with cell membrane to establish the tight seal and rupture the membrane beneath the electrode. In this circumstance there is direct contact between the electrode recording medium and the cytoplasm. This is advantageous for experiments that require the control of ionic concentrations or drug applications, but non-applicable when minimal disturbance of the intracellular milieu is required. First introduced almost 50 years ago, patch-clamp was adapted for *in vivo* use in *Drosophila* only recently (Joesch et al., 2008; Turner et al., 2008; Wilson et al., 2004). That it took so long is mostly explained by the small size of fruit flies' neurons and difficulties associated with accessing them. Nevertheless, in the past decade this technique was successfully used to study neurons in different brain regions (Behnia et al., 2014; Fisher et al., 2019; Joesch et al., 2008; Murthy et al., 2008), and even in head-fixed behaving animals (Fujiwara et al., 2017; Maimon et al., 2010; Turner-Evans et al., 2017). Whole-cell patch clamp provides high-resolution and high-sensitivity recordings of neuronal membrane potential. In combination with various sensory stimuli, applications of drug and dyes, this technique is indispensable to study response properties of neurons, synaptic transmission, circuit connectivity, ion channel activity and cell morphology.

Optical imaging

Any brain function, be it sensory processing or instruction of a behavior, is a result of interaction between numerous neurons of different types. Therefore, the ability to measure the

activity of individual neural populations and brain regions is of great importance. That became possible after the development of genetically encoded indicators of neural activity in combination with powerful imaging techniques. Today, functional imaging of large brain regions is being successfully used for spatial analysis of neuronal activity in multiple model systems.

There exist two types of indicators for optical imaging: 1) genetically encoded calcium indicators (GECIs) and 2) genetically encoded voltage indicators (GEVIs). Using binary expression systems (see above), one can target any neural population in the fly brain for functional imaging. First GECI, GCaMP, is a chimeric protein in which circularly permuted GFP is fused to the calcium-binding protein calmodulin (Nakai et al., 2001). In the presence of calcium, GCaMP undergoes structural rearrangement that significantly increases the intensity of fluorescence. When neurons get activated, rapid depolarization causes opening of voltage-gated calcium channels and a rapid influx of extracellular calcium. Therefore, changes in the intensity of GCaMP fluorescence can be used as a proxy for neural activity. In addition to GFP-based, there were also developed RFP-based GECIs, such as jRGECO and jRCaMP (Dana et al., 2016). Combination of red and green indicators enables simultaneous imaging of activity in two independent cell populations. These chimeric proteins were improved via mutagenesis to enhance calcium-induced fluorescence, increase calcium-binding affinity, and accelerate their response time.

Comparison between the fluorescence of calcium indicators and electrophysiological recordings in fly neurons demonstrate that changes in fluorescence of calcium indicators reliably reflect changes in the membrane potential (Chen et al., 2013; Jayaraman & Laurent, 2007). However, temporal kinetics of changes in intracellular Ca2+ concentration is slow, which largely limits temporal resolution of calcium imaging. Moreover, this technique is not suitable for neurons with strong calcium buffering, as well as for measuring subthreshold events and inhibitory activity.

Stated limitations of calcium imaging can be resolved by using indicators with voltage- instead of calcium-sensing domains. Voltage imaging has substantially better temporal resolution and reflects exact changes in membrane potential. However, high imaging speed and excitation intensity requires very bright and photostable indicators, which is difficult to achieve with genetically-encoded proteins. Therefore, recent advances in development of hybrid systems look particularly promising (Abdelfattah et al., 2019; Kirk et al., 2021; Liu et al., 2021). These systems deploy synthetic fluorophores in combination with cell-targeted genetically-encoded voltage-sensitive proteins. Several of those chemogenetic indicators were successfully tested for various model systems, including *Drosophila*.

In vivo imaging of functional indicators requires high spatial resolution and penetration depth. That can be achieved by using two-photon microscopy, which permits tight restriction of the excitation light and better penetration through scattering tissues with minimal phototoxicity (Denk et al., 1990; Helmchen, 2009; Mostany et al., 2015). Spatial information is gathered by moving the laser focus across the sample, resulting in images with single-cell resolution deep inside brain tissue. Voltage imaging in addition requires very high temporal resolution (kilohertz acquisition rate versus $\leq$ 30 Hz for calcium-imaging), which still remains costly and challenging for a large number of neurons at the same time. However, the high potential of this technique stimulates the development of new microscopy techniques, methods for image analysis and GEVIs, making voltage imaging more accessible for various applications (Platisa et al., 2021; Villette et al., 2019).

1.2.4 Tools for neurogenetics

The ability to study the functional role of neural circuits *in vivo* is provided, to a great extent, by a combination of specific delivery systems and a variety of molecular effectors. Decades of scientific development in multiple fields of biology made *Drosophila* melanogaster a unique model organism that enables specific neuronal targeting with an extraordinary array of effectors (Martín & Alcorta, 2017; Venken, Simpson, et al., 2011).

The spatial control of expression in *Drosophila* is achieved by using transcriptional regulatory elements of cell-type-specific genes (Rubin & Spradling, 1982). Introducing these regulatory elements upstream of a reporter targets its expression to specific cells. Nowadays, almost any neuronal type in the brain of *Drosophila* can be targeted, thanks to well-annotated collections of so-called driver lines (Dionne et al., 2018; Jenett et al., 2012; Tirian & Dickson, 2017). In combination with an extensive range of easily accessible effector lines, driver lines enable comprehensive genetic, morphological and functional characterization of fly neural circuits.

Access to neuronal populations

Cell-type-specific regulatory elements can provide robust spatial control of expression of any effector. However, it is impractical to generate all transgenic animals that would enable expression of all possible effectors in every neuronal type. The development of binary expression systems provided an elegant solution to this problem. These systems are based on a combination of two elements, one of which defines the expression pattern and another the type of effector being expressed. This way a desirable effector can be expressed in any neuronal type as a result of a single genetic cross.

The most widely used binary expression system in *Drosophila* is the GAL4-UAS system (Brand & Perrimon, 1993). GAL4 is a yeast transcription factor that specifically binds a motif called Upstream Activating Sequence (UAS), and initiates the expression of a downstream gene. For spatial control of expression of a desirable effector, transgenic fly lines that drive cell-specific GAL4 expression are crossed to flies that encode effectors controlled by the UAS activator. Yeast UAS/GAL4 system does not interact with the transcription machinery of *Drosophila*, and therefore remains phenotypically neutral.

While the GAL4-UAS system provides efficient targeting of specific neuronal populations, there still exist some limitations to its usage. Firstly, it induces chronic expression of a transgene that can have potential developmental effects or be subjected to homeostatic compensations. Secondly, for the majority of GAL4 promoter drivers the specificity remains low, which results in broad patterns of expression. The temporal restriction of GAL4-driven transcription can be achieved by using the repressor protein GAL80. GAL80 forms a complex with GAL4 and prevents UAS-mediated activation of expression (Ma & Ptashne, 1987). A temperature-sensitive variant of GAL80 was developed (GAL80ts), that degrades at 29°C allowing GAL4 to bind UAS sites (McGuire et al., 2004). This way the GAL4-UAS-mediated expression can be temporarily suppressed at low temperatures (around 20°C), and be induced at any moment by a heat-shock. The GAL80 repressor can provide not only temporal, but also spatial control of GAL4-UAS-mediated expression.

However, applications of GAL80 for spatial control of expression in the nervous system remain rather limited. Instead, the refinement of cell-type specific manipulations is achieved by using a combinatorial split-GAL4 system (Luan et al., 2006; Pfeiffer et al., 2010). In this system the DNA-binding domain (DBD) and the transcription activation (AD) domain of GAL4 protein are expressed independently. Each domain is fused to heterodimerizing leucine zippers that enable reconstitution of GAL4 activity upon their coexpression in the same cell. This way, one can use two different regulatory elements to drive the transcription of these two domains, and induce the expression of an effector only in cells where both elements are active.

Often experiments require independent targeting of several neuronal populations at the same time. For example, when one has to assess the activity of one cell type upon activation of another one. That requires two different systems for targeted expression to drive independently effectors for optical imaging of neuronal activity and effectors for neuronal activation. That is possible due to the development of several alternative binary systems, such as the LexA system (Lai & Lee, 2006) and the Q system (Potter et al., 2010; Riabinina et al., 2015). This way

independent reporters can be expressed in distinct neuronal populations using different binary expression systems.

These days almost every experiment in the field of *Drosophila* neurobiology relies on genetic access to neurons of interest. Since it is not possible to create driver lines to target specific cell types, there exist large libraries of available lines with well-annotated patterns of expression. By selecting and combining available expression systems one can target the neuronal population of choice specifically and reproducibly.

Anatomical and structural analysis of neurons

Drosophila offers an unmatched toolkit of reporters to study neuron morphology and connectivity. Each of the genetic tools often results from years of development and improvement, providing highly reproducible and efficient means to investigate neuron structure.

Visualization of neurons is the primary task of any anatomical and functional investigation. Fluorescent reporters remain the most widely deployed labelling method. A variety of fluorescent proteins is available to be expressed in individual neuronal types as well as in several neuronal types at the same time. While earlier reporters were rather inefficient, labelling the cytoplasm of the entire neuron, modern reporters were significantly improved via codon optimization (Pfeiffer et al., 2010), or multimerization (Shearin et al., 2014). Moreover, some fluorescent markers were fused to targeting elements, enabling specific labelling of the cell membrane (Lee & Luo, 1999), cell organelles (LaJeunesse et al., 2004) and individual synaptic components (Estes et al., 2000; Zhang et al., 2002). Besides fluorescent markers some non-fluorescent reporters are available, such as horseradish peroxidase and peptide tags (Larsen et al., 2003; Viswanathan et al., 2015).

Labelling of neuronal groups does not always permit the resolution of the morphology of individual cells due to their close proximity. That is why recombinase-mediated genetic techniques were developed for sparse labelling of neurons in defined cell populations. These methods permit single-color as well as multicolor stochastic labelling. The sparse expression of a single reporter can be achieved by using FLP-recombinase-mediated MARCM technique (Lee & Luo, 1999), or PhiC31-recombinase-mediated SPARC technique (Isaacman-Beck et al., 2020). For stochastic and combinatorial expression of multiple fluorescent proteins, Brainbow-derived methods can be used, such as FLP-recombinase-mediated Flybow (Hadjieconomou et al., 2011) and Multicolor Flip-Out (Nern et al., 2015). The density of labelling can be regulated by controlled expression of the recombinase (as for FLP-mediated techniques), or by using recombinase recognition sites with different affinities (as in SPARC technique). Recombinase-mediated-techniques can be used not only for fluorescent labelling, but also for molecular and physiological manipulations at the single-cell level.

Analysis of neural circuits often requires identifying and labelling synaptically connected cells, rather than neurons of the same group. Serial electron microscopy remains the gold standard for detailed analysis of neuronal morphology and identification of synaptic connections. Practical considerations, however, limit the use of this technique by the majority of laboratories. For that reason, multiple scientific initiatives are working on developing publicly available electron microscopy datasets of the adult fruit fly brain that can be used for neuronal tracing and synaptic mapping (Scheffer et al., 2020; Zheng et al., 2018). These open-access resources already have a profound effect on fly neuroscience allowing to map neural circuits with unprecedented precision. While offering a unique resolution, electron microscopy, however, remains largely non-versatile and unsuitable for comprehensive analysis of variability among individuals (Briggman & Bock, 2012). Routine visualization of neuronal connections can be achieved using flexible genetic approaches that exploit the proximity of pre- and postsynaptic membranes. For example, individual synapses can be visualized using a split version of the Green Fluorescent Protein (GFP), such as in GRASP method (Feinberg et al., 2008). Anatomical tracing of postsynaptic partners can be achieved with techniques that are based on ligand-induced signaling pathways, such as trans-

Tango (Talay et al., 2017). In addition to fluorescent labelling, this technique provides genetic access to postsynaptic partners for further circuit dissection and manipulation.

Neurogenetics and molecular analysis

Every neuronal cell-type is characterized by a unique pattern of gene expression that ultimately determines their morphology, connectivity and physiology. Establishing a link between genes, neuronal activity and ultimately behavior is a challenging task that requires means for gene manipulation. The most direct way to assess the function of a gene is to remove it and observe the effect. *Drosophila* offers one of the largest collections of well-described null mutants. First functional characterizations of potassium, sodium and calcium channels were achieved by using forward genetics, since disruptions in the activity of these proteins result in strong behavioral deficits (Ganetzky & Wu, 1986; Kaplan & Trout, 1969; Smith et al., 1998).

Even though forward genetics is a powerful method to establish a link between genes and observed phenotypes, there are general problems associated with the use of mutants. Mutated genes can be expressed in nonneuronal tissues, have pleiotropic effect, affect other genes, cause developmental issues, or even lethality. To overcome these difficulties, an array of methods for cell-specific gene inactivation in *Drosophila* were developed. The most widely-used among them in neurogenetics are RNA interference (RNAi), CRISPR/Cas9-mediated conditional mutagenesis, and FLP-mediated gene disruption using FlpStop cassette (Dietzl et al., 2007; Fisher et al., 2017; Xue et al., 2014). The spatial control of inactivation in all these methods is achieved by using the GAL4-UAS system, and therefore can be temporally controlled as well. Each of the methods listed above has some advantages and some limitations, and the final choice is often determined by the exact goals of the experiment.

However, often it is not possible to know the exact gene that is critical for a phenotype. Therefore, the candidate genes have to be identified before a functional study is carried out. A search of candidate genes nowadays is largely simplified by the availability of genome-wide proteomics and transcriptomics datasets in *Drosophila* (Corrales et al., 2022; Davie et al., 2018; Davis et al., 2020; Mangleburg et al., 2020). These data sets provide information about spatial (and sometimes also temporal) pattern of expression of every gene, and can be used to determine which genes are potentially crucial for circuit functions, behavioral responses, or disease development. Further, detailed information about the expression of a candidate gene can be acquired using standard molecular techniques, such as in situ hybridization, or immunohistochemical stainings using antibodies raised against the protein encoded by the gene. However, these methods are not versatile and require a development of gene/protein-specific reagents. Therefore, large libraries of transgenic animals were developed, permitting fluorescent tagging of a large portion of *Drosophila* proteins *in vivo* (Knowles-Barley et al., 2010; Venken, Schulze, et al., 2011). The information about cellular and subcellular localization of a candidate gene can indicate its functional role, which can be further tested by an assessment of a phenotypic effect after a direct manipulation of gene activity. It can be achieved by employing *in vivo* techniques for gene inactivation (described above), gene overexpression (Jia et al., 2018; Roman et al., 2001), or gene rescue (Fisher et al., 2017; Venken et al., 2006) that were successfully developed for use in *Drosophila*. Since the genetic makeup as well as mechanisms of neuronal activity are conserved in *Drosophila* and mammals, this neurogenetic approach is a key to understanding causes of neuronal pathologies and behavioral deficits across phyla.

Manipulation of neuronal activity

A standard way to learn how a system works is to examine its components. Similarly, a lot of progress in our understanding of how the brain instructs behavior was achieved by dissecting the functional role of its individual regions. Even though a lot of studies suggest that the brain is

very integrative and that individual brain regions rarely act independently, this approach remains to be one of the most successful in studying neuronal control of behavior.

Historically, the functional role of individual brain regions and neural circuits was studied by performing neural lesions or using electrical stimulation. Being very informative, these methods, however, have rather limited applications due to their low selectivity. Our growing understanding of neuronal and synaptic physiology enabled the development of non-invasive genetic tools for targeted control of neuronal activity. These genetic tools are based on the disruption of synaptic transmission, or manipulation of ionic channels that directly affect the cell membrane potential. Naturally present ionic channels have large diversity in selectivity and modulation mechanisms, allowing the development of controlled effectors for both neuronal activation and suppression.

Suppression of electrical activity in neurons can be achieved by setting resting membrane potential below the threshold to fire an action potential. One of the ways to achieve it is to overexpress potassium channels that are open at rest and induce a potassium efflux that hyperpolarizes the cell membrane. Kir2.1, human inwardly rectifying potassium channel, was adapted for targeted expression in *Drosophila* via the UAS-GAL4 system (Baines et al., 2001). When expressed in neurons, Kir2.1 strongly suppresses excitability and transmitter release, enabling chronic silencing (Wiegert et al., 2017).

Neuronal silencing can be achieved not only by suppressing excitability, but also by targeting the release machinery of chemical synapses. The chronic disruption of synaptic transmission can be induced using genetically encoded tetanus toxin light chain (TNT-LC). It was the first circuit-breaking effector adapted for use in *Drosophila*, which is still actively used nowadays (Sweeney et al., 1995). TNT-LC cleaves the synaptic protein synaptobrevin, and blocks synaptic vesicle release. It interrupts chemical synaptic connections to the postsynaptic neurons, and prevents further transduction of neuronal activity. The effect of TNT-LC, however, is very slow (several hours to days), and does not allow fast disruption of synaptic transmission (Thum et al., 2006). Rapid and reversible inactivation of synaptic activity is possible using UAS-targeted temperature-sensitive shibire (shi^{ts}) (Kitamoto, 2001). Shibire is a dominant-negative allele of dynamin, a protein involved in the recycling of synaptic vesicles. Temperature shift to 30–37°C in flies expressing shi^{ts} induces depletion of synaptic vesicles in targeted neurons. This way, the silencing of chemical synapses can be achieved within minutes (Thum et al., 2006).

Similarly, to neuronal silencing, some recently developed methods permit chronic and inducible neuronal activation. Constitutive enhancement in the excitability of neurons can be achieved by overexpressing a voltage-gated bacterial sodium channel NaChBac (Nitabach et al., 2006). NaChBac has a lower voltage activation threshold than native *Drosophila* voltage-gated sodium channels, and therefore can get activated even at the resting membrane potential. Though the expression of NaChBac does not increase neuronal activity per se, it provokes hyperexcitability that leads to prolonged periods of membrane depolarization (Sheeba et al., 2008). Inducible activation, in turn, can be achieved by expressing temperature-sensitive or ligand-activated ion channels. TrpA1, a heat-sensitive cation channel, opens at temperatures above 26°C causing strong membrane depolarization (Hamada et al., 2008; Rosenzweig et al., 2005). The activation of TrpA1 is reversible and fast, making it a tool of choice for behavioral studies in fruit flies (Flood et al., 2013; Robie et al., 2017). $P2X_2$, ATP-gated cation channel, provides stronger and better temporally controlled neuronal activation (Lima & Miesenböck, 2005). In *Drosophila* the activation of the channel is achieved by a photo-release of caged ATP. This strategy, however, requires chemicals to be exogenously loaded in the tissue before activation, which complicates its usage in intact animals. Instead, $P2X_2$-mediated activation of neurons is used in electrophysiological experiments, since in this case it can be induced by direct application of ATP (Fujiwara et al., 2017; Hu et al., 2010).

Induction of $P2X_2$ by optically uncaged ATP was the first example of light-induced activation of neurons in *Drosophila*. This approach became widespread after the development of optogenetics, a set of tools that uses genetically targeted expression of light-activated ion channels

and pumps. The first transgene for optogenetics successfully used in *Drosophila* was the blue-light activated cation channel Channelrhodopsin-2 coming from algae (Hwang et al., 2007; Schroll et al., 2006). Nowadays, opsins are routinely used in a wide range of experimental settings across multiple model systems.

A decade of efforts in protein screening and engineering provided researchers with a set of available opsins that differ in their kinetics, light sensitivity, peak absorbance wavelength, and ionic conductance (Britt et al., 2012; Deisseroth, 2015). This broad range of optogenetic proteins enables flexibility of neuronal manipulations. For example, precise temporal control can be achieved by using opsins with increased onset and offset kinetics (ChETA and Chronos), prolonged activation — by using variants with increased conductance or photocurrent amplitude (CatCh, ChIEF, and ChR2-XXL), deep tissue targeting with limited light exposure — by using ultra-light-sensitive opsins (ChR2-XXL, Chronos, and Step-Opsins) (Dawydow et al., 2014; Gong et al., 2020; Klapoetke et al., 2014; Kleinlogel et al., 2011; Lin, 2011). Moreover, simultaneous manipulation of multiple neural populations became possible due to the recent discovery of opsins that respond to yellow/red light (ReaChR and CsChrimson) in addition to traditionally used green/blue light sensitive opsins (Klapoetke et al., 2014; Lin et al., 2013). While optogenetic activation of neurons gained widespread use shortly after the first application of channelrhodopsin, the use of optogenetic silencing remained challenging until recently. Efficient optogenetic inhibition of neuronal activity became possible only after the discovery of perfectly selective anion channelrhodopsins (GtACRs) with high conductance (Govorunova et al., 2015). GtACRs were demonstrated to be effective in multiple model systems, including *Drosophila* (Mahn et al., 2018; Mauss et al., 2017; Mohamed et al., 2017). Optogenetic experiments in fruit flies are made easier to perform due to the transparency of fly cuticle. Combined with other genetic tools for targeted neural manipulation, optogenetics makes *Drosophila* a very attractive model for behavioral neuroscience.

1.3 Neural circuits underlying optic flow processing in Drosophila melanogaster

Navigating through the environment, flies perform course correction and evasive maneuvers with astonishing speed and precision. Such superb motor coordination requires robust detection of motion cues that are generated by the egomotion of the fly and by external objects in its environment. This task is very challenging considering that it requires multistep processing of sensory inputs: the fly brain has to compute local motion vectors throughout the entire visual field, then integrate local inputs in order to reconstruct the pattern of global motion, and only after that, instruct appropriate behavior. Furthermore, information from other sensory modalities is of fundamental importance to interpret visual motion. How neural circuits in the fly brain provide swift and robust computation of motion vision became a topic of extensive research in past decades. It takes its start from a detailed description of optomotor following in insects and theoretical model of motion computations that take place in the insect brain in order to instruct the observed behavior. 70 years later, with the advent of sophisticated neurogenetic methods, we are now discovering neuronal implementations of those models in *Drosophila* brain. Our understanding of the neural mechanisms that underlie motion vision in flies is getting more complete day by day, but there still remain a lot of questions to be answered.

1.3.1 Optomotor response and models for motion detection

Being exposed to coherent motion cues, flies, as many other animals, perform compensatory head and body movements in the direction of the visual stimulus (Wehner, 1981). This so-called optomotor response occurs in nature because unexpected retinal slip mostly results from the animal's own inadvertent movements. These movements therefore are promptly counteracted in order to stabilize the intended course.

Optomotor response is extremely robust, and therefore is often used to assess fly motion vision in laboratory conditions. In tethered paradigms, flies are placed in the middle of a rotating drum, or nowadays of a spherical LED arena or in front of a screen where coherently moving visual patterns are presented (Duistermars et al., 2012; Seelig et al., 2010; Wolf & Heisenberg, 1990). The experiments can also be performed in closed-loop settings, where the velocity of the stimulus is controlled in accordance with the animal's own locomotion. Optomotor response in freely walking animals is evoked by presenting the stimulus on the walls, roof or the floor of the arena (Cruz et al., 2021; Götz, 1975; Werkhoven et al., 2021). Stimuli that mimic rotational flow elicit much stronger compensatory responses than those mimicking translation flow. It can be explained by the fact that the presence of rotational flow is highly undesirable during navigation since it largely distorts visual image. Therefore, animals express strong compensatory mechanisms to minimize the presence of rotational flow during navigation.

The strength of the optomotor response can be quantified by the response gain, i.e. the ratio of the animal angular velocity to that of the moving stimulus. The gain in flying *Drosophila* in closed-loop stimulus of regular vertical gratings approaches the one at the optimum speed of the stimulus (Wolf & Heisenberg, 1990). The optomotor response, therefore, does not operate like a simple speedometer whose output linearly increases with image speed, but has a nonlinear speed dependency with a clear optimum. The optomotor response of flies during walk is weaker than during flight, and does not even approach the gain of 0.5 in comparable conditions (Werkhoven et al., 2021). The low gain during walking can be advantageous since flies are more stable around their body axes, and often navigate in a constantly changing visual environment.

As mentioned above, the optomotor following in flies reaches its maximum at a particular velocity of the stimuli. When presented with a sinusoidal grating which moves at different velocities (v) the response of the flies increases up to a particular velocity of the stimulus, and slowly decreases after this peak (Duistermars et al., 2007). The velocity tuning curve of the

optomotor response is shifted to higher velocities when the pattern wavelength (λ) becomes larger. Hence, the strength of the optomotor response depends on the temporal frequency of the presented stimuli ($f = v/\lambda$) rather than on its velocity. In addition, the gain of the optomotor response increases with increasing pattern contrast (Borst et al., 2010). Those dependencies on stimulus statistics would play a decisive role in natural conditions. When flies navigate freely in a complex and largely uneven visual environment, the choice of a compensatory behavior is often less definite, and largely depends on image texture with respect to the animal's own movement (Lehmann et al., 2012).

In order to respond to motion cues, the visual system of flies have to contain direction-selective neurons. Direction-selective detection of motion is possible if the following general requirements are fulfilled: 1) the presence of at least two input channels, since information from a single position in space is not sufficient to detect any motion cues, 2) asymmetric temporal processing to extract direction of the motion, 3) nonlinear asymmetric interactions between processed output signals (Borst & Egelhaaf, 1989). A thorough analysis of the optomotor responses in beetle Chlorophanus led to the development of a computational model of motion vision that operates in accordance with the stated requirements (Hassenstein, 1951; Hassenstein & Reichardt, 1956). This model, called Hassenstein–Reichardt elementary motion detector (EMD), was developed in the 1950s and still remains one of the most influential models in neuroscience. EMD consists of two mirror-symmetric half detectors (Figure 3B). Each half detector consists of two elements, or input channels, that measure luminance at two neighboring locations in the visual space. The signal from one of the elements gets temporally delayed by linear low-pass filter, while the input from the second is not. Both signals from two channels are subsequently multiplied, resulting in a strong signal in response to the motion in the preferred direction (PD), and weak signal in response to the null-direction (ND). Subtracting the output of the second mirror-symmetric detector results in the direction-opponency: motion in the PD leads to positive signals, while motion in the ND leads to negative signals.

The characteristics of the fly optomotor behavior described above fit the predictions of the Hassenstein-Reichardt model, suggesting that there exist neuronal substrates that provide those computations in the fly visual system. And indeed, the directional responses of wide-field motion sensitive neurons in the fly lobula plate correspond to the outputs of the Hassenstein–Reichardt detectors (Egelhaaf & Borst, 1989; Joesch et al., 2008). This discovery marks the starting point of the search for exact neuronal implementations of motion detectors in the fly visual system that will be described further.

Correlation type motion detectors, such as Hassenstein-Reichardt and its alternative null-direction suppression Barlow-Levick model (Barlow & Levick, 1965) (Figure 3B), have been very influential in the development of composite motion detection models (Torre et al., 1978; van Santen & Sperling, 1985) as well as other classes of motion-detectors, such as gradient detector and motion energy model (Fennema & Thompson, 1979; Limb & Murphy, 1975; van Santen & Sperling, 1984). Applications of those models to both vertebrate and invertebrate motion detection suggest strong similarities in neuronal computations that underlie motion vision across phyla.

1.3.2 Local motion detection

As mentioned above, in the fly lobula plate were discovered motion-sensitive tangential neurons that respond in accordance with the subtraction stage of the Hassenstein-Reichardt detector. These cells show motion opponency and respond with depolarization to visual motion in PD and hyperpolarization to motion in the opposite ND (Hausen, 1984). In addition to motion opponency the response properties of these neurons such as temporal frequency tuning and contrast dependency are in strict agreement with the prediction of Hassenstein-Reichardt model (Borst & Egelhaaf, 1989). These cells, however, are not directly involved in motion computation but rather reflect the output of this process. The exact neuronal processes involved in

transformation of the visual information from photoreceptors to lobula plate motion sensitive neurons remained unclear for over half a century. It is largely related to the fact that there exist tens of cell types across the neuropils of the lamina, medulla, lobula, and lobula plate in *Drosophila* optic lobe. Even though all those cells have been identified and described for a long time, their response properties remained unknown due to technical limitations (Fischbach & Dittrich, 1989; Ramón y Cajal, 1915). The situation drastically changed with the development of advanced neurogenetic techniques for *Drosophila*. Genetic access to all the neuronal classes across optic lobe neuropils in combination with Ca2+ imaging and tools to manipulate neuronal activity enable building up a complete picture of how EMD are implemented in the fly visual system.

The first motion-sensitive neurons along the visual pathway are T4 cells in the medulla and T5 cells the lobula. Genetic silencing of T4 and T5 neurons abolish direction-selective responses in lobula plate tangential neurons as well as motion-guided behaviors, including the optomotor response (Bahl et al., 2013; Schnell et al., 2012). Every column contains four subtypes of both T4 and T5 cells: T4a, T4b, T4c, T4d and T5a, T5b, T5c, T5d. Each of the cell subtypes is tuned to one of the four cardinal directions and project axons to a specific layer of lobula plate (Maisak et al., 2013). Physiological analysis showed that T4 cells respond to moving brightness increments and T5 cells to brightness decrements, therefore representing two independent motion channels. These so-called ON and OFF channels exist in the visual system of vertebrates as well and originate at very early stages of visual processing. In *Drosophila*, inactivation of synaptic transmission in specific lamina neurons showed that L1 and L2 neurons initiate brightness-increment and brightness-decrement detecting pathways, respectively (Clark et al., 2011; Joesch et al., 2010). Some experimental evidence suggests that L3 and L4 neurons provide additional inputs to the OFF pathway (Silies et al., 2013; Takemura et al., 2011). Lamina neurons receive input directly from R1-6 photoreceptors, therefore visual information immediately after its detection gets split into parallel channels depending on the contrast polarity. Physiological data suggests little to no interactions between these two channels. Therefore, EMD in flies was suggested to be described by more elaborate 6-, 4- and 2-Quadrant Detector models, which allow implementation of separate ON- and OFF-input signals (Eichner et al., 2011; Fu & Yue, 2020; Joesch et al., 2013). How do T4 and T5 cells acquire their direction selectivity? The Hassenstein-Reichardt detector suggests that between L1/L2 and T4/T5 neurons there exist cells that provide the necessary stages of motion computation. EM experiments helped to identify all the neuron types that provide inputs to T4 and T5 cells, and to determine the exact locations of each synapse across the dendrites (Shinomiya et al., 2019). The results suggest that presynaptic cells to T4 are medulla neurons Mi1, Tm3, TmY15, Mi4, Mi9, C3, and CT1, while presynaptic cells to T5 are medulla neurons Tm1, Tm2, Tm4, TmY15, Tm9, CT1, LT33, and Tm23 (Figure 3A).

In addition, T4 and T5 neurons form synaptic connections within each subtype. Different subtypes of T4 and T5 receive input from the same medulla neurons but at different dendritic locations. Distinct medulla cell types have different physiological properties (Arenz et al., 2017; Behnia et al., 2014; Gruntman et al., 2018; Meier & Borst, 2019). More specifically, Mi4 and Mi9 neurons ON pathway as well as Tm9 neurons in OFF pathway and CT1 neurons have low-pass characteristic and carry time-delayed visual signals. On the dendrites of T4/T5 cells these signals are spatiotemporally correlated with non-delayed signals coming from other cell-types with band-pass properties. In addition, distinct medulla cell types use different types of neurotransmitters that exert excitatory and inhibitory effects at different locations of T4 and T5 dendrites. Anatomical and physiological properties of synapses between medulla and T4/T5 cells were used to complement the existing model of EMD (Borst, 2018; Gruntman et al., 2018; Haag et al., 2016, 2017). In the new, so-called three-arm detector model, the motion is calculated from three inputs (instead of two): a non-delayed central input that is amplified by a delayed input from the preferred side and suppressed by a delayed input from the null side (Figure 3C). This model represents a hybrid detector that combines Hassenstein-Reichardt half-detector with a Barlow-Levick half-detector.

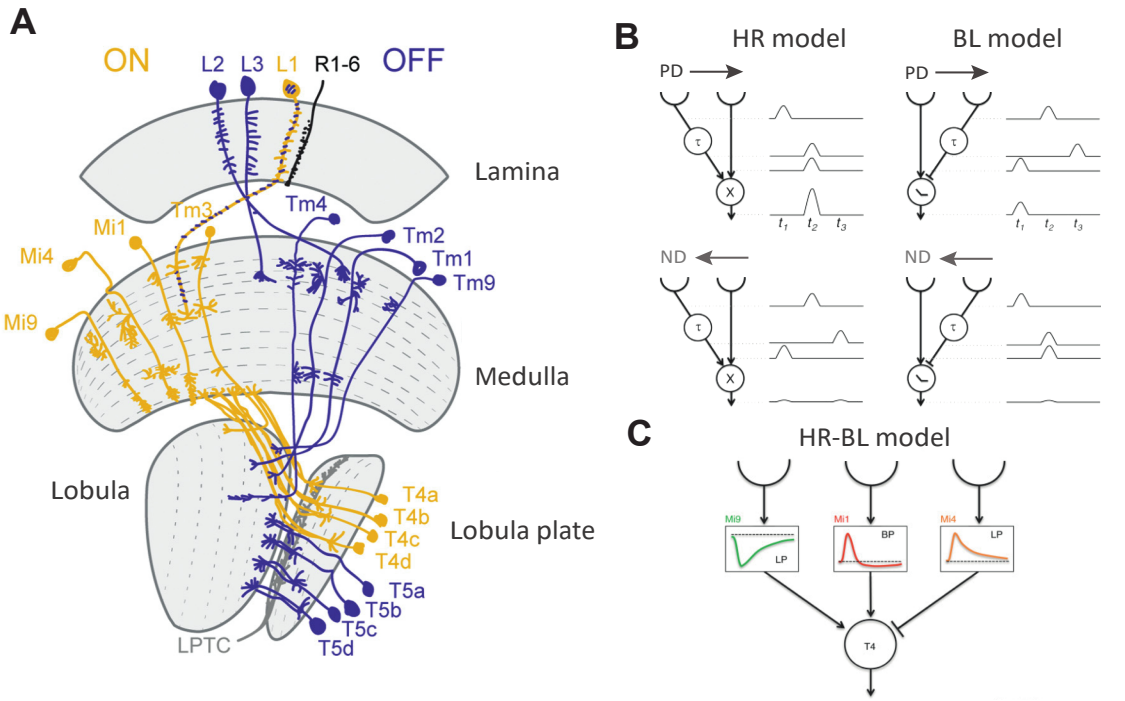

Figure 3. Elementary motion detector in the fly visual system. A) Schematic of the fly visual system with neurons of motion detecting circuits. Neurons of the ON pathway are depicted in yellow, and neurons of the OFF pathway in blue (adapted from Ramos-Traslosheros, 2018). B) The Hassenstein-Reichardt (HR) model and the Barlow-Levick (BL) model. C) The proposed cellular implementation of a HR/BL hybrid motion detector in the ON-pathway (Biswas & Lee, 2017).

1.3.3 Global motion processing

Information about local motion across the visual field has to be pulled together in order to reconstruct the pattern of global motion fields. T4 and T5 cells that serve as EMDs project directly to wide-field motion-sensitive lobula plate tangential cells (LPTCs) mentioned above. These projections are well-structured with each subtype of T4/T5 neurons sending axonal projections to specific layers of the lobula plate, providing this way distinct motion selectivity to different types of LPTCs (Maisak et al., 2013). Front-to-back motion sensing T4a and T5a subtypes send their axons to layer 1 of the lobula plate, back-to-front motion sensing T4b and T5b to layer 2, upward motion sensing T4c and T5c to layer 3, and downward motion sensing T4d and T5d to layer 4. In turn, dendrites of distinct types of LPTCs arborize in different layers of lobula plate receiving retinotopic motion-selective inputs from large areas of the visual field.

It is thought to exist approximately 60 different LPTCs in each hemisphere of the *Drosophila* brain, the majority of which are still poorly characterized (Figure 4). LPTCs can be classified based on multiple characteristics: 1) their preferred direction: vertical direction for the vertical system (VS) cells and V1, or horizontal direction for the horizontal system (HS) cells, H1, and H2, 2) their prevalent electrical responses: whether they respond to motion with graded potentials as centrifugal horizontal (CH) cells, VS, HS cells, or fire action potentials as H1, H2, and V1, 3) their projection area: whether they have purely ipsilateral projections (HS, VS), or connect the two hemispheres (V1, H1, H2).

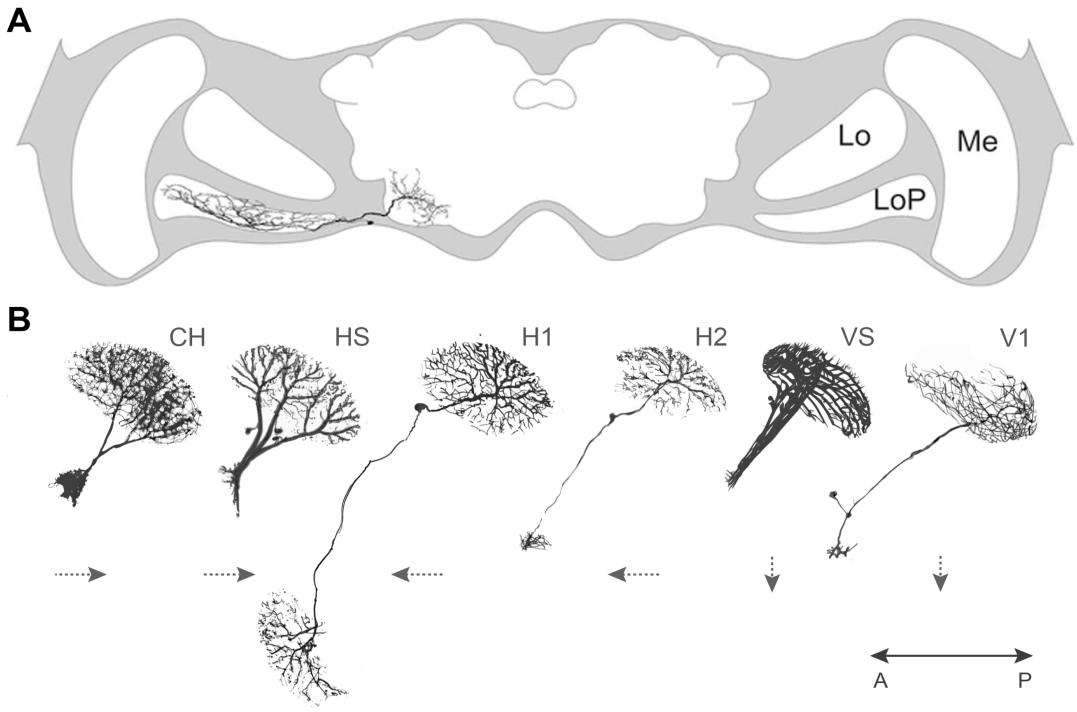

Figure 4. The diversity of lobula plate tangential cells. A) Horizontal section through the brain of blow fly, and the position of a LPTC. Me – medulla, Lo – lobula, LoP – lobula plate (adapted from Douglass & Strausfeld, 2007). B) The diversity of LPTCs. Dashed arrows indicate the direction selectivity of each of the cell type (adapted from Hausen, 1984).

Direction selectivity of LPTCs is defined by the area of their dendritic ramification in the lobula plate. Some wide-field neurons sample local motion information from a particular layer within the lobula plate, while others do not get direct inputs from EMDs and receive inputs only from other LPTCs in corresponding layers. LPTCs located in layer 1 of the lobula plate are horizontal system (HS) cells and centrifugal horizontal (CH) cells (Boergens et al., 2018; Wei et al., 2020). *Drosophila* has three HS cells that are named based on their anatomical location: northern HS cell (HSN, dorsal), equatorial HS cell (HSE, middle), and southern HS cell (HSS, ventral). HS cells respond with depolarizing graded potentials to front-to-back motion and hyperpolarizing in response to back-to-front motion (Schnell et al., 2010). CH cells have not been physiologically characterized in *Drosophila*. However, their anatomical resemblance to eponymous cells in the blow fly may suggest similarities in their visual response properties as well. CH cells in blow flies respond with graded membrane depolarizations to clockwise motion and with graded membrane hyperpolarizations to counter clockwise motion (Eckert & Dvorak, 1983). CH cells, contrary to HS cells, do not receive motion inputs directly from EMDs but only indirectly via dendro-dendritic electrical synapses from HS-cells (Haag & Borst, 2002). We have only sparse information about LPTCs in layer 2 lobula plate in *Drosophila*. There are located spiking cells that seem to be analogous to the well-described H1 and H2 neurons in blow flies. *Drosophila* H1-like neurons innervate lobula plates on both sides of the brain with dendrites located in the ipsilateral side and axons in the contralateral. The ipsilateral dendritic processes innervate only layer 2 of the lobula plate, while the contralateral axonal processes both layer 1 and 2. As layer 2 receives back-to-front local motion inputs, the response properties of H1-like cells presumably are consistent with those of H1 cells in blow flies (Eckert, 1980). H2-like neurons receive back-to-front local motion inputs from layer 2 in the ipsilateral optic lobe (Cruz et al., 2019; Wasserman et al., 2015). These cells send their axonal projections to the contralateral inferior posterior slope where they synaptically interact with other tangential cells. LPTCs in layer 3 have not been characterized, except for V1-like neurons that have dendrites in the ipsilateral posterior slope and contralateral axonal projections in layer 3

and 1. Therefore, it is probable that these cells have similar properties to their analogues in blow flies, i.e. that they receive motion signals from axons of VS cells, transform them into spike activity, and convey this information to the contralateral lobula plate (Kurtz et al., 2001; Warzecha et al., 2003). Layer 4 contains VS cells that have narrow band-like dendrites that span the lobula plate dorsoventrally. There exist six VS tangential cells (VS1-VS6) and three VS-like cells (VSlike1-VSlike3). Both of those subtypes respond with graded depolarizations to downward motion presented at a particular frontal-posterior position (Joesch et al., 2008). While responses of most LPTCs increase with the size of the visual stimulus, in blow flies were also identified small-field tuned FD cells (Egelhaaf, 1985). Recent studies showed that in *Drosophila* there exist neurons morphologically similar to FD cells, FD1-like and FD3-like (Wei et al., 2020). FD1-like neurons innervate layer 1, 2 and 3 of the lobula plate, while FD3-like neurons only innervate layer 2 which suggests their strict back-to-front direction preference consistent with FD3 in blow flies.

The direction selectivity of LPTCs can be easily explained by synaptic connections with specific subtypes of T4 and T5 cells in specific layers of the lobula plate. However, T4 and T5 neurons provide only excitatory cholinergic input and therefore cannot explain hyperpolarizing null direction responses. At the same time, it was demonstrated that inactivation of T4 and T5 cells abolishes hyperpolarizing along with depolarizing potentials in LPTCs (Schnell et al., 2012). These seeming inconsistencies led to a hypothesis that subtypes of T4 and T5 cells do not solely activate LPTCs in the corresponding lobula plate layer but also feed-forward inhibitory elements that inhibit tangential cells in the adjacent layer with opposite direction selectivity. Such bi-stratified Lobula Plate intrinsic (LPi) neurons were discovered to ramify within exactly two adjacent layers (Mauss et al., 2015). LPi neurons convey an inhibitory glutamatergic signal to tangential cells that express glutamate-gated Cl-channels (Richter et al., 2018). Silencing of these inhibitory neurons in layer 3 of the lobula plate resulted in the loss of null-direction hyperpolarizing responses of postsynaptic VS cells in layer 4. Similarly, optogenetic activation of these neurons resulted in fast graded inhibitory postsynaptic potentials. While LPi neurons were not yet identified between lobula plate layers 1 and 2, similarities in response properties of HS and VS cells suggest the existence of inhibitory neurons for translational motion as well.

Tangential cells thus integrate two sources of local motion information: direct excitation from ON- and OFF-selective T4 and T5 cells, and indirect inhibition from bi-stratified LPi cells activated by T4 and T5 cells from the neighboring layer. The presence of the feed-forward inhibitory elements demonstrates that neuronal implementations of Hassenstein–Reichardt model is more parsimonious. First, the subtraction step occurs on the dendrites of LPTCs and not upstream of them, second, computation of the motion direction occurs only once and is used to convert it into an inhibitory signal in the adjacent lobula plate layer. Feed-forward inhibition was shown to play a critical role in the formation of complex receptive fields of LPTCs, that are finely tuned to capture specific optic flow patterns generated during fly maneuvers (Mauss et al., 2015). With LPi neurons silenced, wide-field tangential cells lose their selectivity and respond with equal strength to various motion patterns.

1.4 Network of LPTCs and behavioral implementation of visual motion information

As it was discussed, motion information is extremely important for successful navigation in the visual environment. Our understanding of circuits underlying motion vision in flies is growing fast. However, it is becoming overwhelmingly evident that the complexity of sensory-motor transformation even in seemingly simple organisms like *Drosophila* is phenomenal.

The complexity of circuits underlying optic-flow-based navigation can be explained by the fact that flies have to faithfully extract intricate patterns of motion vectors and decide on appropriate behaviors extremely fast. Execution of prompt responses to complex sensory stimuli has major implications. First, neural circuits for optic flow processing have to receive local motion information very fast and integrate it efficiently across the entire visual field. Second, particular patterns of optic flow have to instruct distinct compensatory responses with a limited number of neurons. Third, the interpretation of the optic flow largely depends on the animal's own locomotion making behavioral responses flexible and context-dependent.

Neural implementation of visuomotor transformation in *Drosophila* therefore evolved to perform extremely complex computations with astonishing speed. Implementing such a complex task with the rather limited computational capacity of the fly brain makes optic-flow-based navigation an excellent example of performance optimization in biological systems.

1.4.1 Optic flow interpretation by LPTCs

The useful information needed for fly navigation cannot be discerned by examining small areas of the visual environment, but rather by estimating its global features. The estimation of global patterns of visual motion is carried out by LPTCs that combine measurements of local motion across large areas of the visual field. The information about the motion vectors of the optic flow in the fly's environment are then used to instruct appropriate motor commands. In natural conditions, faithful reconstruction of the optic flow is challenged by large irregularities in the image texture throughout the visual field. As a result, ambiguous or even conflicting motion cues may arrive from different areas of the visual environment. Together with that, optic flow patterns that result from distinct ego-motions can have extended patterns of identical motion cue patterns. Therefore, LPTCs can faithfully instruct optic-flow-guided navigation only by employing efficient mechanisms that enable them to integrate information between individual tangential cells uni- and bilaterally. That explains why these cells developed a complex pattern of lateral synaptic interactions. These interactions largely enhance the specificity of individual tangential cells to particular motion patterns and improve signal-to-noise ratio, allowing efficient control of visually-guided motor commands.

Receptive fields

In order to reconstruct the global structure of the optic flow, LPTCs spatially pool the outputs of many retinotopically-arranged local motion detectors. Distinct types of tangential neurons have sensitivity to particular motion directions, and are excited by motion in their preferred direction and are inhibited by motion in the opposite direction. Since sampling of local motion information happens on the dendrites of LPTCs, the spatial receptive fields (RFs) of these neurons are broad and defined to a great extent by the regions of their dendritic arborization.

The detailed RF structure of individual tangential cells can be reconstructed by mapping local directional tuning curves in response to a small visual motion stimulus. From the tuning curves, one obtains the local motion direction and the local motion sensitivity of a neuron across the visual field. This analysis was extensively applied to study LPTCs in blow flies (Krapp et al., 1998; Krapp & Hengstenberg, 1996), and to a smaller extent in *Drosophila* (Schnell et al., 2010).

The reconstruction of spatial RFs shows that local computations in the dendrites of LPTCs are more nuanced than the global direction-selectivity, and are composed of areas with distinct PDs. The local directional preferences of individual LPTCs therefore are not strictly unidirectional, and rather reflect the optic flow fields over the entire eye of the animal during different ego movements, such as pitch, yaw and roll (Figure 5A, 5B). For example, VS cells that have overall selectivity to downward motion show responses to horizontal pattern movements in the dorsolateral area. This way, the receptive fields of VS cells appear as curled vector fields matching the optic flow pattern occurring when the animal rotates around horizontally aligned body axes.

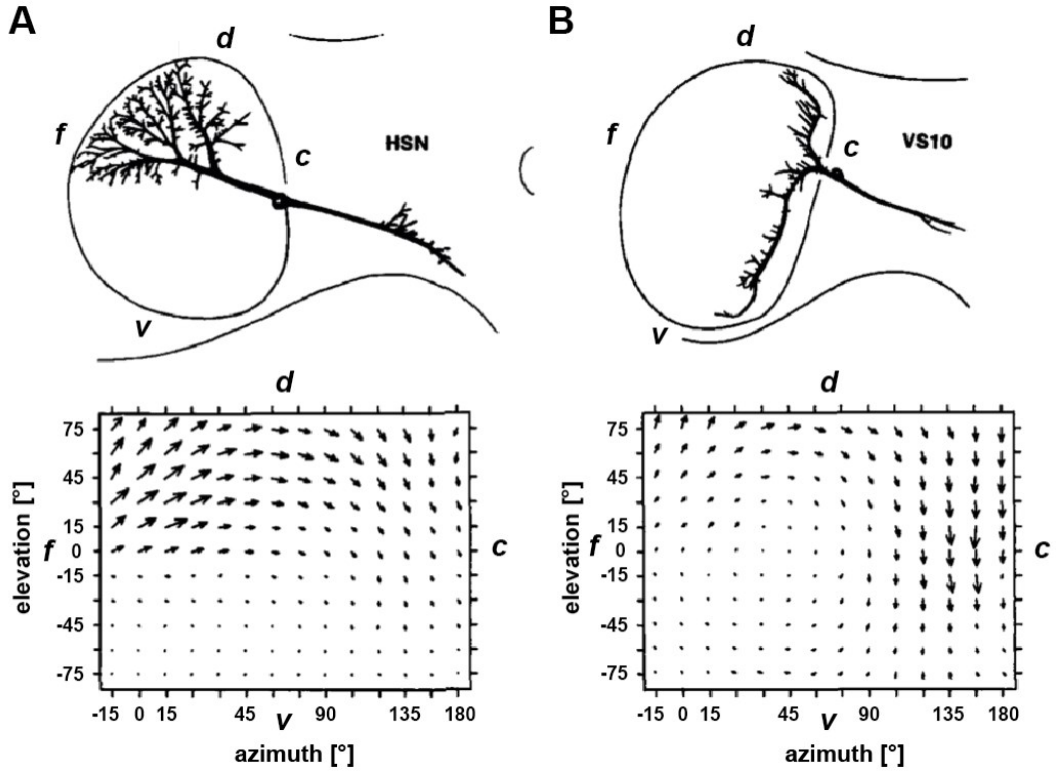

Figure 5. Morphology and spatial receptive fields of A) the HSN neuron and B) the VS10 neuron (adapted from Krapp, 2000); f – frontal, c – caudal, d – dorsal, v – ventral. The images of neuronal morphology were drawn from frontal serial cross sections after staining of individual cells with Lucifer Yellow. The receptive fields were reconstructed from extracellular recordings obtained during a presentation of a black dot with a diameter of 7.6 deg moving clockwise and counterclockwise.

If RFs of individual tangential cells match specific patterns of optic flow associated to a particular self-motion, then each of these neurons can drive compensatory responses to corresponding inadvertent change of the course. This approach would correspond to the idea of efficient information processing though so-called matched filters. The term, borrowed from engineering, was first applied to sensory processing by Rüdiger Wehner (Wehner, 1987). He defined neurons with specialized processing properties that relay only essential information about the sensory world by extracting solely crucial components of stimuli and ignoring irrelevant information. This strategy reflects the adaptive nature of the nervous system, which provides optimal responses to relevant sensory stimuli with minimal energy consumption. VS cells were shown not to operate as "classic" matched filters but rather as a special case that incorporates prior assumptions about environment and the self-motion, reflecting the dynamics of behavioral and sensory contexts in natural conditions (Franz & Krapp, 2000; Krapp, 2000). This way VS cells can maintain a robust behavioral output when the same type of rotatory motion occurs in different situations.

While the global pattern of motion responses in VS cells reflect the rotatory component of the optic flow, in blow flies there exists another type of tangential cells, Hx cells, with RFs matching the translatory component of the optic flow (Krapp & Hengstenberg, 1996). During navigation animals rarely experience pure rotation or translation, but often the combination of both. Therefore, an efficient decoding of self-motion requires a combination of multiple matched detectors. In addition, HS cells are predicted to supply additional correction for both translations and rotations (Krapp, 2000). Encoding of separate optic flow components by distinct tangential cells can potentially increase the flexibility of the sensory-motor transformation and enable monitoring of animal self-motion along any intermediate motion axis.

How do such complex receptive fields with different PDs in different areas arise in LPTCs? Some tangential cells have their dendrites arborizing in multiple layers of the lobula plate, which can result in selectivity to multiple directions (Boergens et al., 2018; Wei et al., 2020). However, it does not explain the exact match between distinct patterns of naturalistically experienced optic flow and RFs of individual tangential cells. Additionally, fields of motion responses in LPTCs often exceed in size the span of neurons' dendritic arbors. It suggests that receptive fields of tangential cells cannot be easily explained just by the inputs arriving from EMDs (Krapp et al., 1998). Indeed, it was discovered that in addition to synaptic connections with upstream local motion neurons, LPTCs form lateral connections between each other (Haag & Borst, 2001, 2004). These connections are highly stereotyped and were shown to improve specificity of tangential cells to particular patterns of self-motion-generated optic flow.

Interactions between LPTCs

Different LPTC subtypes form subnetworks via lateral synaptic interactions (Borst & Haag, 2002; Farrow & Munchen, 2005; Hausen, 1984). The properties of these interactions were studied extensively in blow flies using an array of techniques, including double recordings, dye coupling, photoablation and computer modelling (Farrow, 2005; Haag & Borst, 2001, 2002, 2008; Hausen, 1984). These studies revealed unexpected complexity of circuitry that connects different types of tangential cells: consisting both of bilateral interactions between two lobula plates, as well as unilateral intra lobula plate connections. Interactions between tangential cells were shown to be established both by chemical and electrical synapses, with some of them located between the axon terminals of neurons and others between the dendrites of neighboring cells. So far, two prominent subnetworks of LPTCs were described in blow flies: one consisting of horizontal-motion-sensitive cells, and another of vertical-motion-sensitive cells. One of these subnetworks mostly extracts translations and the other extracts rotations, yet, they do not function completely independently and form several connections with each other. This complex pattern of connections between tangential neurons most likely accounts for the aforementioned complexity of spatial RFs in these neurons.

The horizontal-motion-sensitive subnetwork is formed by distinct types of LPTCs that combine information binocularly. Among them, three HS cells that innervate overlapping regions along the dorsal-ventral axis of the lobula plate, form axonal electrical synapses between each other (Ammer et al., 2022; Haag & Borst, 2003; Schnell et al., 2010). Also, within the same lobula plate HS cells provide motion inputs to CH cells via dendritic gap junctions (Haag & Borst, 2002). Both HS and CH cells, therefore, are sensitive to front-to-back ipsilateral motion. In addition to unilateral integration of horizontal motion, HS cells form connections with spiking bilateral neuron H1 and heterolateral neuron H2 that are both sensitive to back-to-front motion (Farrow et al., 2006; Haag & Borst, 2001). H1 cell forms excitatory chemical synapses while H2 cell forms electrical synapses with CH and HS cells in the contralateral lobula plate. In turn, CH cells send inhibitory projections to ipsilateral H1 and H2 cells. The described subnetwork of horizontal-motion-sensitive neurons allows flies to disambiguate between translation, yaw rotation and side

slip. All these optic flows are dominated by horizontal retinal image shifts along the eye equator, and would be indistinguishable without the binocular recurrent loop.

The vertical-motion-sensitive subnetwork primarily consists of VS cells within each lobula plate. Adjacent VS cells are coupled via axonal gap junctions, enabling the bidirectional passage of electrical signals (Haag & Borst, 2004). These connections can explain the large width of receptive fields in individual VS cells (Farrow et al., 2005). Furthermore, electrical coupling between VS cells was shown to improve estimation of the center of rotation from natural image scenes (Cuntz et al., 2007). In addition to intra lobula plate connections, frontal VS cells are electrically coupled to the spiking V1 cell that relay information to the vertical CH cell in the contralateral side (Kurtz et al., 2001). This way, the V1 cell connects horizontal- and vertical-motion-sensitive subnetworks. There potentially exist other connections that convey information between those two networks, and that most probably explain why local direction selectivity differs in individual tangential cells (Haag & Borst, 2003).

Gap-junctions and functional impact of electrical coupling

As described above, many of the connections found between LPTCs turned out to be electrical in nature. Electrical synapses are structurally simpler, and for a long time were considered evolutionarily "primitive", and not suited for sophisticated computations afforded by the flexibility of chemical synapses. Electrical coupling between neurons provides fast bidirectional flow of the current that is traditionally thought to be used only in rapid stereotyped responses and in neuronal synchronization. The role of electrical synapses in sensory information processing became a subject of extensive research only recently. However, it is already evident that electrical coupling can have profound effects on the properties of neural circuits and the nature of neural computations (Alcamí & Pereda, 2019).

Electrical synapses are an omnipresent feature of nervous systems, and are formed by gap junctions. In insects the molecular substrate of gap junctions is innexin proteins (Phelan, Bacon, et al., 1998). The genome of *Drosophila* encodes 8 innexin genes, each with a distinct pattern of expression (Adams et al., 2000; Bauer et al., 2005). Innexins are structurally similar to all gap junction proteins: they have four transmembrane domains and intracellular N- and C-termini (Figure 6A). Gap junctions in *Drosophila* are formed by two octameric hemichannels in adjacent cellular membranes (Figure 6B). The resulting intercellular channel permits the passage of ions and small molecules between coupled cells. Gap junction channels show a high degree of molecular diversity: composed solely of one innexin type (homotypic) or of several types (heterotypic and heteromeric) (Figure 6C). We have very sparse knowledge about the molecular composition of gap junctions in the *Drosophila* nervous system, however, the majority of innexins studied so far appear to participate in channels of mixed composition and not in homotypic ones (Phelan et al., 2008; Phelan, Stebbings, et al., 1998; Wu et al., 2011). Considering that channels composed of distinct innexins have different properties, this strategy creates significant variability of electrical synapses with limited genetic diversity.

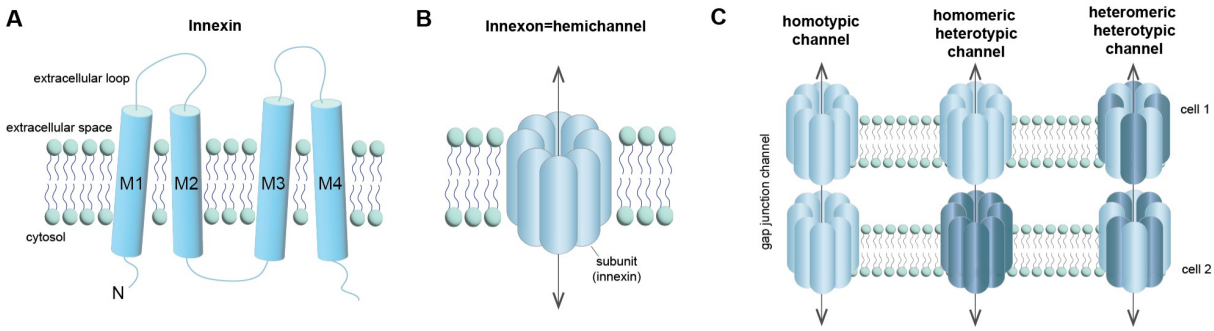

Figure 6. Structure of channels formed by innexins. A) Innexin protein consists of four transmembrane domains (M1-4) connected by two extracellular loops and one cytoplasmic loop; N- and C-loop are both located in cytosol. B) Eight

innexins form hemichannels called "innexons". C) Innexons align to form cell-to-cell gap junction channels. Gap junctions can be formed by identical connexons in adjacent cells, forming homotypic channels, or with different connexons, forming heterotypic channels.

Six out of eight innexins in *Drosophila* are expressed in the brain tissue, with inx1 (ogre), inx2, and inx3 being expressed exclusively in glia cells, and inx5, inx6, inx8 (shakB) in different neuronal populations. While inx5 and inx6 have a very sparse neuronal expression, inx8 is broadly expressed in multiple neuronal types within optic lobes, central brain and the ventral nerve cord (VNC) (Ammer et al., 2022; Davis et al., 2020; Kurmangaliyev et al., 2020).

The precise spatial and temporal expression of distinct types of innexins in the nervous tissues of *Drosophila* suggests that they are implicated in various cellular processes. Indeed, it was shown that gap junctions formed by innexin genes influence the activity of neuronal tissue during the development as well as during the adult stage of the animal (Phelan, 2005). Several innexings, including Ogre in *Drosophila*, are implicated in the development of the nervous system as early as from embryogenesis (Watanabe & Kankel, 1992). Nevertheless, the majority of gap junctions control cellular processes in developing neural circuits during pupal stage. In the optic lobe for instance, Ogre and Shak-B influence the formation of chemical synapses, and the loss of these innexins during development disrupts chemical synaptic transmission in the adult eye (Curtin et al., 2002). In addition, gap junctions are thought to be implicated in the generation of spontaneous neuronal activity during the development of neural circuits in the optic lobe of *Drosophila* (Akin et al., 2019). In other words, gap junctions have a role in synaptogenesis and in the propagation of spontaneous activity waves during development, but it is unclear whether those roles are functionally related. Similar to propagating the waves of activity in developing brain, gap junctions are often implicated in the control of collective neuronal dynamics and rhythmic central pattern generators in the brain of both larvae and adults (Matsunaga et al., 2017; Hürkey et al., 2022; Ramakrishnan & Sheeba, 2021). In addition to establishing collective dynamics of neuronal activity, gap junctions were shown to be critical for the function of various neural circuits (Güiza et al., 2018). Finally, it was recently discovered that gap junctions are involved in complex neuronal processes such as memory formation and sleep control (Troup et al., 2018; Wu et al., 2011).

Inx 8, or *shakB*, that is highly expressed in the optic lobe including LPTCs, has been demonstrated to be important in functional implications of various neural circuits, including early visual processing in photoreceptors and lamina (Joesch et al., 2010), escape response via giant fiber system (Blagburn et al., 1999; Pézier et al., 2016; Phelan et al., 1996), as well as odor processing in olfactory glomeruli (Yaksi & Wilson, 2010). LPTCs in flies that carry a null allele of the shakB gene (shakB2) lose electrical coupling, suggesting that gap junctions in these neurons are formed mostly or solely by this innexin (Ammer et al., 2022). The shakB gene, however, is complex and produces 8 distinct isoforms as a result of alternative splicing. It was demonstrated that distinct isoforms of shakB form heterotypic rectifying channels in the giant fiber system (Phelan et al., 2008). Electrical synapses formed by different protein variants of shakB have different conductance and potentially plasticity mechanisms (Palacios-Prado et al., 2014; Phelan, Stebbings, et al., 1998). Therefore, molecular diversity of innexins can provide extreme complexity of intercellular flow of current across neural circuits. Due to the lack of systematic characterization of gap junctions in *Drosophila* we know very little about the exact properties of electrical synapses in the tangential neurons. Therefore, theoretical predictions and modelling of the LPTC network considers non-rectifying junctions of the same conductance, which may not be biologically accurate.

Despite little understanding about the molecular characteristics of gap junctions in the lobula plate, physiological recordings and dye-coupling analysis enable predictions of their functional role in the circuit. As mentioned above, electrical synapses mediate direct flow of current between tangential cells, thereby influencing the structure of spatial RFs in these neurons. For example, the width of VS receptive field exceeds 100° in azimuth, even though based on the area of their dendritic arborization it should amount only to ~30–40°. Indirect experimental evidence coming from photoablation of individual VS cells suggests that spatial sensitivity of these

neurons increases due to lateral electrical coupling with the immediate neighbors (Farrow et al., 2005). Extended breadth of RFs in VS cells was predicted to provide a robust representation of the axis of rotation from images of complex statistics, which is especially important in the natural environment (Cuntz et al., 2007; Wang et al., 2017). Electrical coupling between horizontal-motion-sensitive cells provides binocular integration of visual information, which is critical for correct interpretation of optic flows that are dominated by horizontal vector fields (Farrow et al., 2006). In addition, gap junctions were predicted to improve motion detection from obscure visual stimuli by signal averaging. All that suggests that even though electrical coupling between tangential cells leads to an apparent loss of acuity, it increases sensitivity of the circuit to behaviorally relevant stimuli.

To directly assess the role of electrical synapses in the optic-flow-based navigation, detailed molecular, physiological and behavioral analysis of innexin mutants would be required. Results of such multifaceted analysis will be presented and discussed in Chapter 3.

1.4.2 Integration of contextual information into visual motion processing

All the properties of LPTCs described so far were mainly concerned with their visual response properties. It is evident that the network is adapted to reliably detect behaviorally relevant optic flow patterns from naturalistic images. Optic flow, however, is directly linked to an animal's own locomotion and therefore cannot be considered independently of it. In other words, to accurately navigate through the environment, animals must be able to account for the changes in their visual field that result from their own ongoing movements. In addition, voluntary movements have to be distinguished from inadvertent ones in order for intentional course changes not to become a subject of stabilizing responses. Multiple physiological studies in walking and flying animals show that the processing of visual information in the lobula plate network is largely modulated by the behavioral state of the animal. In addition, it was demonstrated that LPTCs receive motor-related signals for direct adjustment of the visual processing to the animal's locomotion. These strategies provide flexibility to seemingly rigid sensory matched filters, allowing flies to elicit robust responses in various environmental and behavioral contexts.

State-dependent modulation of optic flow processing

During different behavioral states the animal brain anticipates different sensory inputs. For example, quiescent animals normally do not experience optic flow stimuli, because it is predominantly associated with the animal's self-motion. Therefore, it is critical for neural circuits to assign different weights to the same stimuli in distinct behavioral and environmental scenarios. This adaptation of neuronal activity can be achieved by modulating the gain of individual neurons. Neural gain is a parameter that describes sensitivity of a neuron to a particular stimulus, and can be measured as a slope of the neural input-output relationship. It was demonstrated that during walking and flying the baseline membrane potential of LPTCs rapidly shifts upward and the amplitude of their responses to wide-field motion increases (Chiappe et al., 2010; Maimon et al., 2010). It suggests that the gain of these neurons increases during active locomotion, and therefore greater weight is assigned to behaviorally-relevant motion signals.

In addition to the increase of neural gain to particular direction of the motion, active locomotion changes the speed sensitivity of LPTCs. While in quiescent flies maximum responses of tangential cells are detected when stimulus is presented at the temporal frequency of 1Hz (Joesch et al., 2008; Maimon et al., 2010), the peak sensitivity during walking occurs at around 2 Hz (Chiappe et al., 2010) and at around 5–10 Hz during flight (Schnell et al., 2014). Some experimental results suggest that the changes in speed sensitivity occur already at the level of EMDs, upstream of tangential cells (Arenz et al., 2017; Strother et al., 2018). Therefore, the circuits for motion computation get modulated during locomotion in order to detect stimuli of higher speeds.

It was demonstrated that changes in the motion-processing circuits during active locomotion are induced by the neuromodulator octopamine. Pharmacological application of octopamine or of its agonist chlordimeform during neuronal recordings recapitulates the effects of locomotion on motion vision circuits (Longden & Krapp, 2009; Suver et al., 2012). Similarly, genetic activation and silencing of octopaminergic projection neurons have similar effects on neuronal responses as active and quiescent states, respectively. Neuromodulation is a slow process, that is why the increase in gain in LPTCs decays slowly (in the range of tens of seconds) after the end of the active state. Interestingly, the elevated baseline membrane potential of tangential cells that takes place during flight decreases rapidly after the end of activity. The differences in the time course of the baseline shift and the neuromodulation suggest that adaptation of neuronal sensitivity can be achieved by several distinct physiological mechanisms.

Locomotion is not the only behavioral state that can modulate the activity of visual motion-detection circuits. Another example is odor tracking: it was demonstrated that olfactory cues can increase the fidelity of visual reflexes during flight (Chow et al., 2011). At the neuronal level, high concentrations of attractive odorants activate octopaminergic neurons that modulate the gain of a subtype of LPTCs, Hx cells (Wasserman et al., 2015). These cells are sensitive to front-to-back motion, and are thought to regulate the direction of heading. Therefore, increase in the gain of Hx neurons in the presence of an attractive odorant can facilitate the search for a food source.

Overall, state-dependent modulation is an efficient strategy that provides flexibility of sensory circuits and their optimal performance in different settings. Being extremely efficient, this strategy however is energy-demanding. It was demonstrated that the increase in the gain of LPTCs during locomotion is no longer present in starved blow flies (Longden et al., 2014). Together, these findings demonstrate that tangential cells as visual matched filters are not rigid, and can adapt their responses to distinct behavioral states in a manner that also considers the metabolic state of the animal.

Locomotion-induced feedback and efference copy

Egomotion-induced optic flow cues are in sync with animal locomotion. That is why integration of sensorimotor and visual modalities can result in a substantial increase in the fidelity of optic-flow-based navigation. In *Drosophila* the responses of horizontal-motion-sensitive tangential cells are enhanced by locomotion-related inputs. It was shown that when a fly is walking HS and H2 neurons respond in a direction-selective manner to nonvisual motor-related signals (Cruz et al., 2019; Fujiwara et al., 2017). Interestingly, motor-related inputs enhance visual direction-selectivity in HS cells only when visual cues match those anticipated from the fly's movement. This way, self-induced and externally-evoked motion cues will result in different amplitudes of responses in HS cells. This selective augmentation of visual responses can serve as a mechanism to correct for animals' self-motion during navigation.

Motor feedback to tangential cells is important not only to stabilize the course but also to filter out self-evoked visual cues that are not supposed to be subjected to compensatory responses. Flies perform intended change in the course control using extremely fast saccadic turns. These saccades result in a prompt sweep of the visual scene across the retina and can induce strong motion visual responses in tangential cells and associated stabilizing reflexes. It is clear that it does not happen, because otherwise animals would counteract their voluntary movement. More than half a century ago, von Holst and Mittelstaedt described the principle of reafference that can provide resolution for this sensory conflict. It was suggested that with each motor command that initiates a voluntary turn, also known as an efference, the fly visual system receives a copy of this command, so-called efference copy. This efference-copy signal has to be of a correct sign and magnitude to silence the reafferent visual input caused by voluntary turns, thus preventing the stabilizing response from taking place. Only recently the cellular evidence for efference copy in *Drosophila* was discovered (Kim et al., 2015). It was shown that in alignment with the reafference

principle tangential cells get suppressed during saccades by motor-related inputs. While both HS and VS cells are subjected to saccade-related inhibition, the magnitude of inhibitory potentials differ across cell classes depending on their sensitivity to particular axis of rotation (Kim et al., 2017). This way motor-related inputs to the visual neurons silence visual responses only to saccade-induced yaw turns while preserving sensitivity to other axes of rotation. This indicates that only visual responses that match the ones predicted by voluntary self-motion get suppressed, while responses that are not anticipated remain largely preserved. Thus, the visual system of flies does not go completely blind during voluntary turns and stays responsive if the fly were to experience an unexpected visual stimulus during a saccade. Motor-induced suppression of visual perception was also reported for saccadic eye movement in primates (Matin, 1974). Therefore, the reafference principle can be a common mechanism to regulate sensorimotor processing across phyla.

1.4.3 Behavioral role of lobula plate network

The visual response properties of LPTCs together with the implementation of efference copies and feedback signals suggest that tangential cells control gaze stabilization and course control during locomotion. Indeed, flies with developmental malformation of the lobula plate, such as omb^{H31} mutant flies, demonstrate impaired optomotor responses (Heisenberg et al., 1978).

Visually-guided course control can be achieved by downstream circuits that receive integrated inputs from tangential neurons. Anatomical and physiological studies show that a subset of fly neck motor neurons receive direct inputs from VS and HS cells (Huston & Krapp, 2008; Milde & Strausfeld, 1986; Strausfeld & Seyan, 1985; Wertz et al., 2012). These connections are formed by both electrical and chemical synapses, and are likely to control LPTCs-mediated gaze-stabilizing head movements. In addition to neck motoneurons, HS and VS cells form connections with descending neurons that reach motor centers in the VNC (Haag et al., 2007; Strausfeld & Gronenberg, 1990; Suver et al., 2016; Wertz et al., 2008), and can potentially control steering responses during walking and flight.

How exactly tangential cells command motor circuits for the course control is not yet fully understood. Multiple experiments suggest, however, that bilateral asymmetry in the activity of LPTC-network is a key to instruct adequate steering responses. For instance, unilateral laser beam ablation of HS and VS progenitor cells resulted in reduced optomotor stabilizing responses to globally moving gratings on the ablated side, while having no effect on visual object fixation (Geiger & Nässel, 1981). Similar findings were obtained using microsurgical axonal lesions of HS cells (Hausen et al., 1983). Unilateral lesions led to significant changes in yaw torque responses to full field grating stimuli. In addition, electrical stimulations of distinct regions in the lobula plate of blow flies evoke different maneuvers (Blondeau, 1981). Besides the already mentioned polarity of responses, it was demonstrated that the hosting VS cells posterior layer of lobula plate controls pitch, lift and thrust responses while the anterior region that hosts HS cells controls the yaw responses. Altogether these early experiments suggest that tangential cells instruct steering behavior in accordance with the spatial organization and polarity of their visual motion sensitivity.

Recent advances in genetic tools enable targeted manipulation of neuronal activity. Controlled optogenetic activation of HS cells using a bistable variant of channelrhodopsin-2 and a selective driver line resulted in robust yaw head movement during quiescence and yaw turning responses during flight (Haikala et al., 2013). Unilateral light activation always induced yaw responses towards the simulated side. Similarly, brief unilateral activation of HS cells using optogenetics and ATP-gated cation channel P2X2 in walking flies resulted in ipsilateral steering responses (Busch et al., 2018; Fujiwara et al., 2017, 2022). These results suggest that activation of HS cells alone is sufficient to elicit yaw head movements and turning responses during flight and walking in *Drosophila*. Interestingly, chronic bilateral silencing of HS cells using the inward-rectifier potassium channel Kir2.1 reduces stabilizing head movements but does not firmly affect

optomotor responses in flying or walking flies (Cruz et al., 2019; Kim et al., 2017). At the same time, acute unilateral opto- and chemogenetic silencing of HS induces turns away from the stimulated side (Busch et al., 2018; Fujiwara et al., 2017). These results point to a functional importance of asymmetry in the activity of the LPTC network as well as to the presence of an additional yaw-control pathway that can functionally compensate for the loss of HS cells. Altogether, the described experiments suggest direct involvement of LPTCs in the course control. Nevertheless, our understanding of exact behavioral instructions elicited by this circuit is far from complete, and would require thorough functional and anatomical analyses using novel neurogenetic tools and extensive EM datasets.

1.5 Overall motivation and thesis outline

While physiological properties of optic flow sensing tangential cells are well described, further studies are required to understand how the neural activity in this circuit instructs motor commands. Behavioral studies described in the previous chapter suggest several important aspects of functional encoding in the LPTC network. Firstly, adequate stabilizing responses require asymmetric activation of neurons within the network. Secondly, each subtype of tangential cells potentially regulates fly maneuvers along a specific body axis. Thirdly, there seems to exist several compensatory control systems within the LPTC network that have combined or exclusive effects on each other. All that points to a functional entanglement of individual tangential cells, understanding of which would require novel approaches to tackle the connectivity and the dynamics of neuronal activity within the network.

The aim of my thesis is to unravel how patterns of neuronal activity and connectivity within the LPTC network give rise to optic-flow-based course control. In Chapter 2 I tackle the functional role of neuronal connectivity between tangential cells. I firstly developed a genetic tool to inactivate gap-junction forming innexin ShakB in tangential cells. I characterized the electrical coupling of LPTCs in the wild-type and *shakB* mutant animals. Using *in vivo* patch clamp technique, I compared passive electrical properties and visual response properties of LPTCs in wild-type and mutant animals. Finally, together with collaborators, I analyzed the functional role of electrical synapses in visual compensatory responses. Results of this study are presented in Chapter 2.

In Chapter 3, I address how activity in the LPTC network instructs distinct stabilizing responses. For that I tested existent and developed new genetic mosaic techniques to manipulate neural activity. Firstly, I applied SPARC-based mosaic optogenetic activation for different subsets of LPTCs and tracked induced behavioral responses. I adapted the SPARC toolkit for simultaneous optogenetic activation and inhibition, and characterized new transgenic animals that enable those manipulations. In addition to the optogenetic mosaic tool, I developed and characterized a new method for sparse neuronal inactivation.

Chapter 2

Gap-junctions in LPTCs arbitrate course control via integration of binocular visual information

2.1 Introduction

During navigation, animals largely rely on optic flow as an important source of information about their self-motion and the structure of the environment. These visual cues are critical for instructing motor programs that stabilize and control the animal's course. The classical example is the optomotor response (Reichardt, 1957), a counteractive compensatory reaction to stabilize global motion cues that, e.g., could be elicited by the displacement from its course by a gust of wind.

In the fly's brain, the circuit of LPTCs is thought to be primarily involved in steering compensatory behaviors (Borst & Haag, 2002). In *Drosophila*, LPTCs form a network of ~ 60 cells per hemisphere (Fischbach & Dittrich, 1989), with every single cell type defined by a distinct morphology and connectivity. One of the key response properties of these neurons is cell-specific tuning to particular optic flow patterns resembling sensory matched filters (Krapp & Hengstenberg, 1996). It was demonstrated that this global motion tuning originates from nonlinear processing in the dendrites of LPTCs, and gets further enhanced by stereotyped lateral interactions between specific subsets of tangential cells that mediate stabilizing maneuvers around specific body axes (Barnhart et al., 2018; Borst and Haag, 2002; Elyada et al., 2013). Most of these lateral connections are electrical in nature, and are formed by ShakB gap-junction channels (Ammer et al., 2022; Farrow et al., 2006; Haag & Borst, 2004; Wertz et al., 2008). Electrical synapses formed between LPTCs have been implicated in modulating the receptive field structures, the robust coding of flow-field parameters (Cuntz et al., 2007), improving motion encoding (Wang et al., 2017; Weber et al., 2012), sensory prediction (Wang et al., 2021) and establishing nonlinear binocular interactions (Farrow et al., 2006). Despite this wealth of functional correlations, the understanding of exact behavioral implications of lateral electrical synapses between tangential cells remains rudimentary.

Here, I studied HS cells, a subgroup of horizontal-motion-sensitive tangential cells. Optogenetic and chemogenetic activation of these neurons in *Drosophila* (Schnell et al., 2010) were shown to evoke directed head movement and flight turns, suggesting their involvement in the control of ipsilateral head and body yaw movements (Busch et al., 2018; Fujiwara et al., 2017; Haikala et al., 2013). However, these cells are not activated solely by yaw-induced optic flow patterns. Other ego-motions, such as slip and thrust translation also contain strong horizontal flow components, but require different compensatory reflexes. It was proposed that electrical coupling of HS cells with contralateral spiking H1 and H2 neurons is critical to disambiguate overlapping optic flow patterns in order to instruct appropriate behavioral responses (Hausen, 1984).

To test this hypothesis, I developed a new *shakB* mutant line that enables disruption of gap-junctions in LPTCs without strongly affecting visual motion circuits. In this chapter I will present results of 1) electrophysiological studies demonstrating that the loss of gap-junctions changes the receptive fields and connectivity patterns of HS cells without affecting their direction selectivity, and 2) behavioral studies proving that binocular integration via gap-junctions between HS-cells and contralateral spiking neurons is critical to elicit appropriate optic-flow-induced compensatory responses.

2.2 Methods

2.2.1 Fly stocks and husbandry

Drosophila melanogaster were reared on a standard cornmeal-molasses agar medium at 18°C and 60% humidity, and kept on a 12 h light/12 h dark cycle. Behavioral experiments were performed with 2-to-6-day old male flies, patch clamp experiments with 1-day old male flies.
To generate FlpStop^{shakB} flies, pFlpStop-attB-UAS-2.1-tdTom (Addgene #88910) donor plasmid was injected into shakB[*MI15228*] flies together with φC31 integrase-expressing transgene (BestGene Inc.). The orientation of the FlpStop cassette was identified using primers MiL-F, FRTspacer_5p_rev, and FRTspacer_3p_for from (Fisher et al., 2017).

The following fly stocks were used in the study:

Canton S (BDSC_64349)
shakB^{2}; +; + (Rodney Murphey)
shakB^{FlpStopND}, w+; +; +
shakB^{FlpStopD}, w+; +; +
shakB^{FlpStopND} DB331-GAL4; 20XUAS-FLPG5.PEST/+; +
shakB^{FlpStopD} DB331-GAL4; 20XUAS-FLPG5.PEST/+; +
shakB^{FlpStopND}; 10XUAS-IVS-mCD8::GFP; VT058487-GAL4
shakB^{FlpStopD}; 10XUAS-IVS-mCD8::GFP; VT058487-GAL4
shakB^{2}; 10XUAS-IVS-mCD8::GFP; VT058487-GAL4
shakB^{FlpStopD} UAS-myrGFP.QUAS-mtdTomato-3xHA; trans-Tango; +
shakB^{2}; 20XUAS-SPARC2-I-mCD8::GFP/VT058487-p65.AD, 20XUAS-IVS-PhiC31; VT000343-GAL4.DBD
shakB^{FlpStopD}; 20XUAS-SPARC2-I-mCD8::GFP/VT058487-p65.AD, 20XUAS-IVS-PhiC31; VT000343-GAL4.DBD

2.2.2 Immunohistochemistry and confocal imaging

Brains were dissected in PBS and fixed for 25 min in 4% PFA/PBS, washed 2 h in PBS and then 4 times for 15 min in 0.3% PBST, blocked in 10% Donkey normal serum in 0.3% PBST for 3 h, (all at RT), and incubated with primary antibodies diluted in 0.3% PBST containing 5% Donkey normal serum for 24 h at 4°C. Samples were washed for 5 h in PBS at 4°C and then 4 times for 15 min in 0.3% PBST at RT, and incubated with secondary antibodies diluted in 0.3% PBST containing 5% Donkey normal serum for 12 h. Samples were washed again 4 times for 15 min in 0.3% PBST and in PBS for 5 min at RT. The samples were mounted on glass microscope glasses with 0.12mm-deep spacers in VECTASHIELD® mounting medium (Vector laboratories). Z-stack images were acquired on Zeiss LSM800 confocal microscope using 10X and 20X air objectives. The images were processed using Fiji software.
For quantitative and qualitative analysis of ShakB localization brains of 2-day-old male flies were used, for the analysis of neuronal morphology - brains of 2-to-5-day-old male flies, for trans-Tango-mediated trans-synaptic tracing - the whole CNS of 10-to-15-day-old flies
The following antibodies were used: Anti-shakB rabbit serum antibody (kind gift of Alexander Borst, Max Planck Institute for Biological Intelligence, Martinsried, Germany; 1:800), goat anti-GFP (Abcam, 1:500), goat anti-RFP (Rockland, 1:500), rabbit anti-GFP (Thermo Fisher, 1:500), donkey anti-goat AF488 (Abcam, 1:1000), donkey anti-goat AF594 (Thermo Fisher, 1:1000), donkey anti-rabbit AF594 (Thermo Fisher, 1:1000), CF594 rabbit anti-RFP (Biotium, 1:500).

2.2.3 Protein isolation and quantification

To extract insoluble protein fraction, approximately 150 brains of 3-to-5-day-old male flies were homogenized in 300 µl of extraction buffer (20 mM Tris pH 7.6, 50 mM NaCl, 1% Triton X-100, 1XHalt Protease inhibitor Cocktail (Thermo Fisher)), and incubated for 30 min on ice. Homogenates were centrifuged for 60 min at 15 x 1000 g in 4°C. Supernatant was discarded, and the remaining pellet was used for isolation of insoluble proteins. For that the pellet was resuspended in SDS extraction buffer (50 mM Tris pH 7.6, 5 mM EDTA, 4% SDS), and incubated at 95°C for 10 min. Supernatants were collected after centrifugation for 10 min at 15 x 1000 g at room temperature, and were used for protein quantification with BCA protein assay (Thermo Fisher).
For western blot analysis, 10 µg of each protein sample were mixed with Laemmli's buffer, boiled for 5 min, and subjected to SDS-PAGE using 4–20% TGX Stain-Free Precast Gels (Bio-Rad). Gels were activated by UV exposure for 2 min using a Bio-Rad Chemidoc MP imager. Proteins were transferred to LF PVDF membranes (Bio-Rad) using a Transblot Turbo apparatus (Bio-Rad). The membrane was incubated in EveryBlot Blocking Buffer (Bio-Rad), and immunoblotted following standard protocols. The following antibodies were used for the western blot analysis: anti-ShakB (1:3000), IRDye 800CW goat anti-rabbit (1:15000). Total lane signal was detected using Stain Free Blot application and ShakB signal was detected using IRDye 800 CW application (Bio-Rad Chemidoc MP imager). The immunoblots were repeated three times. ShakB signal was quantified and normalized to the total lane signal using Imagelab 4.1 (Bio-Rad).

2.2.4 Proteomic analysis

For protein sample preparation, brains of 2-5 days old flies were dissected. All samples (3 genotypes, 4 replicates; 10 or 6 pooled dissected fly brains per sample for replicate 1 and replicates 2, 3 and 4, respectively) were processed in 4 replicate-specific batches with the iST-NHS kit from PreOmics GmbH using the standard manufacturer's protocol; samples were trypsin digested for 2 h 30 min, then labelled with TMT-6plex (ThermoScientific) according to the manufacturer's instructions. Combined TMT samples were dried, re-dissolved in 45 µL 100 mM NH4OH, then loaded onto an ACQUITY UPLC BEH C18 column (130Å, 1.7 µm, 2.1 mm x 150 mm, Waters) on an Ultimate 3000 UHPLC (Dionex) and fractionated into 24 fractions by High pH Reversed Phase chromatography. Fractions were combined at mid-gradient, yielding 12 final fractions which were dried, re-dissolved in 50 µL iST-LOAD and sent for MS analysis.
All samples were analyzed by LC-MS/MS on an Ultimate 3000 nano-HPLC (Dionex) coupled with a Q-Exactive HF (ThermoFisher Scientific). Acquired raw files were searched in MaxQuant (1.6.17.0) against a *Drosophila melanogaster* fasta database downloaded from UniProtKB. The output "evidence.txt" files were then re-processed in R using in-house scripts. The long format evidence table was transformed into a wide format peptidoforms table, adding up individual values where necessary. Peptidoform intensity values were $\log_{10}$ transformed. The TMT/replicate-specific batch effect was corrected using Internal Reference Scaling, then values were re-normalized (Levenberg-Marquardt procedure). Protein groups were inferred from observed peptidoforms, and, for each group, its expression vector across samples was calculated by averaging the log10 intensity vectors across samples of individual unique and razor peptidoform, scaling the resulting relative profile vector to an absolute value reflecting the intensity level of the most intense peptidoform according to the best flyer hypothesis (phospho-peptides and their unmodified counterpart peptide were excluded). Peptidoform and protein group log2 ratios were calculated per replicate to the corresponding control (FlpND) sample. Statistical significance was tested with the limma package, performing a moderated t-test for all other genotypes against the FlpND genotype. Protein groups with a significant P-value were deemed to be regulated if their absolute log2 ratio was larger than the 90% least extreme individual control to control $\log_2$ ratios.

2.2.5 Analysis of isoform expression

Quantifying the expression of shakB isoforms was performed with Salmon (Patro et al., 2017). The transcriptome of Drosophila melanogaster was indexed with decoys following the instructions of the Salmon documentation. Briefly, the files dmel-all-chromosome-r6.43.fasta.gz and dmel-all-transcript-r6.43.fasta.gz were downloaded from Flybase on December 16 2021. The chromosome sequences were used as decoy and the index was constructed with default k-mer length 31.
The RNA-seq data from (Kurmangaliyev et al., 2020) was downloaded from ENA (European Nucleotide Archive) using accession numbers PRJNA658010. Each replicate was quantified independently using Salmon default parameters with options -lA to detect the library type automatically.

2.2.6 Reconstruction of neuronal morphology

To label individual HS cells we used 2-3 days old male flies of the following genotype: *+; 20XUAS-SPARC2-I-mCD8::GFP/VT058487-p65.AD; VT000343-GAL4.DBD*. Only flies with single labelled HS cells were used. After IHC and imaging (see above), confocal z-stacks of individual HS cells were used for neuronal reconstruction using Neutube (Feng et al., 2015). The generated .swc files were loaded into Imaris software (Imaris9.3.1) as filaments using PylmarisSWC extension, implemented in Python. The diameter of each segment was manually readjusted based on the confocal images. Parameters for Filament dendrite area (sum) and Filament dendrite length (sum) for each neuron were normalized to the size of the optic lobe. For sholl analysis, the step resolution was adjusted to the total length of the dendrite to obtain the equal amount of sholl intersections for each cell type. The Excel files were extracted for individual cells and used for further analysis.

2.2.7 Trans-synaptic tracing

To identify postsynaptic partners of HS cells, trans-Tango flies carrying a wild-type or a mutant *shakB* allele were crossed with HS-specific GAL4 driver line R81G07. This way the genetic diversity and growth conditions between individuals were reduced due to the comparison of wild-type and mutant flies from the same progeny (siblings). The crosses were maintained at 18 °C, the male flies from the progeny were collected after eclosion and kept for another 14-16 days at 18 °C. Fly CNS were dissected and immuno-stained as described above. The variant of shakB allele of each dissected fly was identified using primers MiL-F and FRTspacer_3p_for for FlpStopNDshakB batch, and primers 5'-cacaccaacgcaacggttatata-3' and 5'-cggccctgtgaattgtgaac-3' with subsequent sanger sequencing for *shakB*^{2} batch.

2.2.8 Electrophysiology

1-day-old male flies were briefly anaesthetized on ice and tethered using beeswax to a 3D-printed holder with a hole in the middle fitting the head and the thorax. The flies were positioned and prepared for recordings as in (Joesch et al., 2008). The holder with tethered fly was placed on the set-up under 40× water-immersion objective in front of a screen for stimulus presentation, and cell bodies of LPTCs were additionally cleaned under visual control using a low-resistance patch pipette (tip ~4 μm) filled with extracellular saline solution. Patch electrodes of 5-7 MΩ resistance (thin wall, filament, 1.5 mm, WPI, Florida, USA) were pulled on DMZ Zeitz-Puller (Zeitz-Instruments Vertriebs GmbH) and filled with intracellular solution. Using a Multiclamp 700B amplifier (Molecular Devices, Sunnyvale, USA), the signals were filtered at 4 kHz, digitized at 10 kHz, and recorded via a digital-to-analog converter (PCI-DAS6025, Measurement Computing, Massachusetts, USA) with Matlab (Vers.9.2.0.556344, MathWorks, Inc., Natick, MA). The recorded membrane potential was corrected for junction potential (12 mV).

The solutions used for *in vivo* whole-cell patch-clamp recording: extracellular saline solution (in mm): 103 NaCl, 3 KCl, 5 *N*-tris(hydroxymethyl) methyl-2-aminoethane-sulfonic acid, 10 trehalose, 10 glucose, 2 sucrose, 26 NaHCO3, 1 NaH2PO4, 1.5 CaCl2, and 4 MgCl2, adjusted to 275 mOsm, bubbled with 95% O2/5% CO2, and pH equilibrated around 7.3; the intracellular solution (in mm): 140 potassium aspartate, 10 HEPES, 1 KCl, 4 MgATP, 0.5 Na3GTP, and 1 EGTA, pH 7.26, adjusted to 265 mOsm. In most experiments, 0.5% Neurobiotin was added to the intracellular solution.

2.2.9 Visual stimulation for electrophysiology

Visual stimuli were presented on the screen with the shape of a quarter sphere (diameter 40 mm) using an LED projector (Texas Instruments DLP LightCrafter Evaluation Module). The refresh rate of the projector was set to 120Hz and the frame update was at the rate of 60Hz. An optical filter was positioned in front of the projector to block the red light, which was projected outside the visual field for synchronization. The reflected red light was captured by a photodiode and saved for further analysis. The stimulus was presented in green and blue light. The scripts to present visual stimuli were written in Matlab using Psychtoolbox library (Brainard, 1997). To compensate for spherical distortions of the screen, we created a customized lookup table that pre-deforms each frame on the GPU. The span of the visual field covered by the stimuli is ca. 140° horizontally and 85° vertically.

2.2.10 Neurobiotin cell filling and visualization

After the recordings were accomplished, cells were filled with Neurobiotin using a positive current of 1 nA for 10 min. After filling, the tissue was left in the recording bath for another 10 min for the dye to diffuse. The heads of flies were fixed in 4 % PFA/PBS at RT for 1 h, and washed 3 times for 15 min in PBS. The brains were dissected out of head capsule in cold PBS. To visualize neurobiotin we used TSA-mediated streptavidin labelling, as described in (Vega-Zuniga et al., 2018) with some modifications. The neurobiotin-filled neurons were revealed using Streptavidin-Alexa 546 (Thermo Fisher) or Streptavidin-Alexa 488 (Thermo Fisher) diluted 1:500 in 0.5 % PBST/4 % NaCl solution at 4 °C overnight. The mounting and imaging of brains was performed as described above.

2.2.11 Analysis of patch-clamp recordings

Cell voltage activity was recorded using the custom designed software in LabView and analyzed in Matlab.

Full field flashes
Full field flashes were interleaved with intervals of dark screen in between. The average response per animal was computed across repetitions. The population average is the average of the responses of all flies with the same genetic background.

Gratings (contrast, direction and velocity selectivity)
To quantify the tuning of the cells to contrast, direction, and velocity we presented a moving grating stimulus with spatial frequency 0.04 cycle/° (that in our hands elicited the strongest direction-selective responses in HS cells), while changing one of the aforementioned parameters. The moving gratings were interleaved with intervals of the stationary gratings. The baseline computed during the stationary gratings was subtracted from the responses to the moving gratings. Population responses are averages of the responses of individual cells. For the direction tuning analysis (Figure 1F), responses were normalized to the maximum response for each cell and then averaged across animals with the same genetic background.

Power spectrum analysis
For the power spectrum (PS) analysis we first extracted the raw responses during the flash OFF periods and subtracted the global mean, such that the contribution of the lowest frequencies does not overshadow the contribution of higher frequencies. We used Matlab fft function to compute the Fourier transform of the traces. One-sided spectrum was normalized with respect to the bin size and squared to convert to the power of frequencies. Whenever multiple repetitions of the stimuli were available, we computed the PS for each repetition and averaged them to obtain the PS of the responses of one cell. The PS of each cell was normalized such that the total energy was 1. The PS of the population is the average of PS of individual cells with the same genetic background. To quantify the contribution of three different ranges of frequencies we subdivided the frequency range into three intervals: 0-10 and 11-50. The sum of power of the frequencies within these groups is depicted in Figure 7C as a percentage of the total power over all the frequencies to give the relative contribution of each interval.

Scanning stimulus (RFs)
The rectangle of the size of 10° high and 2° wide was scanning the visual field horizontally and vertically. The baseline voltage value recorded during the experiment was subtracted, so that only the deviations from the baseline are used for the analysis.
The responses were discretized into bins of 16.6ms. The position and motion direction of the rectangle in each frame was weighted with the discretized voltage response at the time of the frame. We take the vector sum of the responses to the four cardinal directions and average across multiple repetitions to compute the mean response of a cell which can be represented as a vector field, called receptive field optic flow (RFOF). The location of each arrow in the RFOF corresponds to a specific azimuth and elevation in the visual field of the fly, the direction represents local preferred direction and the length indicates the relative strength of response. After normalizing the responses of each cell to the unit maximum, we average the responses of multiple cells from animals with the same genetic background to obtain the RFOF of the population. In order to represent the deformations that are due to the spherical shape of the screen we deform the RFOF similarly to how the stimulus is pre-deformed during the experiment. The horizontal/vertical profiles of the RFOF were computed as length of the average arrow in the corresponding azimuth/elevation.

2.2.12 Freely-walking behavioral arena

Individual flies walked freely on a 55mm circular arena made of IR-transparent Perspex acrylic sheet with 3mm tall walls. The walls were heated with an insulated nichrome wire to prevent the flies from walking on the walls and to encourage them to spend more time close to the center of the arena. The arena was covered with an IR-transparent acrylic sheet coated with Sigmacote™ (Merck) to prevent flies from walking on the roof. The entire behavioral setup is placed inside a custom-designed temperature-controlled compartment that maintains the internal temperature at 27°C.
Visual stimulus was projected from the top on the outer face of the roof which is covered with a projection screen (Gerriets OPERA® Grey Blue Front and Rear Projection Screen). Stimulus was presented by an LED projector (Texas Instruments DLP LightCrafter Evaluation Module) at a framerate of 60Hz and pixel size of 12px/mm using green LED (peak around 520-560 nm) of the projector. The fly was video recorded from the bottom using a monochrome USB3.0 camera (Flea3 FL3-U3-13YM) at a frame rate of 60Hz and resolution 1024x1024 pixels (~10px/mm). The arena was illuminated from the top by a custom-made panel of IR LEDs (850nm SFH 4235-Z). Since the projection screen, the roof and the arena are all made of IR-transparent material, the backlit flies appear as dark silhouettes on a bright background.
The stimuli were presented by a custom python script and the various textures were generated and updated using the Psychopy library (Peirce et al., 2019). The stimuli were updated every frame in

a closed-loop fashion by tracking the position and orientation of the fly online (see Data analysis). The delay between the fly movement and the update of the stimulus was 3 frame updates (~50ms). We presented a radial sinusoidal grating pattern, akin to a sinusoidal pinwheel, that was centered over the fly body. Rotating this pinwheel in either clockwise or counterclockwise direction evoked a turning response, the optomotor response of the fly. The diameter of the pinwheel was kept 45 mm since the optomotor response of the fly, which increased with an increase in size of the pinwheel, saturated at 45 mm and did not change for larger pinwheels. An experiment session consisted of approximately 200 trials of 5s pinwheel rotation preceded by 5s without rotation. The direction, contrast and speed of rotation of the sinusoidal pinwheel were changed across trials. The contrast of the grating pattern was computed as

$$Contrast = \frac{Max\ Intensity - Minimum\ Intensity}{Max\ Intensity + Minimum\ Intensity}$$

For experiments with localized motion, the pinwheel was divided into 2 or 4 segments and the direction of rotation of each segment (counterclockwise, clockwise or no rotation) was changed independently across trials to produce different combinations of translational and rotational optic flow.

2.2.13 Extraction and pre-processing of behavioral data

The position and orientation of the fly were determined for each frame during the experiment. The contour of the fly was extracted after performing a pixel intensity thresholding and an ellipse was fitted to this contour. The position of the centroid and the angle of the major axis of this fitted ellipse were used to determine the position and orientation of the fly, respectively. While this method is quick (a requirement for performing online experiments) and works well for determining the direction of the fly body, it does not provide the head direction of the fly since there is no way to distinguish between the head and the abdomen. This was done by processing the saved videos post-experiment. Otsu's binarization was used to obtain two thresholds from the image, one for the body of the fly and one for the wings which are translucent and allow some light to pass through. The direction of the line joining the center of mass (COM) of the body and the COM of the wings was used to determine the head direction of the fly which was then used as the correct orientation for further analysis. All machine vision computations were performed using functions from the OpenCV python library.

The speed and angular velocity of the fly were calculated from the change in position and orientation respectively. In order to remove noise, we used a rolling median followed by a rolling average with a window length of 5 frames (~40ms). Events where the fly jumped were detected using a threshold of 100 mm/s or 1000 degrees/s. Trials in which the fly either jumped or went close to the walls of the arena (within 5 mm of the wall) were excluded from further analysis.

Estimation of the path straightness and saccades

Fly locomotion is composed of long bouts of relatively straight motion interspersed with sharp turns, called saccades. We detected these saccades by using a wavelet transform strategy inspired by Cruz et al. 2021. The stationary wavelet transform (swt) of the angular velocity was computed using a biorthogonal 2.6 wavelet. The swt signal in the 10-20 Hz band was isolated and used to reconstruct the angular velocity data with an inverse stationary wavelet transformation. Peaks in this reconstructed angular velocity data that had a maximum angular speed higher than 200 degrees/s and with a width more than 50ms and less than 250 ms were deemed to be saccades.

In order to calculate the local curvature of locomotion, we first defined forward walking bouts as periods between two saccades that are longer than 333ms (20 frames) where the average speed of the fly is more than 5 mm/s. Then, a window of 333ms was selected centered around each point of a walking bout. The length of the straight line connecting the two end points of this

window (the shortest distance between two points) and the perpendicular distance between this line and the midpoint of the actual trajectory (deviation from the shortest distance) was calculated. A straight walking bout will have minimal deviation from a straight-line trajectory. As such, the straightness of a walking bout was defined as the ratio of the sum of the shortest distances and the sum of deviations from the shortest distance.

2.3 Results

2.3.1 Development and validation of an inducible ShakB mutant

The role of electrical synapses in *Drosophila* neural circuits is an object of extensive research. However, it remains challenging to manipulate them genetically. Widely used EMS-induced mutants such as shakB^2 offer the advantage of robust gene inactivation but frequently carry background mutations. Together with that, cell-specific inactivation of gap-junctions in the fly visual system had rather limited success (Ammer et al., 2022). For these reasons, pinpointing the contribution of electrical synapses within neural circuits remains challenging.

To attempt a detailed description of the role of electrical synapses in fly neural circuits for visual motion processing, we generated transgenic animals that carry FlpStop cassette inside the shakB gene (Figure 7C). This approach offers the advantage of creating both full and cell-specific mutants maintaining homogeneous genetic background, which is an advantage for adequate interpretation of behavioral experiments (Colomb & Brembs, 2014; de Belle & Heisenberg, 1996).

FlpStopNDshakB (non-disruptive orientation) and FlpStopDshakB (disruptive orientation) flies were created by integrating FlpStop-cassette into an intronic MiMIC insertion between exons 5 and 6. This insertion allows inactivation of 6 out of 8 isoforms of the shakB protein, leaving isoforms shakB-PA and shakB-PE intact (Figure 7A, 7B). Notably, the widely-used shakB^2 mutant carries a null mutation in 5 isoforms, leaving shakB-PF undisrupted in addition to shakB-PA and shakB-PE.

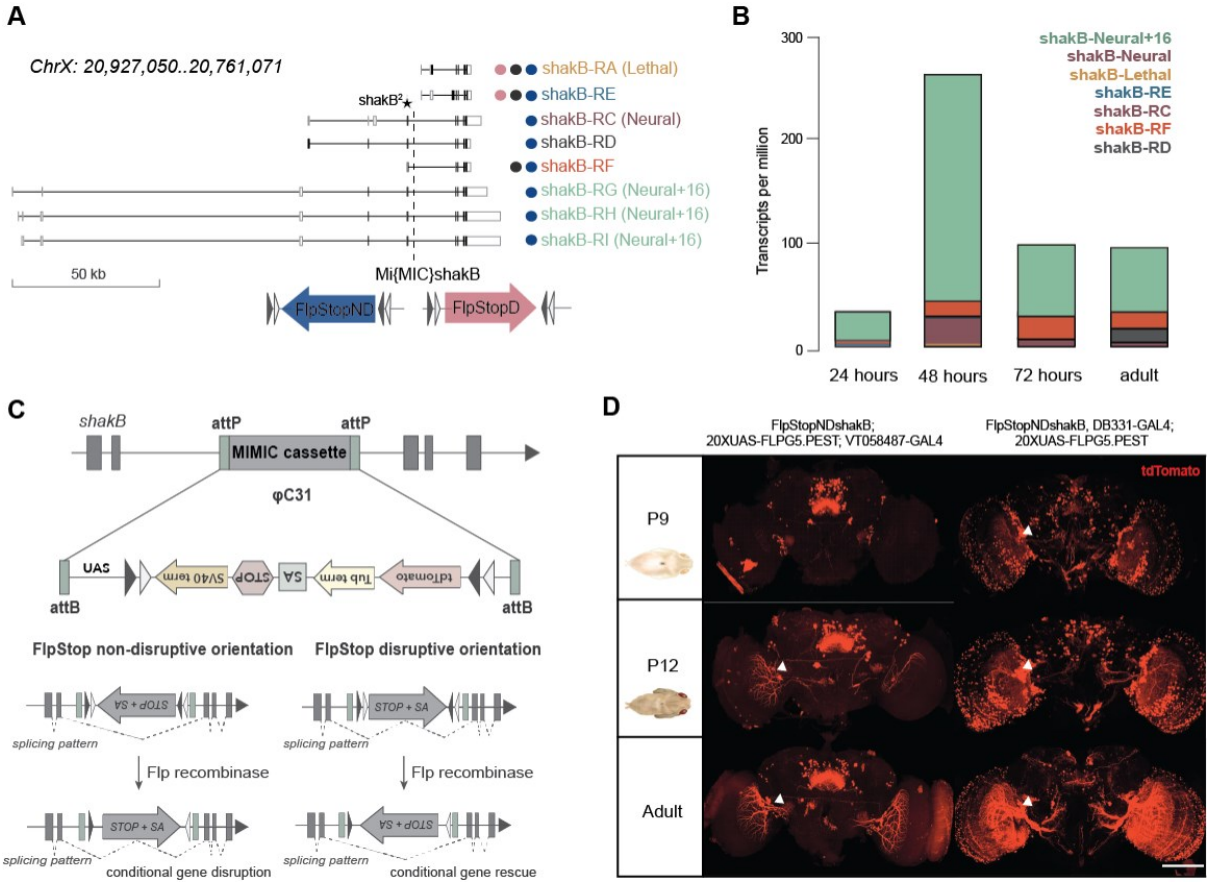

Figure 7. FlpStop technique for ShakB inactivation. A) Gene map of *shakB* isoforms. Nonsense mutation carried by shakB^2 flies is indicated with a star, the dashed line indicates the position of the intronic MiMIC cassette used for the integration of FlpStop cassette in disruptive (FlpStopDshakB, magenta) and non-disruptive (FlpStopNDshakB, blue) orientations. The circles indicate isoforms that are intact in FlpStopNDshakB (blue), FlpStopDshakB (magenta) and shakB^2 (black) flies. B) The expression of shakB isoforms in the optic lobe of Drosophila throughout the pupal

development. C) Schematic of the structure of the FlpStop cassette and of the gene disruption mechanisms. The cassette is integrated into MIMIC insertion using PhiC31-integrase. FlpStop cassette contains a splice acceptor (SA), transcriptional terminators (Tub α 1 terminator and the SV40) and stop codons in three frames (STOP). The cassette can be integrated in disrupting (FlpStopD) or non-disrupting (FlpStopND) orientation. Disrupting orientation can be used for a gene knock-out, while non-disrupting orientation can trigger cell-specific gene inactivation in combination with flippase (Flp) and a GAL4-driver line. D) The dynamics of the inversion of the FlpStop cassette using two distinct LPTC-specific driver lines - DB331-Gal4 and VT058487-Gal4. The expression of the tdTomato was used as a marker of the cassette inversion. The onset of the cassette inversion is around P9 for DB331-Gal4 and around P12 for VT058487-Gal4, somas of LPTCs are indicated with white arrows (scale bar 100 μm).

We observed a significant reduction in the total amount of ShakB protein in the brain tissue of FlpStopDshakB flies in comparison to FlpStopNDshakB flies (Figure 8A, 8B). Recent studies suggest that cell-specific inactivation of ShakB protein using driver lines selective to LPTCs is not efficient (Ammer et al., 2022). It can be related to an early onset of expression and a slow turnover rate of innexins in these neurons. Potential influence of the developmental timing on the efficiency of cell-specific inactivation of ShakB prompted us to trigger the inversion of FlpStop cassette using two LPTC-specific driver lines - DB331-Gal4 and VT058487-Gal4. DB331-Gal4 line initiated Flp-mediated cassette inversion in LPTCs at around pupal stage P9 while VT058487-Gal4 at around P12 (Figure 7D). ShakB immunolabelling in LPTC axons showed that DB331-Gal4 driver line induced stronger gene knock-down than VT058487-Gal4 driver line (Figure 8C, 8D), suggesting that timing of gene inactivation is critical determinant of the phenotype. Even though the expression of DB331-Gal4 driving line is not restrained to LPTCs, we did not observe strong qualitative changes in the spatial distribution of gap junctions in other regions of optic lobe after the induced inversion of FlpStop cassette (Figure 8A). Therefore, we used LPTC-specific mutant induced by DB331-Gal4 driver line for further physiological studies.

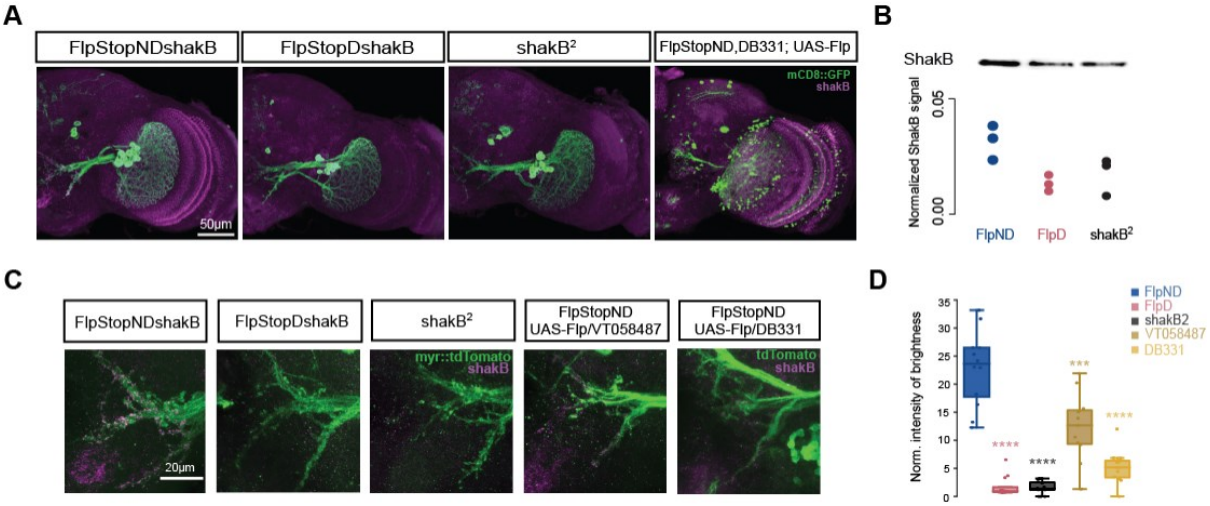

Figure 8. FlpStop cassette reduces the amount of ShakB protein in *Drosophila* brain tissue. A) Immunostainings for the gap junction protein ShakB in the optic lobe of wild type line FlpStopNDshakB and two mutant lines FlpStopDshakB and shakB². B) The western blot analysis of protein extracts from fly brain tissue using antibodies against ShakB. ShakB protein signal was normalized to the total amount of the protein sample per line. C) LPTC axonal staining of ShakB protein in wild-type, full and induced mutant flies. D) Quantification of the ShakB signal in LPTC axons (Mann-Whitney U test, ***p < 0.001, ****p < 0.0001).

Overall, the newly developed FlpStop-based system allows efficient inactivation of ShakB protein. Cell-specific protein inactivation is driver-line-dependent, and can be achieved efficiently by early pupal inversion of FlpStop cassette.

2.3.2 FlpStopDshakB disruptive cassette does not have additional phenotypic effects

Loss of gap junction may severely affect the development of brain tissues (Baker & Macagno, 2014). Therefore, it is crucial to rule out the potential effects of developmental phenotypes to correctly interpret the behavioral phenotypes in FlpStopNDshakB flies.

To account for the potential effects of shakB disruption on the expression of other proteins in the fly brain, we performed the proteomic analysis of brain tissue in FlpStopNDshakB, FlpStopDshakB and shakB^2 flies. Out of 5755 proteins identified, 7 had a different expression between FlpStopDshakB and FlpStopNDshakB flies (Figure S1). In comparison, 41 proteins had a different expression between shakB^2 and FlpStopNDshakB flies, probably due to the distinct genetic background. Proteins Acbp2, Primo-1, and CG31345 were significantly up-regulated in both FlpStopDshakB and shakB^2 flies, indicating their functional connection with ShakB protein.

Gap-junctions were previously shown to be involved in the processes that refine neuronal morphology (Baker & Macagno, 2014) and control the formation of chemical synapses (Todd et al., 2010). To identify potential differences in the morphology of HS cells in wild-type and mutant flies, we fluorescently labelled and imaged individual HS cells using the SPARC technique (Isaacman-Beck et al., 2020). The confocal image stacks were used for 3D reconstructions of neurons, which were then used for the analysis of dendrite morphology. We observed the variability in the dendritic structure of HS cells of the same type within the same genotype, suggesting the intrinsic variability in the morphology of LPTC cells, similar to what was described in other flies (Hausen, 1984). Nevertheless, we did not observe any consistent or significant differences in dendritic branching, area and volume between HS cells in wild-type and mutant flies (Figure S2).

To label postsynaptic partners of HS cells in mutant and wild-type flies we used the trans-Tango technique (Talay et al., 2017). The postsynaptic partners of HS cells were detected in the optic lobe, in the inferior posterior slope, and in the ventral nerve cord (Figure S3). All the postsynaptic partners of HS cells observed in the wild-type were also observed in FlpStopDshakB flies. Meanwhile, the trans-synaptic labelling in shakB^2 flies revealed fewer synaptic partners of HS. Also, the sibling control animals of shakB^2 mutants exhibited higher variability in the overall number of postsynaptic partners than sibling control animals of FlpStopDshakB flies, suggesting the phenotype observed in shakB^2 flies may originate from background mutations (Figure S3).

Altogether, the analysis of brain tissue in FlpStopNDshakB mutant flies suggests that the inactivation of ShakB has little-to-no influence on the proteome and on the morphology of HS cells as well as on the formation of their synaptic connections.

2.3.3 Loss of gap-junctions changes passive membrane properties but not the tuning of direction-selective responses in HS cells

To characterize passive membrane properties and visual responses of HS cells lacking gap-junctions, we used *in vivo* whole-cell patch clamp recordings in tethered flies (Figure 9A). Membrane potential of HS cells in FlpStopDshakB flies displayed spontaneous fluctuations (Figure 9B, 9E), similar to those described in shakB^2 mutant flies (Ammer et al., 2022). Interestingly, while we detected fast β-oscillations of similar frequency band as in shakB^2 (Figure 9F, 9G), we did not observe strongly hyperpolarizing ultraslow waves in FlpStopDshakB flies (Figure 9B). In shakB^2 mutant flies Na_v channels-dependent β-oscillations were suggested to be primary and causal to ultraslow waves that in turn can be mediated via I_h channels (Ammer et al., 2022). Since the molecular mechanism that generates the oscillations in LPTCs lacking gap junctions is not understood, it is not clear why fast oscillations cause slow hyperpolarizing waves in shakB^2, but not in FlpStopDshakB flies.

Importantly, we seldom observed membrane fluctuations in flies with cell-specific inactivation of ShakB in HS cells, suggesting that the reduction of gap junction channels is

insufficient to trigger the membrane oscillations. It is in line with the observation that HS cells after cell-specific inversion of FlpStop cassette still preserved dye-coupling with other LPTCs (Figure S4). Several examples of VS cells that lost the dye-coupling after LPTC-specific inactivation of ShakB exhibited fast membrane oscillations, similar to ones observed in FlpStopD and shakB^2 flies (Figure S4). This observation is in line with the results showing that calcium oscillations in LPTCs from shakB^2 mutant flies persist after the block of all chemical synaptic inputs to these neurons (Ammer et al., 2022). Together these experimental results suggest that membrane fluctuations in HS cells lacking gap junctions are generated via cell-intrinsic mechanisms. However, it cannot be fully excluded that membrane oscillations are additionally reinforced by the synaptic network of LPTCs.

The resting membrane potential of HS cells in the FlpStopDshakB mutant was on average higher in comparison to the wild type, which is consistent with observations made for shakB^2 mutant (Figure 9D).

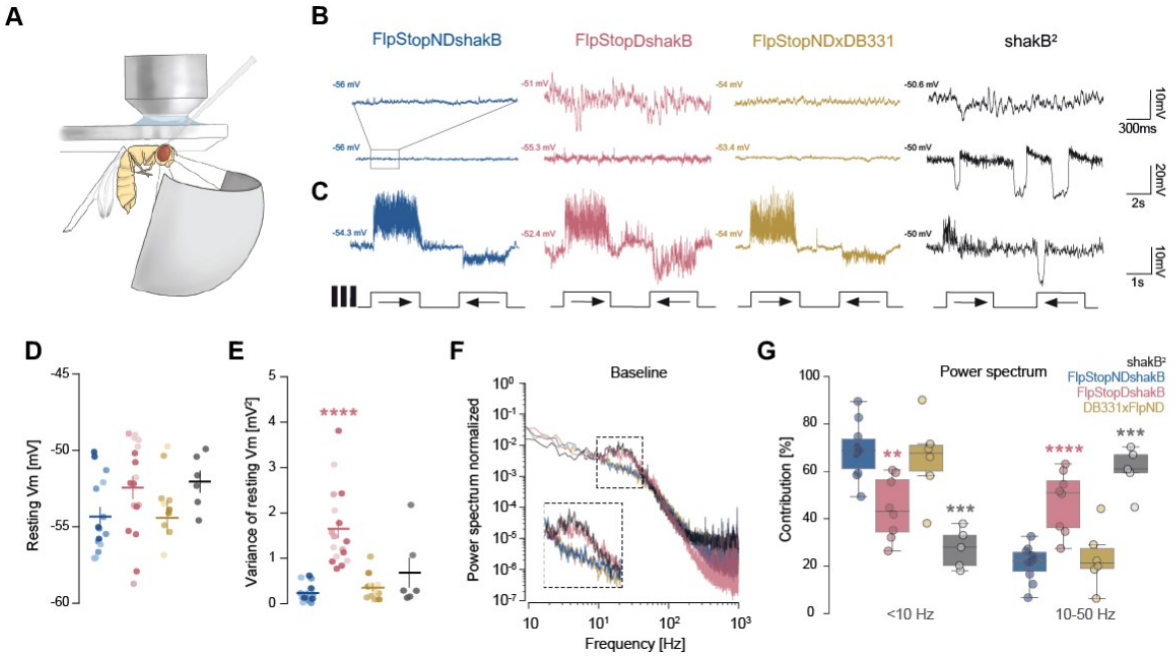

Figure 9. Loss of electrical synapses affects passive membrane properties of HS cells. A) Set-up for *in vivo* whole-cell patch clamp recordings in tethered flies. B) Example traces of membrane potential of HS cells while at rest and C) during direction-selective responses. D) Resting membrane potential of individual HS cells computed for a period of 2s (mean± SEM). The saturation of the color depicts distinct HS types: the highest - HSN, the middle - HSE, the lowest - HSS (distinct cell types were not identified for shakB^2). E) Variance of resting membrane potential computed for a period of 2s (mean± SEM), HS types are depicted as in (D) (Mann-Whitney U test, ****p < 0.0001). F) Normalized power spectrum of baseline membrane potential in HS cells. G) Contributions of low-range (<10 Hz) and mid-range (10-50 Hz) frequencies to the total power (Mann-Whitney U test, ***p < 0.001, ****p < 0.0001).

When presented with full-field flashes, ON-transient responses of HS cells in all animals had similar amplitude, while OFF-transient responses were reduced in FlpStopDshakB flies (Figure 10D). The level of reduction in OFF-transient, however, is smaller than one previously reported for shakB^2 flies; it implies that early stages of visual processing are largely preserved in FlpStopDshakB mutant flies. Even though the amplitude of the transient response to ON-flash is similar across genotypes, the adaptation to bright light happens faster in wild-type FlpStopNDshakB than in FlpStopDshakB flies. Interestingly, HS cells after cell-specific inactivation of ShakB in LPTCs show in-between dynamics of adaptation to bright light,

suggesting that this phenomenon can be cell-intrinsic and not necessarily originating from the upstream visual circuits.

Responses of HS cells to large-field moving gratings suggest that the loss of gap-junctions does not affect the overall direction selectivity of HS cells (Figure 10A). HS cells in FlpStopDshakB mutant flies did not show the reduced amplitude of direction-selective responses, which was previously described for $shakB^2$ flies. On the contrary, we observed enhanced hyperpolarizing responses to gratings moving in null-direction in FlpStopDshakB mutant flies but not in cell-specific DB331xFlpND flies. These results may suggest that strong membrane hyperpolarization in HS cells lacking gap junctions in response to motion in ND is not solely a result of changes of cell-intrinsic properties, but are additionally reinforced by the circuit dynamics within LPTC-network or with other types of neurons.

The enhanced hyperpolarizations, however, were not observed when a drifting dots stimulus was presented instead of gratings (Figure 10B, 10C). Therefore, the enhanced response to motion in null-direction manifests itself only when HS cells receive hyperpolarizing inputs that induce strong instantaneous responses.

It is nonobvious why absence of gap junctions has such a prominent effect on the dynamics of membrane hyperpolarization in HS cells, and not on their membrane depolarization. One of the reasons could be the kinetics of glutamate-activated chloride channels that are implicated in visually-induced hyperpolarizations of LPTCs. Upon a strong presynaptic release of glutamate these channels induce strong transient hyperpolarization followed by a sustained hyperpolarization much weaker in the amplitude (Barbara et al., 2005). While the kinetics of glutamate-activated chloride channels is reflected in the dynamics of hyperpolarization of HS cells in FlpStopNDshakB flies, it is not the case for FlpStopDshakB flies. It can be that change in the passive membrane properties of HS cells lacking gap junctions directly change the kinetics of these channels. Alternatively, the absence of gap junctions can change hyperpolarization-induced membrane processes, such as activation of hyperpolarization-activated cation channels, that regulate cell's excitability. In addition, overexpression of Acyl-CoA-binding protein Acbp2 in the neurons of FlpStopDshakB flies points to some changes in their lipid metabolism. These changes can have direct implications on the dynamics of ionic currents, since some lipids can act as ligands to numerous ion channels, including hyperpolarization-activated cation channels (Hansen, 2015).

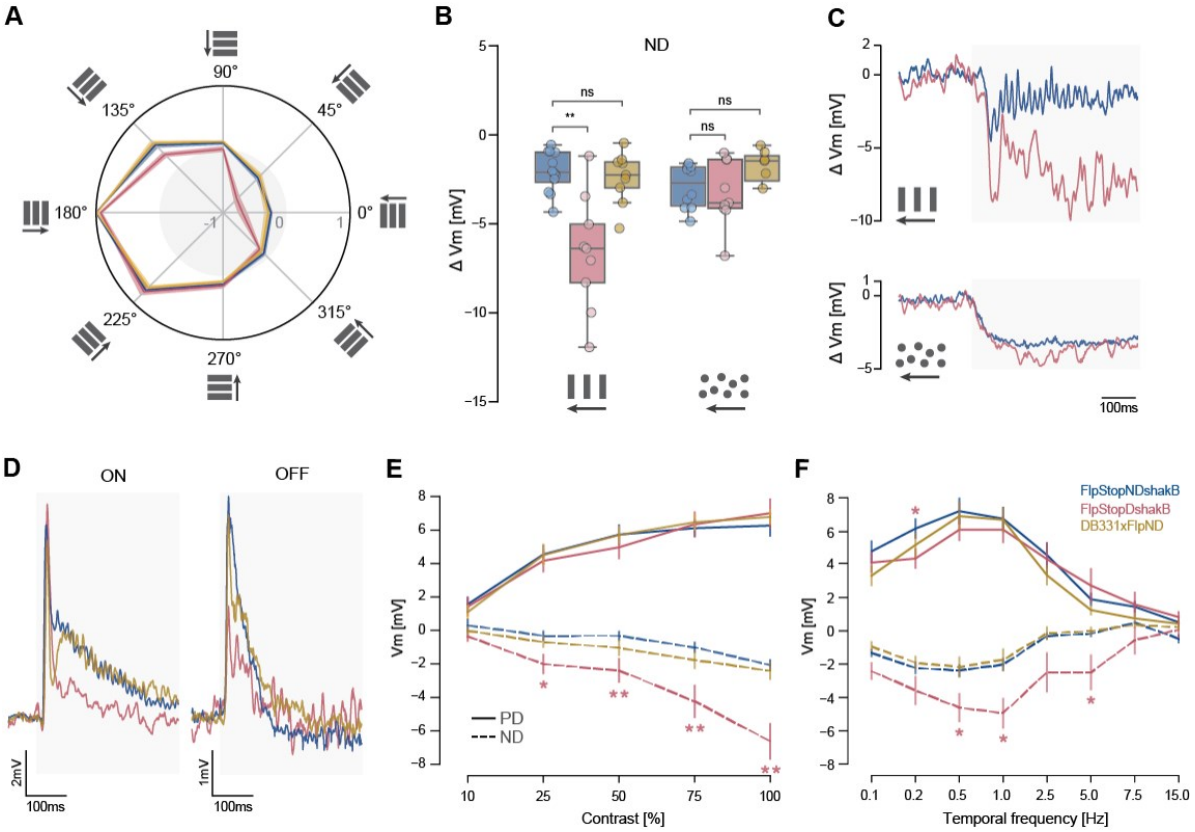

Figure 10. Gap junctions do not influence the tuning of direction-selective responses in HS cell. A) Normalized average voltage changes during 2 s presentation of square-wave gratings moving in 8 different directions (mean±SEM). B) Hyperpolarization of HS cell membrane in response to gratings and drifting dots moving in null direction. C) The transient hyperpolarizing responses differ in response to grating and dot stimuli. D) Average response traces of HS cells during the first 0.5 s after onset of the ON/OFF flash. E) Average responses of HS cells during 2 s of presenting gratings with different contrast moving in PD and ND (1Hz temporal frequency) (mean± SEM). M) Average responses of HS cells during 2 s of presenting gratings moving with different temporal frequency (mean± SEM).
For (B), (E), (F) all the mutant lines were compared to FlpStopND shakB wild-type flies using Mann-Whitney U test, $*p < 0.05$, $**p < 0.01$.

Responses of HS cells to grating patterns moving at 8 different temporal frequencies (velocity/spatial frequency) showed that enhanced hyperpolarizations do not affect the overall velocity tuning of HS cells, the maximum responses for all genotypes being at around 0.5-1Hz (Figure 10F). Similarly, HS in wild-type and mutant flies showed the characteristic increase in the amplitude of response with an increase in grating contrast (Figure 10E). Even though FlpStopDshakB showed enhanced responses to gratings moving in null-direction throughout the contrast range of 25%-100%, the relative increment of response amplitude remains similar across genotypes.

Altogether, the analysis of physiological properties shows that the membrane potential of HS cells in FlpStopDshakB flies exhibits strong fluctuations that do not affect overall direction selectivity in these cells. Nevertheless, the absence of gap junctions increases the amplitude of hyperpolarization in response to grating moving in ND direction. Therefore, the gap junctions primarily influence the hyperpolarizing responses of HS cells in a stimulus-dependent manner.

2.3.4 Lateral connectivity between tangential cells is disrupted in FlpStopDshakB mutants

To visualize electrical coupling, we injected neurobiotin into HS cells, a molecule that can diffuse through gap-junctions. Staining with streptavidin revealed that HS cells in FlpStopNDshakB flies are electrically coupled to each other as well as to postsynaptic interneurons, motoneurons and descending neurons (Figure 11A, 11B), as shown in numerous previous studies (Ammer et al., 2022; Haag et al., 2010; Schnell et al., 2010; Suver et al., 2016; Wertz et al., 2012). We observed strong dye coupling between the three HS cells in the same hemisphere in FlpStopNDshakB flies. HSN cells showed strong coupling with two descending neurons, including DNp15 (DNHS1). Similar to blow flies, HS cells form gap junctions with neck motoneurons. We observed that HSN, together with HSE, neurons form electrical connections with VCNM-like neurons (Ventral Cervical Nerve Motor Neuron), and HSS cells form electrical synapses with CNM-like neurons (Cervical Nerve Motor Neuron).

FlpStopDshakB mutant flies, showed little to no dye coupling between ipsilateral HS cells, indicating that axo-axonal gap junctions between HS neurons are absent or severely perturbed (Figure 10D, 10E). We also observed coupling of HS cells with ipsilateral LPTCs of another type, presumably CH cells. These connections as well were largely abolished in FlpStopDshakB mutant flies.

While connections between LPTCs in FlpStopDshakB mutant flies were abolished, electrical coupling between HS cells and postsynaptic neurons were largely preserved. This suggests that gap junctions formed between HS cells and postsynaptic neurons differ molecularly from those formed between LPTCs, and are likely to be composed of undisrupted ShakB isoforms or of other innexins. Interestingly, HS cells in $shakB^2$ mutant flies do not show any dye coupling (Ammer et al., 2022), which can suggest an involvement of shakB-PF isoform in refining electrical coupling in LPTCs.

Apart from ipsilateral electrical coupling, HS cells were observed to form extensive connections with the contralateral hemisphere. We observed that all three HS neurons were coupled to bilateral neurons in the inferior posterior slope (IPSN), that form a bridge between the tangential cells of the two hemispheres. This coupling is maintained in FlpStopDshakB mutant flies. We observed dye coupling between HSS and contralateral VS2 and VS3 neurons. This coupling was reported in blow flies, where it is mediated via the neck motor neuron CNMN (Cervical Nerve Motor Neuron) (Wertz et al., 2012). It indicates that in *Drosophila*, similar to blow flies, output of HSS and contralateral VS2 and VS3 neurons are combined in CNMN. HSE cells form electrical synapse with contralateral tangential cells H2. This connection was extensively characterized in blow flies, and was suggested to be involved in the integration of horizontal motion coming from two eyes (Farrow at al., 2006). H2-HSE connection is substantially weakened in FlpStopDshakB mutant flies, which can affect the binocular integration of horizontal visual motion.

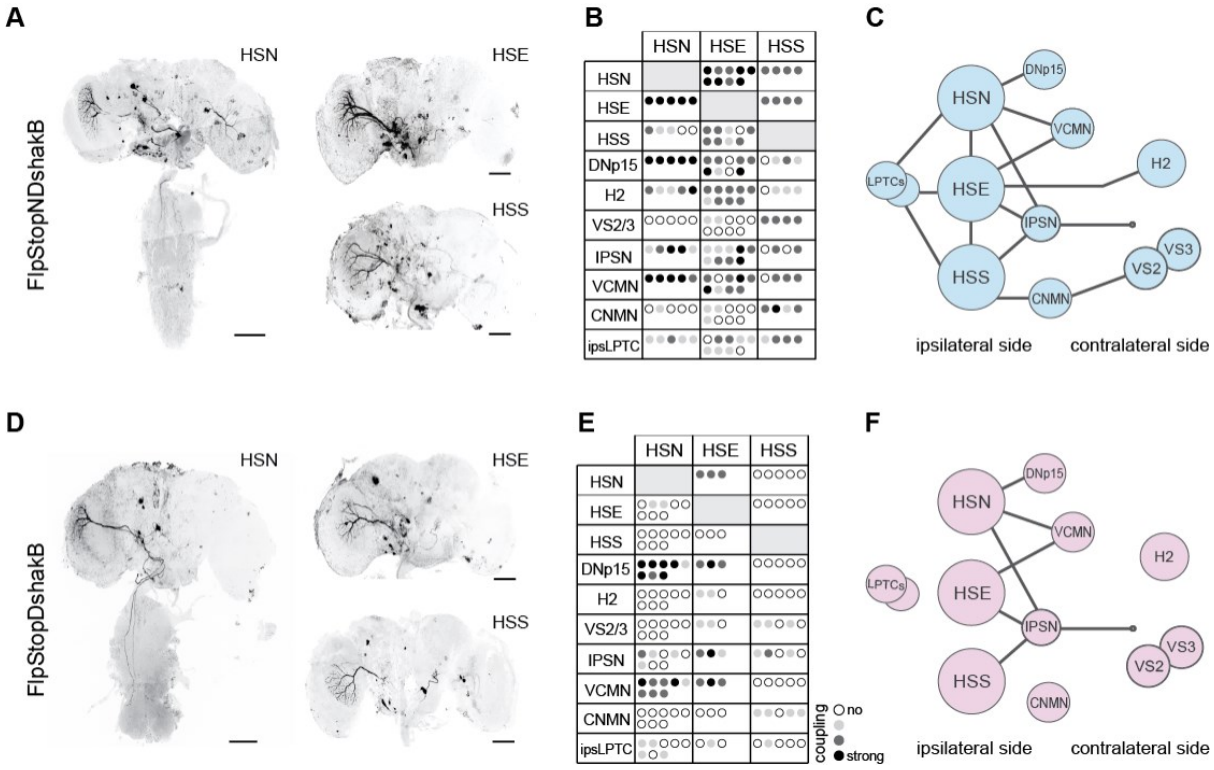

Figure 11. Neurobiotin coupling is significantly abolished in FlpStopDshakB mutant flies. A) Example of neurobiotin injection stained with streptavidin-Alexa488 in individual HS cells in FlpStopNDshakB flies (scale bar 50 μm). B) Identified electrical synaptic partners of HSN, HSE and HSS cells in FlpStopNDshakB flies. C) Schematic of electrical coupling in HS-network in FlpStopNDshakB flies. D) Same as A) for FlpStopDshakB flies. E) Same as B) for FlpStopDshakB flies. F) Same as C) for FlpStopDshakB flies.

Overall, the neurobiotin injections into HS cells reveal significant reduction in the strength of their electrical coupling in FlpStopDshakB mutant flies (Figure 11C, 11F). The reduction prevails for connections between LPTCs, and not for HS connection with postsynaptic interneurons, descending neurons, and motoneurons, making FlpStopDshakB mutant more advantageous for behavioral studies.

2.3.5 Gap-junctions improve motion estimation in noisy conditions

As it was mentioned, lateral electrical coupling between HS cells is absent in FlpStopDshakB mutant flies. However, the absence of gap-junctions in HS cells does not change the direction selectivity of these neurons when tested using full-field square-wave gratings. Despite being widely used to study fly motion circuits, this stimulus does not reflect the statistics of natural stimuli and triggers strong saturating responses in HS cells. Using this stimulus, therefore, can mask subtle effects that gap-junctions may have on the discrimination of motion cues. To address the role of electrical coupling in the discrimination of motion cues under more naturalistic visual conditions, we developed a stimulus consisting of a field of drifting dots, contaminated with an increasing amount of visual noise (Figure 12A). More precisely, dots with size 10° and 100% contrast were moving in PD and ND of HS neurons fully coherently or with 10%, 20%, 30%, 40%, 50%, 75% of the total amount of dots moving in random directions.

The amplitude of direction HS selective responses in both FlpStopNDshakB and FlpStopDshakB gradually decreased with the amount of noise present in the stimulus (Figure 12B).

While FlpStopDshakB showed weaker responses to dots moving in PD, the overall dynamics of the response drop were similar for both genotypes.

To quantify how well HS cells, discriminate motion in noisy conditions, we analyzed the distributions of membrane potentials during stimulus presentation in PD and ND, and computed the ROC curve for each pair of distributions. The closer the ROC curve gets to the top-left corner, the better the ability of the neuron to classify PD and ND direction, and therefore to discriminate visual motion. ROC curves for three pairs of PD-ND response distributions of HS cells in FlpStopNDshakB and FlpStopDshakB flies are shown on Figure 12C.

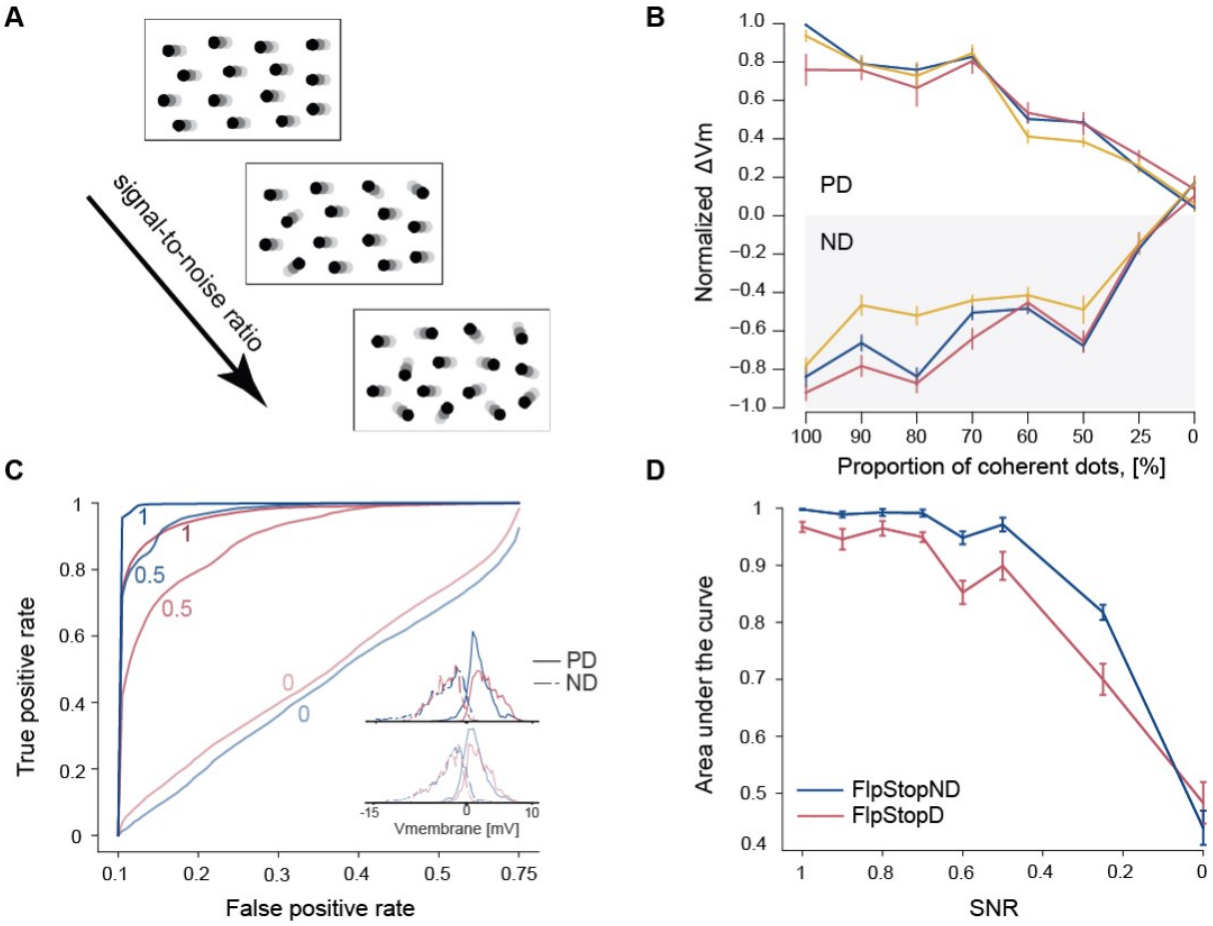

Figure 12. Gap junctions between HS cells improve motion discrimination in naturalistic conditions. A) The schematic of the stimulus used to test the motion discrimination in HS cells in noisy conditions. B) Averaged normalized changes of HS membrane potential in response to drifting dots with increasing proportion of noise. C) ROC curved for three values of signal-to-noise ratio, and average distributions of HS Vm throughout the stimulus for 100% and 50% of dots moving coherently for two genotypes. D) AUC for 8 different values of signal-to-noise ratio for two genotypes.

To summarize the performance of HS cells in wild-type and mutant flies throughout the whole stimulus, we computed the area under the ROC curve for each ratio of signal to noise (Figure 12D). The analysis showed that HS cells lacking gap-junctions discriminated motion signals less accurately than HS cells in the wild-type animals throughout the whole spectrum of the noise level. Interestingly, the differences in performance of HS with and without gap-junctions were observed even for the visual stimulus with purely coherent motion. However, this difference increased with the presence of noise, reaching a maximum of 40–100% noise ratio.

Altogether, the present analysis suggests that the loss of gap-junctions compromises the ability of HS cells to discriminate visual motion in ambiguous and noisy visual environments.

2.3.6 Spatial receptive fields of HS cells reflect their electrical connectivity

The motion sensitivity of HS cells is not fully determined by local motion inputs coming from T4 and T5 cells but also by lateral interactions with other tangential cells. Therefore, the structure of receptive fields in these neurons can provide information about their connectivity. In order to assess the influence of gap-junctions on local directional tuning, we recorded motion responses of HS cells in FlpStopNDshakB and FlpStopDshakB flies to a local stimulus scanning the visual field in four cardinal directions. This way we could identify preferred local direction and local motion sensitivity of individual HS cells across the fly's bilateral visual field (140° in azimuth and 80° in elevation). The size and dorsally displaced positioning of the screen did not allow us to resolve the receptive fields of HSS cells. Therefore, only HSN and HSE cells were considered for detailed analysis.

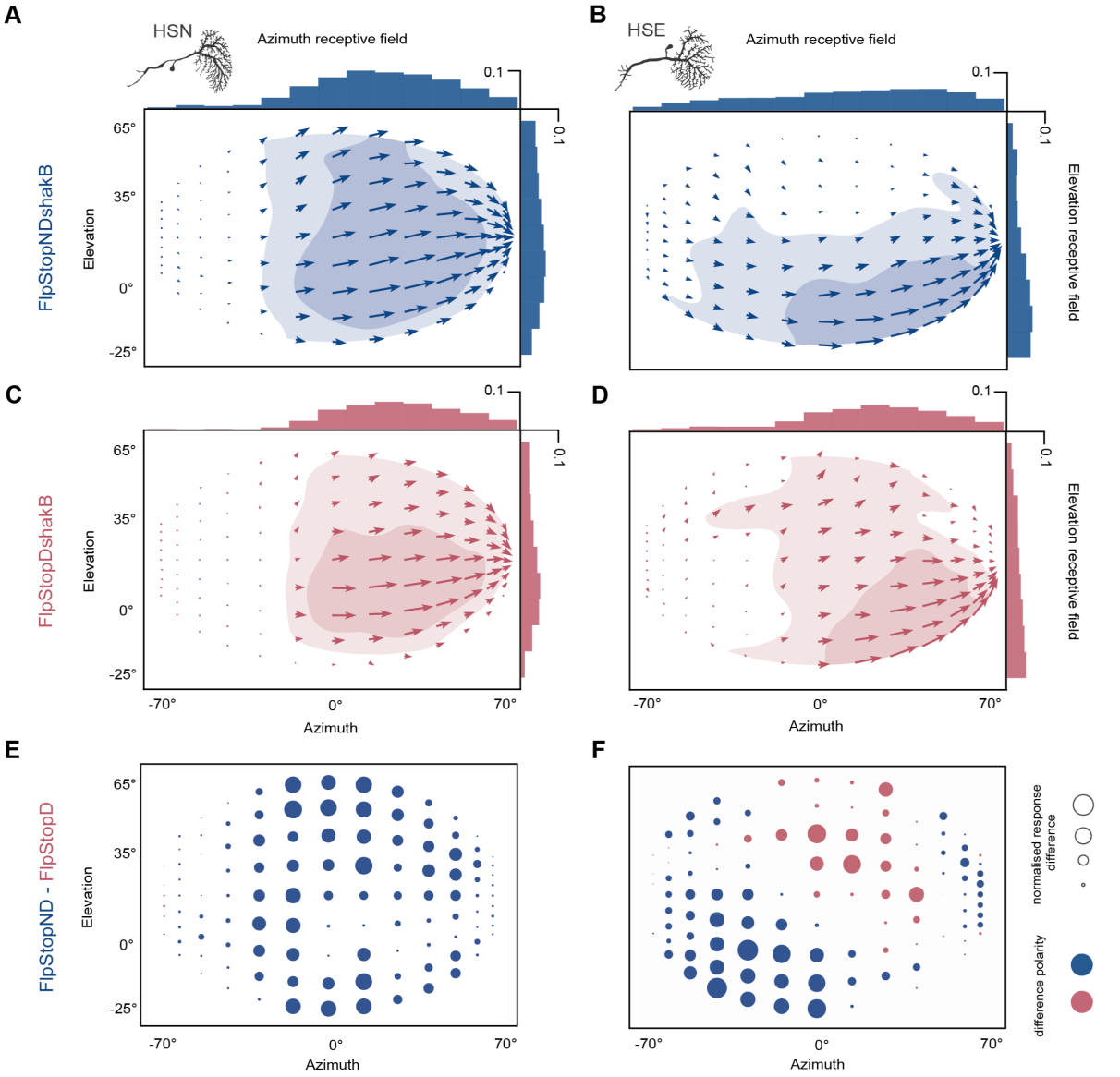

Figure 13. Loss of gap junctions changes the structure of spatial receptive fields in HS cells. Spatial receptive fields reconstructed from the responses to local motion stimulus (see description in the text) and the distribution of the local motion sensitivity along the azimuth and elevation (computed as sum of all response vectors at a given elevation or azimuth) for A) HSN and B) HSE cells in FlpStopNDshakB wild type flies, and C) HSN and D) HSE cells in FlpStopDshakB mutant flies. Light-shaded areas represent 30% and dark-shaded 60% of the maximal strength of the response for each cell type. E) Differences in the amplitude of motion responses in HSN cells and F) HSE cells

between FlpStopNDshakB and FlpStopDshakB flies across the recorded visual area. The size of the circle depicts the magnitude of the response difference, and the color represents polarity with blue circles showing stronger responses in FlpStopNDshakB flies and pink in FlpStopDshakB flies.

Spatial receptive fields of HSN and HSE cells in wild-type and mutant flies are shown on Figure 13A and 13B as vector fields. The root of each arrow corresponds to a specific azimuth and elevation in the visual field of the fly, the direction represents preferred local direction and the length indicates the relative strength of response. In FlpStopNDshakB wild type flies, as expected, the response fields of HS cells, on average, are aligned horizontally. As expected, in FlpStopNDshakB wild type flies the response fields of HS cells, on average, are aligned horizontally. For HSN cells, purely horizontally-aligned response fields were observed mostly in the equatorial region, while in the fronto-dorsal area preferred local directions were tilted upward. The maximum of direction-selective responses of HSE cells was shifted ventrally in comparison to HSN cells, corresponding to their dendritic arborizations. These features of HS receptive fields are consistent with what was shown before in both blow flies and *Drosophila* (Krapp et al., 1998; Schnell et al., 2010).

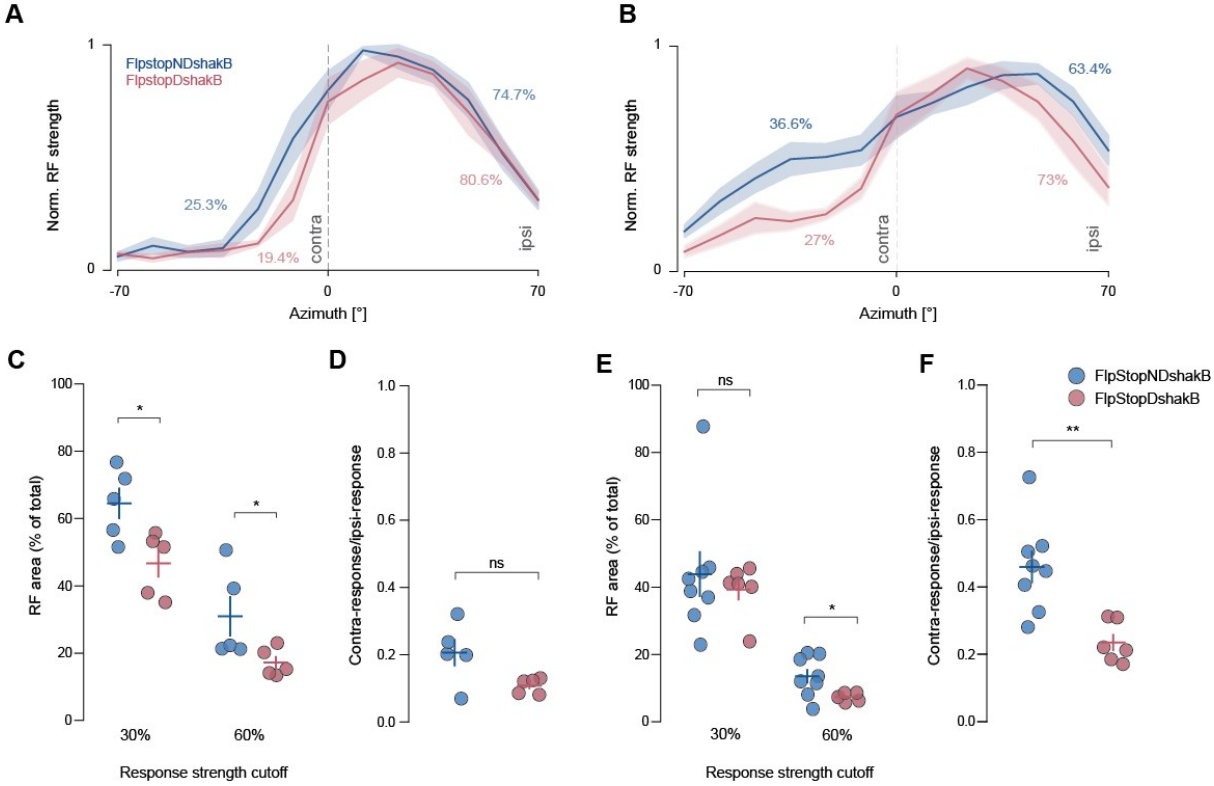

Figure 14. Loss of gap junctions causes the reduction in the overall size of RF in HSN cells and sensitivity to the contralateral motion in HSE cells. A) Normalized strength of responses of HSN neurons across the azimuth (computed as a sum of all response vectors across elevations at a particular azimuth). B) Same as C, for HSE cells. C) Size of the receptive field (computed by applying cutoffs of 30% and 60% of the maximal strength of the response) as a proportion of the total recorded visual field for HSN cells in FlpStopNDshakB and FlpStopDshakB flies (mean± SEM). D) Ratio of the amplitude of visual responses (computed as the sum of all the response vectors) to motion in the contralateral visual field and ipsilateral visual field (mean± SEM). E) Same as in (C), for HSE cells. F) Same as in (D), for HSE cells.
For (C-F) Mann-Whitney U test was applied, $*p < 0.05$, $**p < 0.01$.

Both types of HS cells showed sensitivity to local back-to-front motion in the contralateral visual field, which comprised on average 25.3% of the total sensitivity of HSN cells and 36.6% of HSE cells (Figure 14A, 14B). The motion sensitivity of HSE cells was detected along the entire span of measured azimuth (-70° to 70°), with local preferred directions tilted downward in the

fronto-lateral region around an azimuth of -30° to -50°. This complex structure of local motion sensitivity in the contralateral side is mediated by heterolateral elements connected to HS cells.

In FlpStopDshakB mutant flies, spatial receptive fields of both HSN and HSE cells were significantly reduced (Figure 13C, 13D; Figure 14C, 14E). While strong responses to ipsilateral horizontal motion along the equator were largely preserved in both HSN and HSE cells, HSN cells showed reduced responses in the fronto-dorsal and ventral areas, and HSE cells lost sensitivity to the motion in the contralateral field (Figure 13E, 13F; Figure 14D, 14F). These changes suggest that motion sensitivity in these areas is a result of lateral interactions of HS with other tangential cells: mostly horizontal-motion-sensitive ipsilateral neurons for HSN cells, and contralateral horizontal-motion-sensitive neurons for HSE cells. Interestingly, direction-selective responses of HSE cells in mutant flies were enhanced in the fronto-dorsal area, suggesting a potential role of gap junction-mediated inhibitory inputs in shaping the receptive fields of these cells.

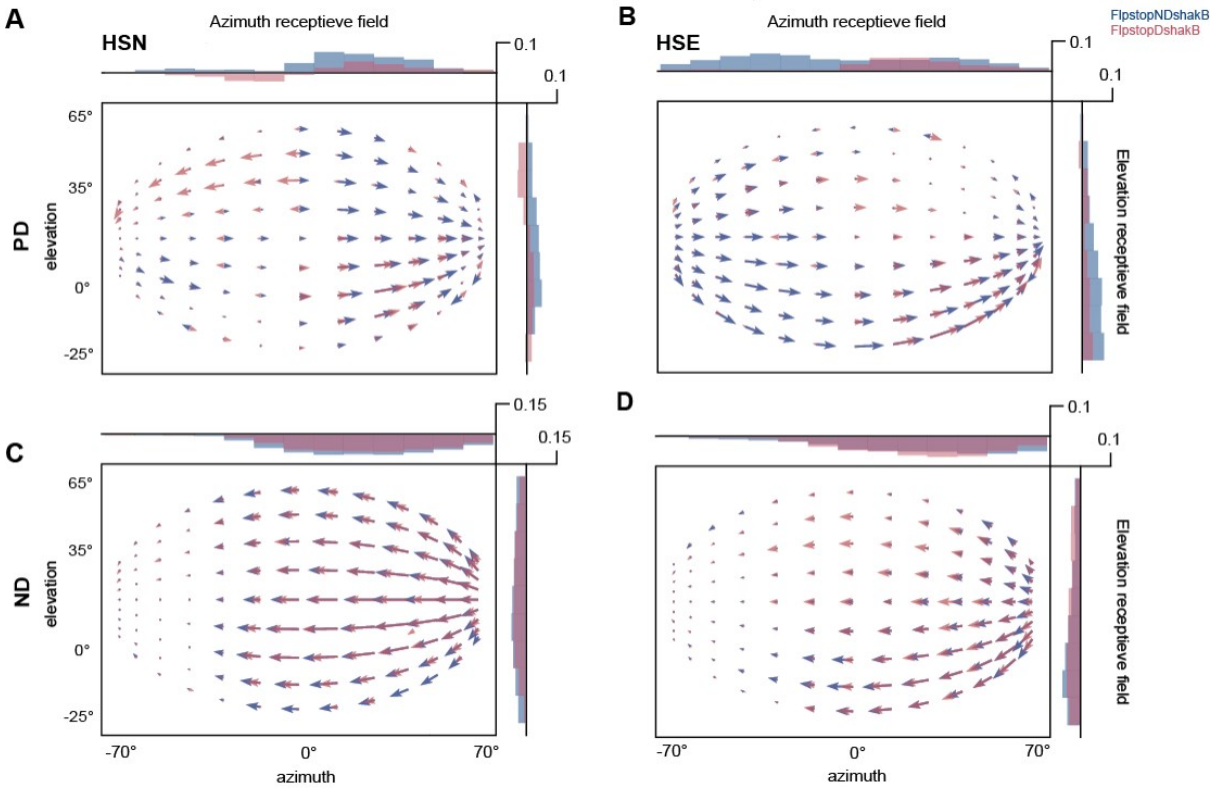

Figure 15. Changes in the structure of RFs of HS cells in FlpStopNDshakB mutant flies are mostly caused by changes in their responses to local motion in PD. The pattern of local motion sensitivity of A) HSN cells and B) HSE cells in FlpStopNDshakB and FlpStopDshakB flies to PD motion, and the distributions of the sensitivity to local PD motion along azimuth and elevation. C) Same as (A) but for local motion in ND. D) Same as (B) but for local motion in ND. The vectors for PD and ND receptive fields were normalized to the maximal amplitude across receptive field for each cell of a particular genotype.

While the distribution of responses of HSN and HSE cells to local motion in ND were similar in FlpStopNDshakB and FlpStopDshakB flies, responses to PD differed substantially (Figure 15). Therefore, described changes in the overall structure of receptive fields of HS cells in FlpStopDshakB flies are largely explained by their responses to local motion in ND.

HS cells in DB331xFlpND flies did not show changes in the pattern of their receptive fields similar to ones observed for FlpStopDshakB flies (Figure S4). This result is in line with the pattern of dye coupling that shows gap junctional connections of HS cells being largely unaffected after LPTC-specific inactivation of ShakB despite an apparent reduction of protein amount in LPTC terminals.

Altogether, the analysis of local motion sensitivities in HS cells suggests the reduced size of spatial receptive fields in HS cells lacking gap junctions. It confirms that lateral interactions between LPTC refine the structure of receptive fields in these neurons, and improve their tuning to a certain pattern of the optic flow. Specifically, HSE neurons acquire back-to-front motion sensitivity in the contralateral area through a direct electrical coupling with contralateral horizontal-motion-sensitive neurons. This way binocular interaction enhances yaw-rotation tuning in HS neurons.

2.3.7 ShakB mutant flies show altered responses to binocular optic-flow patterns

To check if the described changes in connectivity and response properties of tangential cells influence the accurate integration of visual motion cues, we studied visually-guided locomotion in wild-type and mutant flies. More precisely, we compared the behavior of FlpStopNDshakB fly to the FlpStopDshakB mutant fly for unilateral front-to-back, unilateral back-to-front and full-field rotation. Freely walking flies were shown a sinusoidal grating pattern, on the roof of the arena, where each half could be rotated independently (Figure 16A). FlpStopNDshakB wild-type flies and FlpStopDshakB mutant flies did not show locomotion biases when the stimulus was not rotating (Figure 17B), and showed strong optomotor responses to full-field rotation of the pinwheel (Figure 16B). The optomotor response in both genotypes was weaker to the stimulus of lower contrast. Interestingly, the dynamics of the response changed with the decrease in the contrast of the stimulus (Figure 16C).

The wild-type flies displayed a robust turning response to all three stimuli. They turned in the same direction as the pinwheel for back-to-front and full-field motion, as expected, but turned opposite to the motion of the pinwheel for front-to-back motion (Figure 16D, 16E). To our knowledge, this behavior has not been described in prior studies and suggests that the fly visual system does not perceive back-to-front and front-to-back stimuli as simple antagonistic motions. Additionally, we found that the dynamics of the two responses were also very distinct, with the front-to-back response being slow and steady whereas the back-to-front response is sharp and transient (Figure 16E). The response to full-field motion followed a similar dynamic as the back-to-front response except the decay in the response was much more gradual. A closer analysis of the behavior of the animal showed that the response to front-to-back motion is a combination of smooth turning interspersed with lots of anti-saccades (saccades opposed to the motion), reminiscent of the optokinetic nystagmus in mammals.

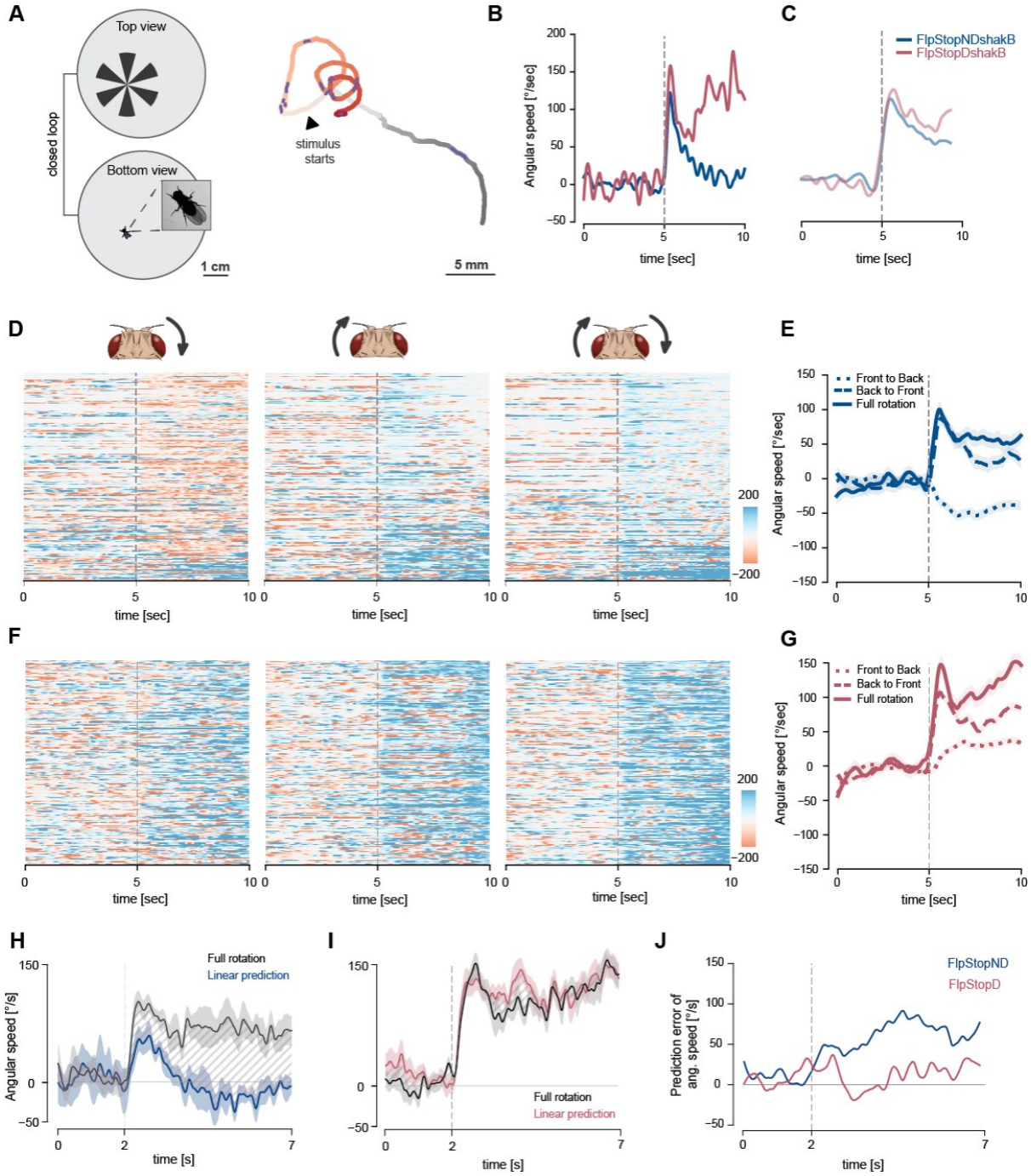

Figure 16. Gap junctions mediate integration of motion information from the two eyes. A) *left* Schematic of pinwheel stimulus presentation (top view, not to scale); *right* trajectory of a fly in the arena during an experimental session with multiple trials; *inset* trajectory across one trial (10s) with pinwheel rotating in clockwise direction. B) Mean angular speed for full rotation under open loop conditions with temporal frequency 10 Hz and 100% contrast as a function of trial duration. Dashed line shows the beginning of the stimulus rotation. C) Same as in B, for pinwheel with 25% contrast. D) Angular speed raster for a random subset of trials from multiple flies for three stimulus conditions: - front to back, back to front, full rotation (*left to right*) under closed loop condition. Each row corresponds to one trial and each column to one frame (~16 ms). Dashed line shows the beginning of the stimulus rotation. E) Mean angular speed across a trial for the three stimulus conditions corresponding to D (mean ± SEM [shaded region]). Dashed line shows the beginning of the stimulus rotation. F) Same as D for FlpStopDshakB flies. G) Same as (E) but for FlpStopDshakB flies. H) Mean angular speed of FlpStopNDshakB flies in response the full rotation stimulus vs the sum of responses to back-to-front and front-to-back stimuli. I) Same as (H) but for FlpStopDshakB flies. J) The difference in angular speed between responses to full rotation stimulus and the sum of responses to back-to-front and front-to-back stimuli for FlpStopNDshakB and FlpStopDshakB flies.

Finally, the optomotor response of the fly was not integrated linearly across space. For linear integration, the average turning response to full-field rotation across many flies and multiple trials, is expected to be a sum of unilateral front-to-back and back-to-front responses which was not the case for wild type flies.

FlpStopDshakB mutant flies, strikingly, did not turn opposite to the motion of the front-to-back stimulus (Figure 16F, 16G). This was primarily due to a reduction in anti-saccades, that were observed in wild-type flies (Figure 17A, 17C, 17D), and will be discussed in more details in the Chapter 4.

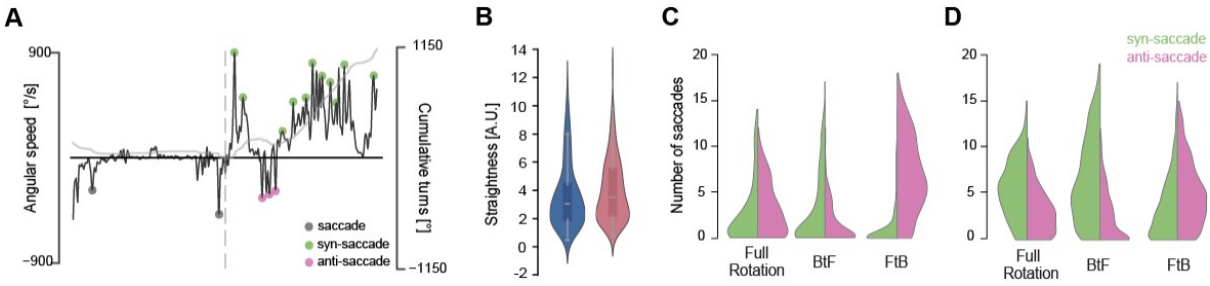

Figure 17. Anti-optomotor responses are primarily mediated by anti-saccades. A) An example of extracted saccades through a single presentation of a full rotation stimulus; dashed line indicates the onset of the stimulus. B) Mean path straightness of walking bouts with rotating pinwheel across all trials for FlpStopDshakB and FlpStopNDshakB flies. C) Distribution of the number of syn- and anti-saccades per each 5s stimulus period in FlpStopNDshakB flies. D) Same as (C) but for FlpStopDshakB flies.

Contrary to wild-type flies, the average turning response to full-field rotation for FlpStopDshakB mutant flies was a simple summation of the unilateral back-to-front and front-to-back responses (Figure 16H-J). This pattern of behavior was similar for shakB^2 flies, suggesting that regardless of the discrepancies at a physiological level, the two mutants of gap-junctions demonstrate similar changes in responses to unilateral front-to-back rotation.

We also observed a clear difference in the dynamics of the response to full-field rotation. While the turning response for mutant flies was sustained for the period of the trial (5s), for wild-type flies, there was a clear decay after the initial response (Figure 16E). This was accompanied by an increase in the probability of anti-saccades over the period of the trial. Interestingly, the response became increasingly sustained, for wild-type flies, as the contrast of the stimulus was decreased (Figure 16C).

Overall, the behavioral results indicate that the removal of gap-junctions from the LPTC network alters the interpretation of motion vision cues, even though the classical optomotor response to full-field rotation remains intact. This is manifested in a striking reversal in behavior of the animal to front-to-back motion suggesting that electrical synapses are crucial for optic-flow-based course control. In addition, these results point to an importance of saccades, along the smooth pursuit, in shaping the dynamics of optomotor response.

Supplementary data 1

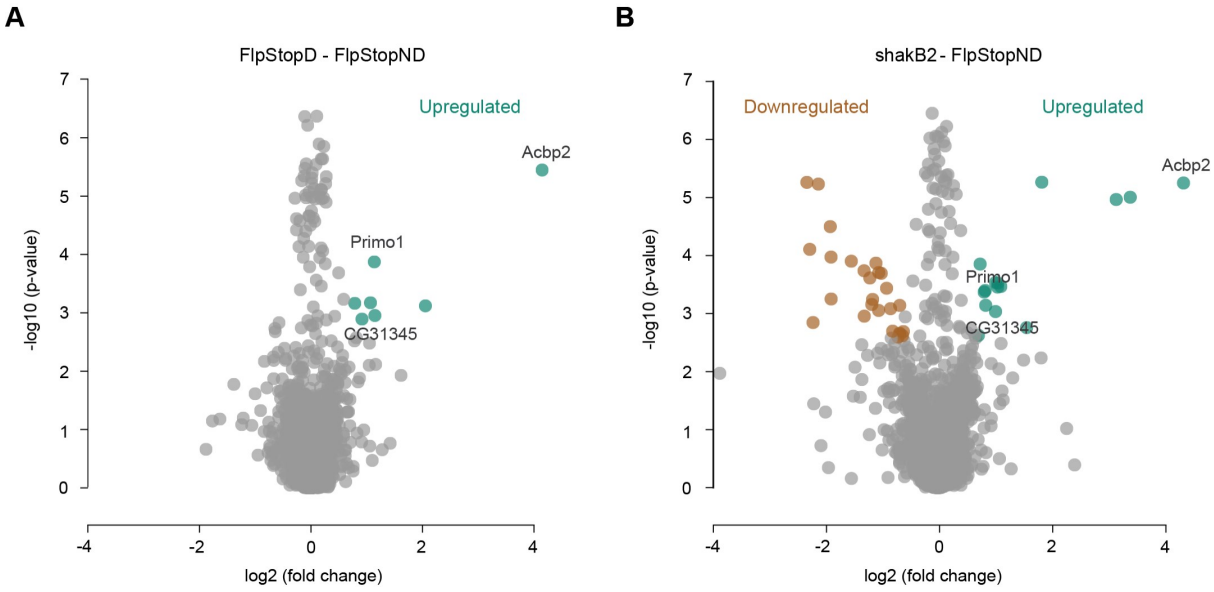

Figure S1. Proteomic analysis of FlpStopDshakB and shakB^2 mutant brains. Total protein lysates obtained from fly brains were analyzed through liquid chromatography mass spectrometry (LC-MS). A) Protein level quantification (fold change) and statistical significance assessment (p-value) for FlpStopDshakB mutant model were performed against FlpStopNDshakB control flies. Proteins that showed significant changes in expression levels are depicted in brown (down-regulated) and green (up-regulated). B) The same for shakB^2 mutant model.

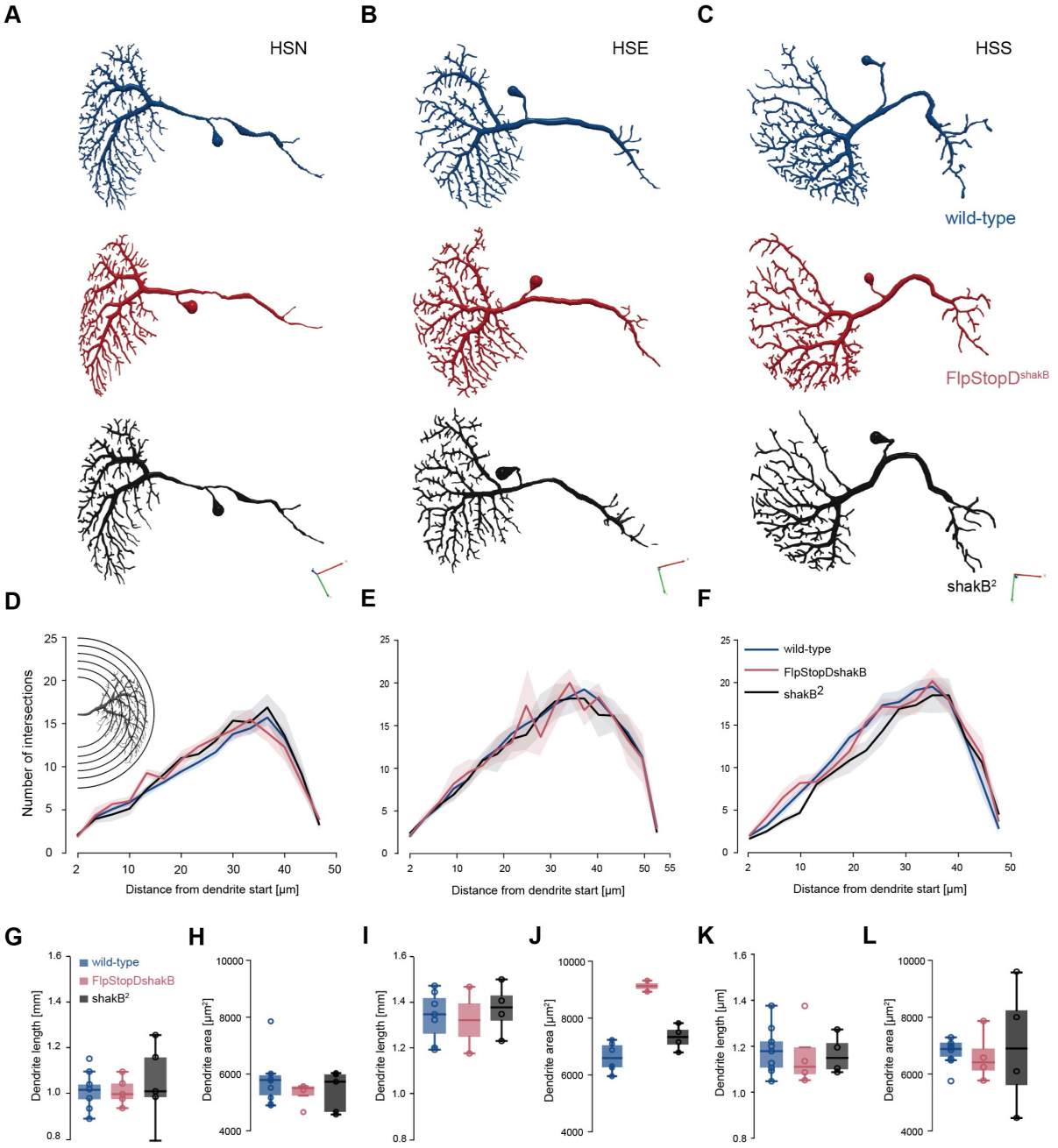

Figure S2. Loss of gap junctions does not affect the morphology of dendrites in HS cells. (A-C) Examples of reconstructed HSN, HSE and HSS cells for every genotype. (D-F) Sholl intersection profile of HS dendrites in the wild type and two mutant lines (mean± SEM). The number of intersections for each HS type was equalized between genotypes. (G, I, K) Total length of HSN, HSE and HSS dendrites in the wild type and two mutant lines. (H, J, L) Dendritic field area for HSN, HSE and HSS in the wild type and two mutant lines.

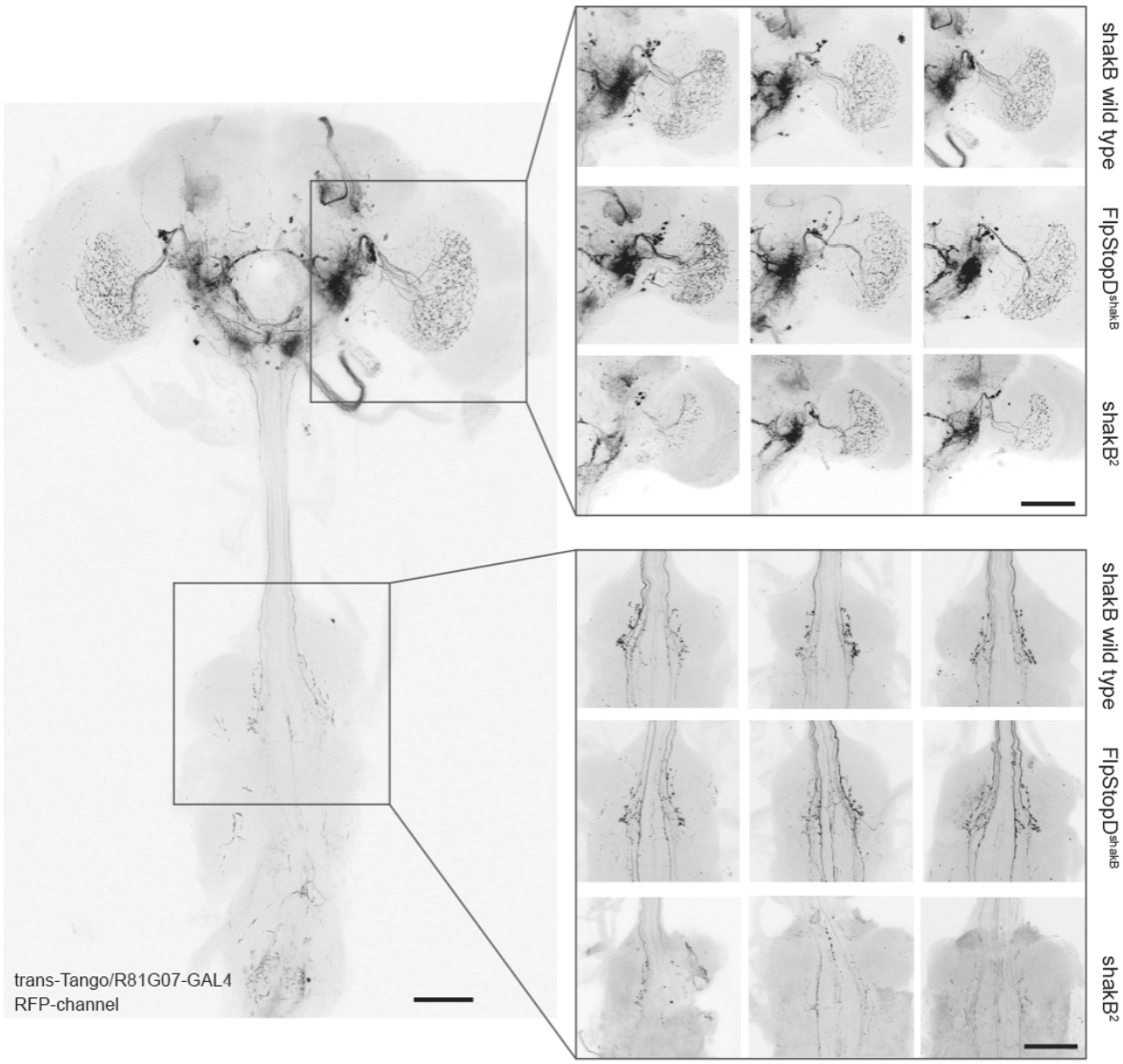

Figure S3. Trans-synaptic labelling does not reveal the loss of chemical postsynaptic partners of HS cells in FlpStopDshakB flies. The examples of trans-Tango-mediated labelling of HS postsynaptic partners: while FlpStopDshakB does not differ from FlpStopNDshakB wild-type flies, shakB^{2} flies demonstrate weaker connections with postsynaptic partners (scale bar 50 μm).

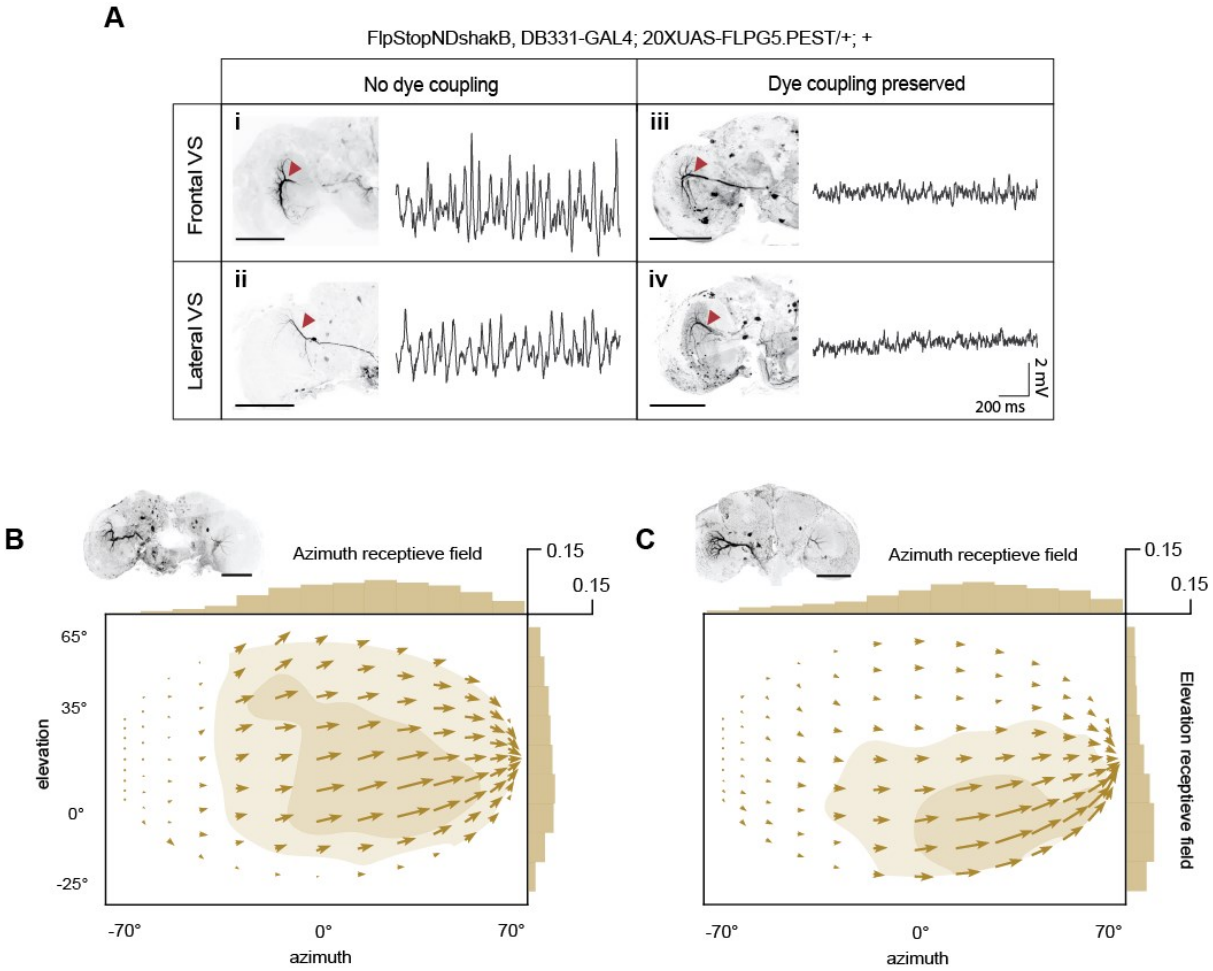

Figure S4. Cell-specific inactivation of gap junctions in LPTCs does not change spatial receptive fields of HS cells. A) Fast membrane oscillations of LPTCs are cell-intrinsic. Example traces of membrane potential and neurobiotin coupling of VS cells in flies with LPTC-specific inactivation of ShakB protein. In contrast to VS cells preserving neurobiotin coupling (iii, iv), VS cells lacking neurobiotin coupling with other LPTC cells (i, ii) exhibit fast membrane fluctuations (scale bar 50 μm, red triangle indicates injected/recorded cell). B) Spatial receptive fields reconstructed from the responses to local motion stimulus and the distribution of the local motion sensitivity along the azimuth and elevation of HSN cells in flies with induced inversion of FlpStop-cassette in LPTCs (FlpStopNDshakB, DB331-GAL4; UAS-Flp/+;+). Light-shaded areas represent 30% and dark-shaded 60% of the maximal strength of the response for each cell type. C) Same as (B) but for HSE cells.

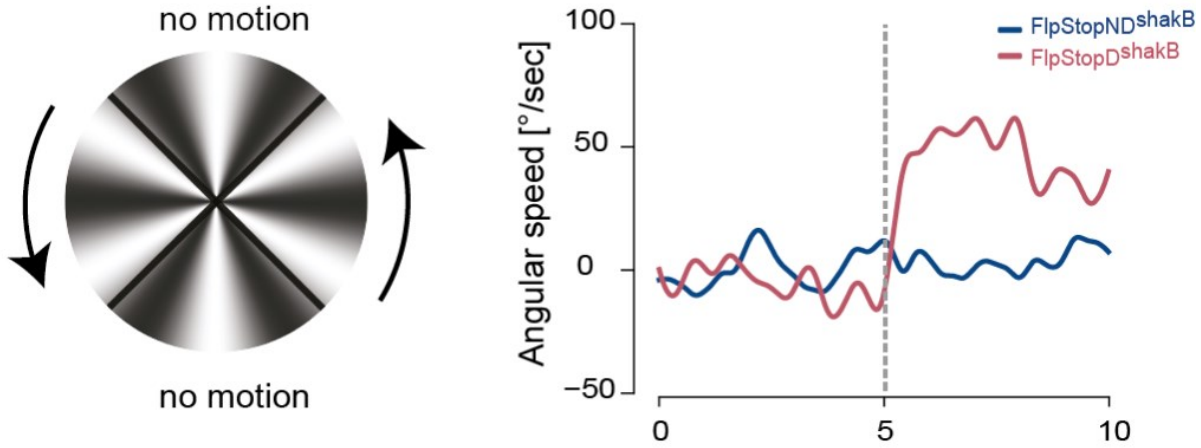

Figure S5. FlpStopDshakB flies, but not FlpStopNDshakB flies, respond to a lateral rotational stimulus. Mean angular speed for lateral CCW rotation of pinwheel gratings with temporal frequency 10 Hz and 100% contrast as a function of trial duration. Dashed line shows the beginning of the stimulus rotation.

Chapter 3
Genetic mosaic approach for mapping neural substrates of fly course control

3.1 Introduction

As described in previous chapters, LPTCs directly instruct optic-flow-based course control in flies. These cells, each having unique physiological and morphological properties, do not operate in isolation. Instead, they form multiple subnetworks which mediate distinct steering maneuvers in response to different optic flows. Even though we do not know how exactly these subnetworks operate, we can make some predictions based on the studies of neuronal activity and connectivity within the LPTC network. For instance, a subnetwork of VS cells is thought to mediate roll-induced compensatory responses, and HS cells mediate stabilizing yaw turns.

Despite these well-reasoned predictions, a direct link between neuronal activity in LPTCs and fly behavior still hasn't been made. This can be attributed to the limitations of existing tools for mapping neuronal substrates of behavior in flies, such as GAL4-UAS controlled neuronal silencing and optogenetics. These methods induce strong homogeneous effects in a large population of neurons. LPTCs, however, are largely heterogeneous and their behavioral role cannot be addressed by uniform bihemispheric neuronal activation or silencing. Indeed, unilateral optogenetic and chemogenetic activation of HS-cells in *Drosophila* were shown to evoke directed head movement and flight turns, suggesting that spatial distribution of neuronal activity within the LPTC network defines the behavioral output. However, only a limited amount of stabilizing behaviors can be instructed by unilateral activity of tangential cells. To address these shortcomings, I developed a system for stochastic manipulation of neuronal activity. This strategy enables generation of numerous distinct patterns of neuronal activity within the LPTC network, each potentially driving distinct behavioral commands.

To achieve stochastic manipulation of neuronal activity, I employed a genetic mosaic approach, based on the SPARC method. I further expanded the toolkit by creating transgenic lines that enable 1) simultaneous optogenetic activation and inhibition, and 2) sparse neuronal inactivation. In this chapter, I will present characterization of the newly developed tools for stochastic neuronal manipulation, and will demonstrate that their application can help to unravel the complexity of behavioral commands instructed by the LPTC network.

3.2 Methods

3.2.1 Generation of transgenic animals

To generate plasmid for the assembly of SPARC cassette, we cloned the construct containing attB and two attP sites separated by MCS into pJFRC7-20XUAS-IVS-mCD8::GFP plasmid (Addgene #26220), replacing the mCD8::GFP insert, to obtain pJFRC7-20XUAS-IVS-SPARC plasmid. We used two wild-type attP sites for optogenetic cassette to obtain an even distribution of effectors, and attP38/wild-type attP sites for Kir2.1 effector to get a sparse neuronal inactivation. csChrimson::tdTomato was amplified from plasmid 5XUAS-IVS-CsChrimson tdtomato_tr (Addgene #111545), GtACR1::eYFP - from plasmid pUC57-dGtACR1::eYFP (Adam Claridge-Chang laboratory) and Kir2.1::eGFP (KCNJ2) - from genomic DNA of the following flies: *w[*]; P{w[+mC]=UAS-Hsap\KCNJ2.EGFP}1* (BDSC 6596). The effector genes were clones into pJFRC7-20XUAS-IVS-SPARC plasmid. The SPARC cassette with the promoter was amplified and cloned into pHD-3XP3-dsRed-DattP-CRISPR-donor-attP40 donor plasmid (Addgene 133560) using Gibson Assembly Cloning Kit (NEB).
pHD-3XP3-dsRed-DattP-CRISPR-donor-attP40-SPARC donor plasmids were injected into flies *y[1]sc[*]v[1]sev[21];P{y[+t7.7] v[+t1.8]=nos-Cas9.R}attP40* together with pCFD5-U6-3-t-attP40 vector (Addgene 133561) by BestGene Inc. Flies that expressed DsRed marker were selected, and crossed to *y[1] w[67c23]; sna[Sco]/CyO, P{w[+mC]=Crew}DH1 f*les (BDSC 1092) to excise dsRed gene.

3.2.2 Fly husbandry and fly stocks

Transgenic flies were reared on a standard cornmeal-molasses agar medium at 25°C and 60% humidity, and kept on a 12h light/12h dark cycle. For optogenetic activation experiments, flies were collected after eclosion and reared in darkness on standard food supplemented with 1 mM all-trans retinal for 3-5 days.

The following fly stocks were used in the study:

1. *norpa[7];20XUAS-SPARC2-I-Syn21-CsChrimson::tdTomato,VT058487-p65.AD/20XUAS-IVS-PhiC31; VT000343-GAL4.DBD*
2. *norpa[7];20XUAS-SPARC2-I-Syn21-CsChrimson::tdTomato,VT058487-p65.AD/20XUAS-IVS-PhiC31; VT058488-GAL4.DBD*
3. *w[1118];20XUAS-Opto-switch,VT058487-p65.AD/20XUAS-IVS-PhiC31;VT058488-GAL4.DBD*
4. *w[1118];20XUAS-Opto-switch, 20XUAS-IVS-PhiC31; VT058487-GAL4*
5. *norpa[7];20XUAS-Opto-switch,R27B03AD-p65.AD/20XUAS-IVS-PhiC31;VT058488-GAL4.DBD*
6. *w[1118];20XUAS-SPARC2-I-Kir2.1::eGFP,R27B03AD-p65.AD/20XUAS-IVS-PhiC31; VT058488-GAL4.DBD*

3.2.3 Immunohistochemistry and confocal imaging

The immunostaining and image acquisition of fly brains were performed as described in Chapter 2. The following antibodies were used: goat anti-RFP (Rockland), rabbit anti-GFP (Thermo Fisher), donkey anti-goat AF594 (Thermo Fisher), donkey anti-rabbit AF488 (Thermo Fisher).

3.2.4 Animal behavior

The freely-walking fly arena described in Chapter 2 was used for behavioral analysis.
For optogenetic stimulation, we used 3 LEDs, mounted above the roof, that illuminated the whole arena. We measured the intensity of light at several points in the arena to make sure that the

illumination was reasonably uniform (25-30 μW/mm2). For excitation of LPTCs by activation of csChrimson, we used LEDs with peak wavelength of 589 nm and for inhibition by activation of GtACR1, we used LEDs with peak wavelength of 505 nm. Optogenetic stimulation was triggered using an Arduino microcontroller that was controlled by a custom python script for varying lengths of time (0.2s, 0.5s, 1s and 2s). Stimulation was continuous and was triggered only when the fly entered a small region [15mm X 15mm] at the center of the arena to avoid any effects due to the heated walls. The smaller field of view also allowed us to record at a higher speed (200 Hz) with a higher resolution (720 x 720 pixels with a pixel size of 50 pixels/mm) while using the same camera we used for visual experiments. Two consecutive bouts of stimulation were separated by at least 10s to allow for the refractory period of the optogenetic proteins.

3.2.5 Analysis of behavioral data

Preprocessing of recordings and analysis of behavioral responses were performed as described in Chapter 2.

3.3 Results

3.3.1 SPARC-mediated approach for sparse optogenetic stimulation of HS cells

Identifying the full range of compensatory responses instructed by tangential cells requires a combinatorial activation of neurons within the network. This can be achieved by a spatial control of photostimulation during optogenetic experiments. This approach, called holographic optogenetics, enables recreation of specific neural activity patterns in both space and time within a neuronal population (Adesnik & Abdeladim, 2021). While it is becoming increasingly popular in mammalian systems, holographic optogenetics has not been applied to flies due to their small size. As an alternative, researchers use a targeted light beam for optogenetic stimulation or spatially constrained electrical stimulations. However, the spatial control of neuronal activation using these methods remains rather limited.

Contrary to difficulties associated with the physical restriction of neuronal activation in *Drosophila*, the possibilities for genetic control of neural manipulations in flies are unmatched. Therefore, the use of genetic tools is the method of choice for spatial and temporal control of neuronal activity in fruit flies. In addition to a wide range of available driver lines, more refined genetic access can be gained by recombinase-mediated stochastic labelling. Among these methods, a recently developed PhiC31-mediated SPARC toolkit provides the simplest and the most versatile stochastic targeting of neurons. The specificity is achieved by a variety of effectors and at different labelling sparsity.

In order to map the behavioral repertoire of tangential cells, we expressed *20XUAS-IVS-PhiC31* and *SPARC2-D-CsChrimson::tdTomato* reporter using 2 driver lines: 1) HS/VS-specific split-GAL4 driver line *VT058487-p65.AD/VT058488-GAL4.DBD*, and 2) HS-specific split-GAL4 driver line *VT058487-p65.AD/ VT000343-GAL4.DBD* (Figure S6). To prevent visual stimulation of HS cells by light we used blind flies that carried norpA(7) mutation. This approach resulted in an efficient stochastic targeting of HS cells (Figure 18A, 18B). Every fly, therefore, was carrying a unique pattern of *CsChrimson::tdTomato*-expression in the HS-network.

To test if distinct patterns of neuronal activation result in distinct behavioral responses, we developed a pipeline for a combinatorial behavioral assay. First, we generated a library of genetic mosaic flies, each with a unique spatial distribution of neuronal activity in HS cells. Then, behavioral responses, induced upon photostimulation, were assessed independently for every fly using a freely-walking behavioral area. Finally, after the recording of behavioral data, the brain of each mosaic fly was dissected and imaged. This strategy enabled establishing a direct link between activity patterns of HS cells and corresponding behavioral responses.

We processed 57 flies from the two aforementioned batches. The density of targeting was 36% for the VS/HS-specific line and 27% for the HS-specific line (Figure 18B). However, we also observed labelling of additional cells in both of the driver lines. We therefore excluded those flies, and performed the final analysis only on flies that had a clean pattern of CsChrimson expression limited to only HS cells. We observed that excitation of different combinations of HS neurons elicited distinct behavioral responses in mosaic flies. The activation of HSE and HSS neurons lead to initiation of walking while activation of HSN neurons caused walking flies to stop locomotion and extend their wings (Figure 18C, 18D). This could hint at a fundamental difference in the behavioral role of the three HS neurons that was suggested based on their visual responses and connectivity (Hausen et al., 1983).

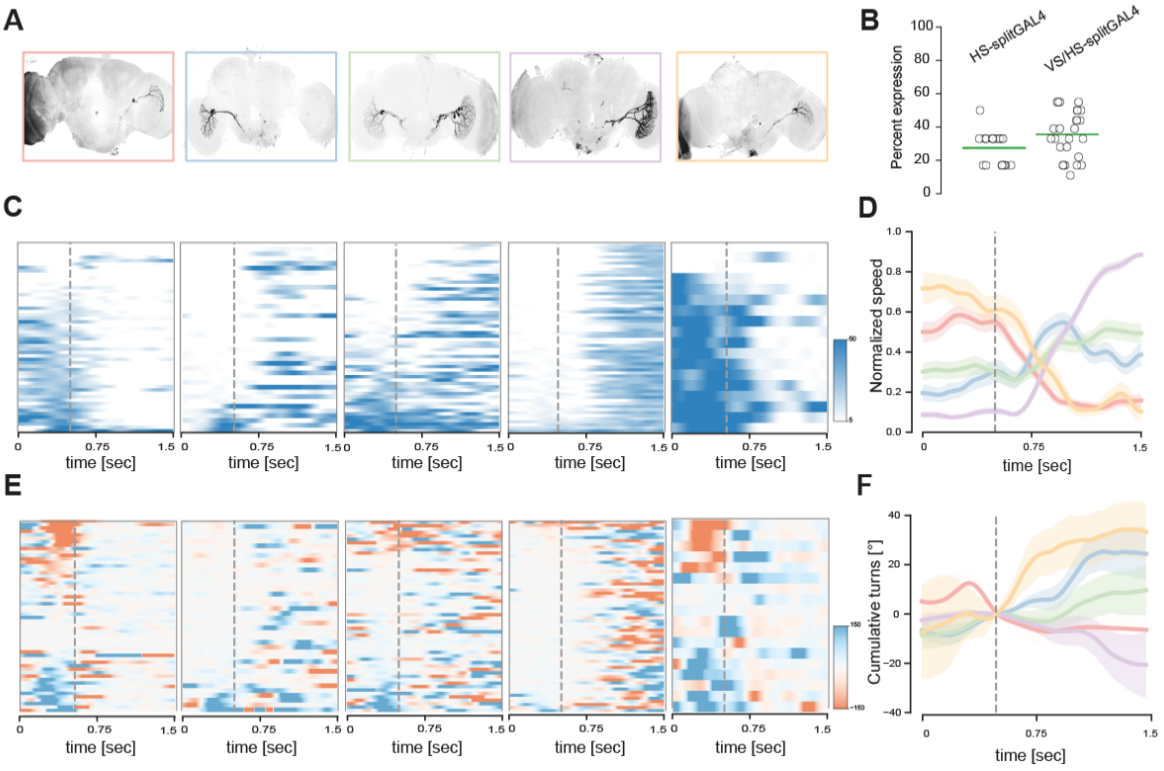

Figure 18. Behavioral assay of flies with mosaic expression of CsChrimson in HS cells. A) Expression of csChrimson::tdTomato in HS neurons of 5 different flies. B) Percentage of HS neurons labeled by CsChrimson::dTomato protein. Each circle represents a single mosaic brain, bars indicate the mean percentage value. C) Speed raster plots, each showing responses after multiple repetitions of optogenetic excitation in a single fly, corresponding to the mosaic flies in A. Each row corresponds to one trial and each column to one frame (5ms). Optogenetic stimulation begins at the 0.5s (dashed line) and continues for 1s. D) Average normalized speed for each individual fly, corresponding to the speed rasters in C (mean ± SEM[shaded region]). E) Angular speed raster plots for multiple repetitions of optogenetic excitation, same as in C. F) Average cumulative turns for each individual fly, corresponding to the angular speed rasters in E (mean ± SEM[shaded region]).

Several studies in the past have shown that excitation of HS neurons in one hemisphere of the brain elicits strong ipsilateral turning responses (Busch et al., 2018; Fujiwara et al., 2017, 2022). Flies that had a clear bilateral asymmetry in the expression of csChrimson in HS cells, provided us an opportunity to replicate those studies in freely walking animals. While we observed turning bias after photostimulation in some of the mosaic animals, an exact correspondence between the direction of turning and the asymmetric expression could not be inferred (Figure 18E, 18F). One explanation for this puzzling discrepancy is that unlike previous studies, flies could walk freely in our experiments. It is possible that the direction of turning after optogenetic stimulation depends on the behavioral state of the animal and therefore, tethered and freely walking flies respond differently to the same optogenetic stimulation.

Altogether, the application of *SPARC2-D-CsChrimson::tdTomato* construct using LPTC-specific split-GAL4 lines induces sparse stochastic expression of the effector in these neurons. The preliminary behavioral analysis of the mosaic flies suggests that distinct patterns of activation in HS cells initiate different behavioral responses. To our knowledge, it is the first experimental evidence that different HS cells have distinct behavioral roles in freely walking conditions. Therefore, a large-scale combinatorial analysis using this approach can be very effective for mapping the full behavioral repertoire of LPTC subnetworks.

3.3.2 Opto-switch tool for simultaneous neuronal activation and inhibition

Multiple subtypes of tangential cells transmit electrical signals via graded membrane-potential changes, and not via action potentials. Therefore, these neurons can mediate hyperpolarizing and depolarizing signals equally. It was demonstrated that unilateral optogenetic inhibition and activation of HS cells result in yaw-turning responses with opposite polarities (Busch et al., 2018). This suggests that accurate instruction of stabilizing responses by HS cells may require a fine balance of neuronal activation and inhibition. Inducing such an activity state on a neural network is, however, not possible with currently available methods, and would require a development of new genetic tools.

In order to induce simultaneous activation and inhibition in distinct cells within a neuronal population, I used a SPARC-inspired bistable Opto-switch genetic construct. This construct utilized PhiC31 recombinase-dependent genetic competition between two optogenetic effectors - CsChrimson and GtACR1. The two effectors were designed to have equal probability of expression within each cell. This way every neuron within a network expresses either CsChrimson or GtACR1, and can be subjected to optogenetic activation or silencing respectively (Figure 19A). The optogenetic proteins were fused to different fluorescent tags (tdTomato for CsChrimson and mVenus for GtACR1) for identification of their expression pattern.

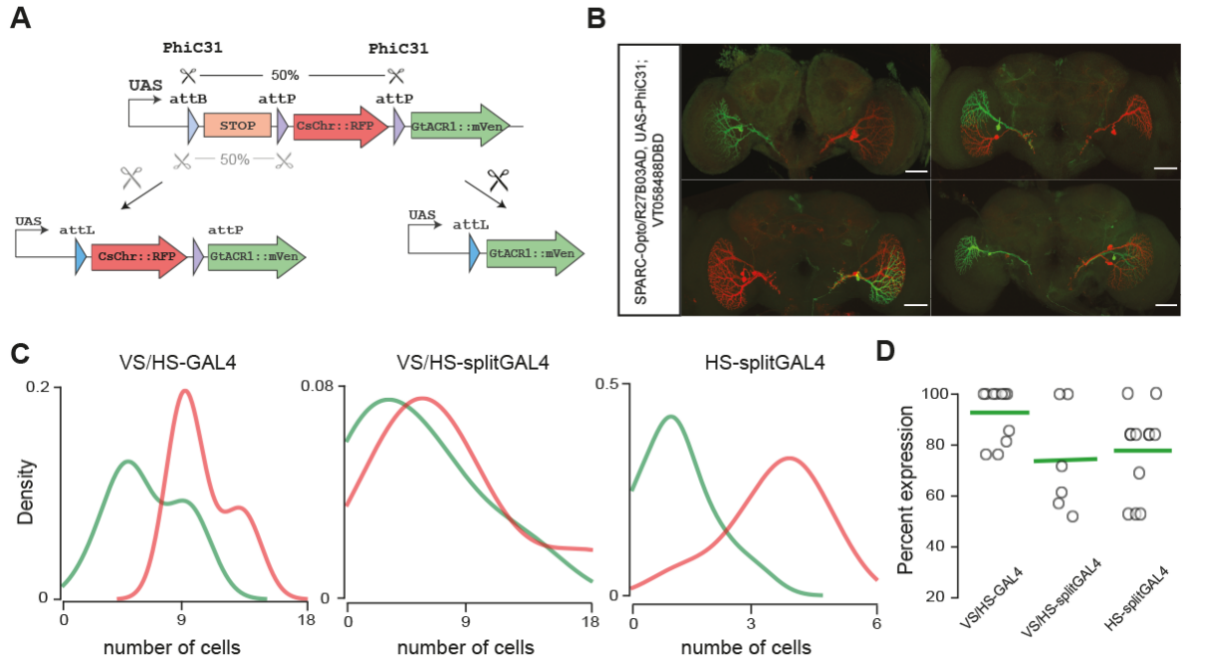

Figure 19. Opto-switch tool enables stochastic expression of CsChrimson and GtACR1. A) The schematic of the opto-switch cassette. PhiC31 integrase recombines one of two competing *attP* target sequences with the *attB* target sequence. Each of the recombination events results in a discriminative expression of one of the two effectors. B) Examples of stochastic labelling of HS-cell generated by PhiC31-mediated recombination induced by HS-specific split-GAL4 line (GtACR1::mVenus in green, CsChrimson::tdTomato in red, scale bar 50 μm). C) The distribution of neurons expressing CsChrimson and GtACR1 optogenetic proteins for three tested driver lines. D) Percentage of LPTC neurons labeled by CsChrimson or GtACR1 protein.

The cassette was integrated inside the attp40 landing site on chromosome 2 using CRISPR/Cas9 technique. To test the expression of the construct in tangential cells we used several driver lines: 1) HS/VS-specific GAL4-driver line *VT058487-GAL4,* 2) HS/VS-specific split-GAL4 driver line *VT058487-p65.AD/VT058488-GAL4.DBD*, 3) HS-specific split-GAL4 driver line *R27B03AD-p65.AD/VT058488-GAL4.DBD* (Figure S6). Similarly to SPARC construct, in the absence of PhiC31, Opto-switch construct retained the stop sequence, and the split-GAL4

driver line failed to drive the expression of the optogenetic proteins. When *20XUAS-IVS-PhiC31* was introduced, the stochastic discriminative expression of one out of the two optogenetic proteins was observed in individual tangential cells (Figure 19B). We noted, however, that not all the neurons targeted by the driver lines were labelled, suggesting that the excision did not occur in all the neurons. We traced the temporal dynamics of neuronal labelling using line *VT058487-GAL4*. From 2 to 5 days of eclosion the average percent of targeted cells increased from ~70% to ~90%. The labelling efficiency using split-GAL4 driver lines largely depends on their stability, and therefore Opto-switch has to be used in combination with stable lines if 100% of total expression is needed to be achieved. The overall efficiency of PhiC31 integrase-mediated excision in 5-day-old flies using three driver lines mentioned above is shown on Figure 19D. The average percentage of labelled cells was higher for the tested GAL4 (91%) line in comparison to split-GAL4 lines (76% and 69%). In addition, tested driver lines showed different excision biases. While VS/HS-specific lines showed no substantial expression bias towards one of the two optogenetic proteins, the HS-specific line had a very prominent bias towards the expression of CsChrimson (Figure 19C). The excision bias can be explained by differences in the distance between PhiC31 integrase binding sites. Sites flanking CsChrimson::tdTomato effector are further away than ones flanking GtACR1::mVenus, which can lead to a higher probability of GtACR1::mVenus being excised. Why the bias would differ for different driver lines, however, is not clear. A more thorough analysis of the expression of the Opto-switch construct would be required to exclude batch effects, as well as the potential influence of other parameters, such as temperature of development, animal sex, etc.

Overall, the preliminary analysis of the newly developed Opto-switch method shows that it can be used for stochastic expression of either an excitatory or an inhibitory optogenetic protein in distinct cells within a population of LPTC neurons. This approach therefore can be used in combinatorial experiments that were applied for SPARC2-D-CsChrimson in order to study the behavioral role of neuronal activation and silencing in the LPTC-network.

3.3.3 SPARC-Kir2.1 for sparse chronic neuronal silencing

Although optogenetics is a powerful tool for mapping neuronal substrates of fly behavior, it cannot be used to study visua responses. To address sensory-motor processing in LPTCs we decided to develop a genetic tool for sparse neuronal ablation. For that, we used SPARC-inspired bistable construct that induces expression of effector protein Kir2.1 in a smaller or a larger fraction of cells within a targeted neuronal population (Figure 20A). In analogy to the SPARC toolkit, we called the construct for sparse genetic targeting *SPARC2-I-Kir2.1::eGFP,* and the construct for dense genetic targeting - *SPARC2-D-Kir2.1::eGFP*. Similarly to Opto-switch, the cassettes were integrated inside the attp40 landing site on chromosome 2 using CRISPR/Cas9 technique.

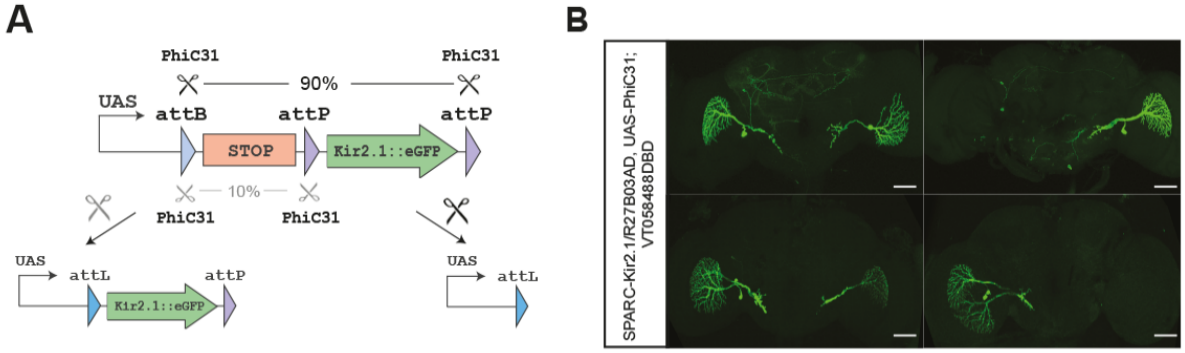

Figure 20. Mosaic genetic tool for sparse silencing of neurons. A) The schematic of *SPARC2-I-Kir2.1::eGFP* cassette. PhiC31-mediated recombination results in higher probability of excision of the STOP sequence, and therefore in sparse expression of Kir2.1 inward-rectifier potassium channel in targeted neurons. B) Examples of stochastic targeting of HS cells using a cell-specific split-GAL4 driver line (Kir2.1::eGFP in green, scale bar 50 μm).

In order to test sparse chronic silencing approach in HS cells we used *SPARC2-I-Kir2.1::eGFP* in combination with *20XUAS-IVS-PhiC31* and a recently described stable and very specific split-GAL4 line *R27B03AD-p65.AD/VT058488-GAL4.DBD* (Figure S6) (Fujiwara et al., 2022). These flies showed a stochastic expression pattern of Kir2.1::eGFP with the average sparsity of 36% (Figure 20B).

We created a library of mosaic flies, and performed combinatorial behavioral assay, similar to the one described for SPARC2-D-CsChrimson experiments. Instead of optogenetic excitation, we used visual stimulation with a rotating sinusoidal pinwheel. As described earlier, flies elicit a robust optomotor response to the rotating pinwheel. This is a simple assay to assess the function of motion vision in flies, and therefore suits well as a readout for the genetic silencing of HS cells. The results of the assay for a subset of in total 22 tested SPARC2-I-Kir2.1 flies are presented on the Figure 21.

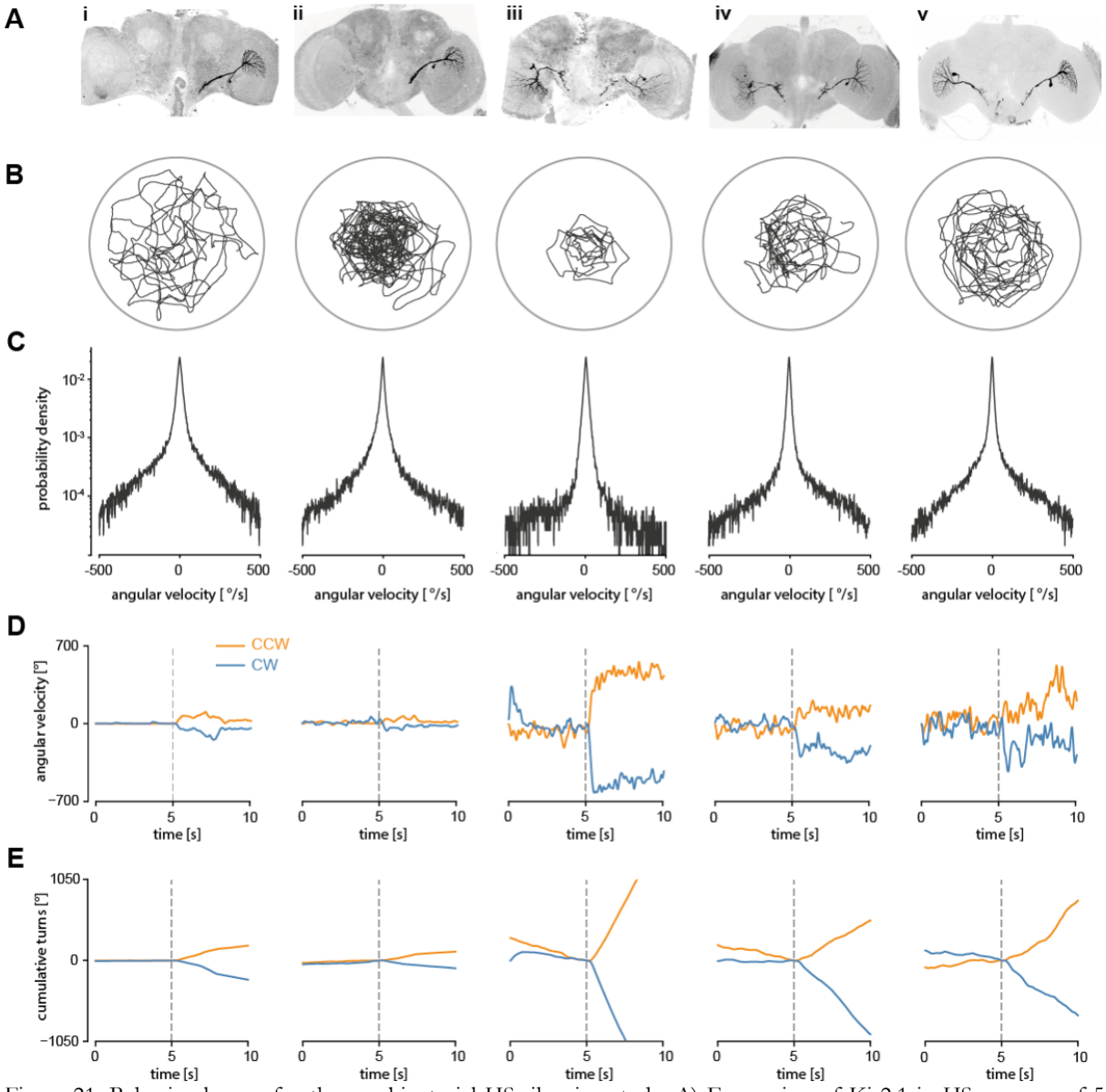

Figure 21. Behavioral assay for the combinatorial HS-silencing study. A) Expression of Kir2.1 in HS neurons of 5 different flies. B) Trajectories of flies walking in darkness, corresponding to the brains in A. Each trajectory is 2 min long and was selected randomly from an experimental session of 30 min. C) Probability density function for angular velocity of flies walking in darkness for 30 min. D) Average angular velocity of flies responding to clockwise (blue) and counterclockwise (orange) rotation of the pinwheel. Dashed line demarcates beginning of rotation. E) Mean

cumulative turns made by each fly over a trial for clockwise (blue) and counterclockwise (orange) rotation. Dashed line demarcates beginning of rotation.

For every fly, we first assessed the behavior in the darkness to estimate if stochastic silencing of HS cells caused biases in the animal locomotion without any visual stimulations. We observed that some flies were more active than others, and were rapidly exploring the arena (Figure 21B). Since the arousal state of an animal can significantly alter responses to sensory stimuli, this parameter has to be accounted for in the behavioral analysis. Another important parameter to consider is the turning bias of animals during locomotion in the absence of any visual input since LPTCs are known to receive feedback from motor centers. We addressed this by computing the distribution of angular speeds throughout navigation in the darkness for a period of 30 minutes. The flies represented on the figure 18 did not show significant turning biases towards any one side (Figure 21C). After recording the behavior of the fly in the darkness, we presented a full-field sinusoidal pinwheel stimulus rotating clockwise and counterclockwise. The stimuli were presented for 5 sec with 5 sec intervals of static pinwheel, and were repeated in a randomized order 90 times in total. For each fly we quantified the cumulative turns and angular velocity throughout the presentation of the stimulus. We observed that the strength of the optomotor following in flies varied significantly, however, flies with identical pattern of Kir2.1 expression (Fly i and Fly ii) showed similar strength of the responses (Figure 21D, 21E). Finally, some flies showed bias in the responses towards one of the stimulus directions. For example, Fly iv showed a stronger turning response to clockwise rotation than counterclockwise rotation. This might be due to asymmetric inhibition of HS cells in the fly (HSE and HSS in left hemisphere and HSE in right hemisphere).

Overall, the preliminary behavioral assay using newly developed transgenic animals for sparse neuronal silencing suggests that flies with stochastically ablated HS cells show a significant variability in their optomotor responses. Therefore, this approach can help to address the mechanism of visuomotor transformations in the tangential cell network. Moreover, *SPARC2-I-Kir2.1::eGFP* and *SPARC2-D-Kir2.1::eGFP* constructs can be used in diverse neural circuits in order to achieve sparse neuronal silencing, and address its behavioral or physiological effects.

Supplementary data 2

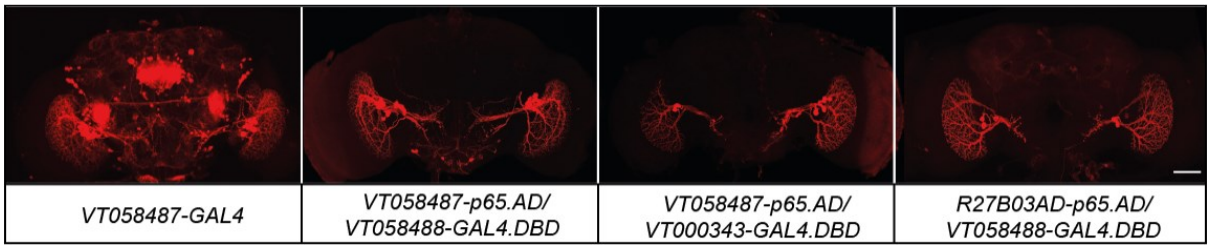

Figure S6. Driver lines used for the mosaic genetic tools. For SPARC-CsChrimson: 1) HS/VS-specific split-GAL4 driver line *VT058487-p65.AD/VT058488-GAL4.DBD*, and 2) HS-specific split-GAL4 driver line *VT058487-p65.AD/ VT000343-GAL4.DBD*; for Opto-switch: 1) HS/VS-specific GAL4-driver line *VT058487-GAL4,* 2) HS/VS-specific split-GAL4 driver line *VT058487-p65.AD/VT058488-GAL4.DBD*, 3) HS-specific split-GAL4 driver line *R27B03AD-p65.AD/VT058488-GAL4.DBD*; for SPARC-Kir2.1: HS-specific split-GAL4 driver line *R27B03AD-p65.AD/VT058488-GAL4.DBD*.

Chapter 4

Discussion

Anyone who observes animals in their natural habitat notes an extraordinary coordination of their behavioral responses. This coordination is achieved through a long process of evolutionary adaptation that enables neural circuits to extract only the information that is relevant for behavior from complex environmental stimuli. Such a strategy significantly reduces the amount of energy and time spent on instructing stimulus-induced behavioral commands. How do neurons acquire this tuning for specific and often composite sensory stimuli? I addressed this question by studying neural circuits responsible for optic-flow-based course control in flies. Tangential cells that comprise this circuit operate as sensory matched filters, each detecting a specific pattern of ego-motion-induced optic flows. This sensitivity is not provided solely by inputs from upstream local motion detectors, but also by stereotyped lateral connections between individual tangential cells. Therefore, the stimulus tuning in these cells reflects overall circuit dynamics and connectivity, and cannot be addressed without considering these two aspects.

The majority of lateral connections between tangential cells are electrical in nature, and formed by ShakB gap junction channels. The application of FlpStop-mediated disruption of the *shakB* gene demonstrated the key role of gap junctions in sensory tuning of horizontal-motion-sensitive tangential cells. The loss of electrical coupling and subsequent decrease in optic-flow sensitivity in these neurons changed the integration of wide-field motion patterns without abolishing optomotor reflexes. It shows that gap junctions are not important for motion-induced responses *per se*, but rather for accurate assessment and interpretation of binocular motion stimuli as a whole.

The aforementioned connectivity between tangential cells creates subcircuits that operate largely independently to mediate steering behaviors in response to particular optic flows. Therefore, by mapping exact components of these subcircuits and by probing their behavioral role we can achieve a good understanding of how optic flow cues instruct course stabilizing responses in flies. This task can be achieved by changing the activity of tangential cells in multiple combinations and tracking behavioral effects of those changes. To implement that in practice, I adapted and further expanded the SPARC toolkit for genetic mosaic manipulation of neural activity in chronic and acute manners. Preliminary results of employing these tools in a subpopulation of HS cells suggest that targeting these neurons in a combinatorial manner can elicit distinct behavioral responses. Further scaling-up of this approach can help to map subnetworks of tangential cells, and annotate a full array of behavioral commands that are instructed by this circuit.

4.1 From molecules to behavior: role of gap junctions in optic flow processing

4.1.1 Mutants of gap junctions, challenges arising from molecular complexity

We showed that FlpStop-mediated knockout of the *shakB* gene can be used as an efficient method to disrupt gap junctions without pleiotropic effect on neural phenotypes. Insertion of a FlpStop cassette into the shakB gene in disrupting orientation can serve as an alternative to widely-used mutant lines in *Drosophila*, while insertion in non-disrupting orientation can be used for cell-specific gene inactivation via FLP-mediated inversion. An additional advantage of this technique is that the obtained mutant lines have maximally similar genetic background to corresponding wild-type animals, and therefore are well-suited for direct behavioral comparisons.

The FlpStop cassette inserted in disrupting orientation between exons 5 and 6 is expected to have similar patterns of *shakB* disruption, and therefore similar phenotypic effects to a nonsense mutation in exon 5 carried by the EMS-mutagenized shakB^2 line. Nevertheless, we observed significant phenotypic discrepancies between shakB^2 and FlpStopDshakB mutant flies. Firstly, dye-coupling suggests that tangential cells in shakB^2 mutant flies lose all their electrical synaptic partners, while in FlpStopDshakB flies, electrical connections with postsynaptic DNs and motoneurons remain. Secondly, LPTCs in shakB^2 mutant flies exhibit so-called ultraslow waves, strong spontaneous membrane hyperpolarizations (15-25mV in amplitude) occurring with a frequency of 0.02–0.2 Hz. This type of oscillations was not observed in FlpStopDshakB flies. Thirdly, HS cells in shakB^2 mutant flies show significantly weaker ON/OFF-transient responses as well as direction-selective responses in comparison to both wild-type and FlpStopDshakB mutant flies.

Potential sources of phenotypic discrepancies between the two mutant lines can be either the reduced penetrance of FlpStopDshakB mutant allele, or the expression of the shakB-RF isoform that remains unaffected in shakB^2 mutant flies (Figure 5B). The *shakB* gene is located on the X-chromosome. The pattern of dye-coupling in LPTCs suggests that in female flies the FlpStopDshakB allele has reduced penetrance in comparison to male flies. Therefore, all described experiments were performed in male flies. In addition, I also observed that high temperatures of pupal development increase phenotypic variability, therefore all the flies were kept at 18°C. In my hands, male FlpStopDshakB flies that developed at 18°C showed strong penetrance and consistent physiological phenotype. Phenotypic variability in shakB^2 male flies grown at 18°C remained considerable (HS neurons in ~40% of the flies did not show any visually-induced responses). These observations suggest that phenotypic variability and penetrance of FlpStop alleles may depend on experimental settings, and therefore have to be carefully tested for each study. Largely variable and strongly deleterious effects of the shakB^2 mutation point to additional genetic agents that may influence the phenotype in this mutant line. It can be additional background mutations that were accumulated or generated during EMS-induced mutagenesis. Alternatively, or additionally, the nonsense mutation in the shakB^2 mutant line does not affect the shakB-RF isoform. The product of this isoform is a truncated ShakB protein that has only three out of four transmembrane domains. This protein variant cannot form functional membrane channels, and therefore, by binding other variants can reduce the amount of gap junction channels in cell membrane. Since shakB-RA(Lethal) and shakB-RE isoforms remain intact in both shakB^2 and FlpStopDshakB flies, the presence of the shakB-RF isoform can reduce the number of channels formed by these two isoforms, and this way cause phenotypic differences in these two mutant lines. Moreover, expression of this isoform in *Drosophila* optic lobe remains at relatively high level throughout the development and during adult stage, suggesting that it is functionally significant (Figure 5C).

Neither the LPTC-specific disruption of *shakB* by FlpStop nor its previously attempted knock-down by RNAi resulted in significant reduction of electrical coupling formed by these cells (Ammer et al., 2022; Haag & Borst, 2003; Schnell et al., 2010)). These technical challenges are rather puzzling, considering that the predicted lifespan of gap junction proteins is in the range of several hours to several days (Curtin et al., 2002; Thévenin et al., 2013). The analysis of several driver lines for LPTC-specific inversion of the FlpStop cassette shows that this prediction may not be accurate for ShakB protein comprising gap junctions in tangential cells. The induction of gene disruption at around developmental stage P9 results in stronger reduction of protein signal in adult animals than induction at later stage P12. It is also possible that ShakB protein expressed during the early development of LPTCs is important to define the area of gap-junction plaques. Since even a severe reduction in the amount of ShakB protein (in the case of induction of gene disruption at around stage P9) did not result in a loss of electrical synapses formed by LPTCs, it may suggest that even a small amount of protein is enough to form sustainable gap junction channels.

All the listed challenges and seeming discrepancies are potentially rooted in the complex structure of the *shakB* locus. The *shakB* gene produces eight isoforms that give rise to six distinct protein variants. Each of these isoforms has a specific pattern of temporal and spatial expression, which points to their involvement in the formation of distinct types of gap junction channels. We have very little knowledge about the molecular diversity of gap junction channels in *Drosophila* neural tissue. Detailed genetic and molecular studies would be of high importance to understand structural and functional properties of electrical synapses in each concrete neural circuit.

4.1.2 Pattern of LPTC electrical coupling

HS cells in shakB^2 mutant flies lose connection to all their electrical synaptic partners, while in FlpStopDshakB flies electrical connections with postsynaptic DNs and motoneurons are preserved. Partial loss of electrical synapses in FlpStopDshakB flies can be a result of incomplete penetrance of the mutant allele. However, this is unlikely to be the only explanation, since all of the HS cells injected with neurobiotin in these flies show a similar pattern of partial loss of electrical coupling.

Why would the disruption of one innexin gene differentially affect electrical synapses formed by HS cells? Given that the *shakB* gene produces multiple isoforms, the most obvious explanation is that HS cells utilize different protein variants to form gap junctions with distinct synaptic partners. Several lines of evidence corroborate this hypothesis. Different isoforms of the ShakB protein form various types of channels with distinct properties that shape a unique pattern of current flow in a given neural circuit (Phelan et al., 2008). For example, heterotypic ShakB-channels were demonstrated to form structurally and functionally asymmetric electrical synapses in the giant fiber system. Specifically, the giant fiber neuron was shown to express the ShakB(N+16) variant to form gap junction channels with postsynaptic motoneurons PSI and TTM that express the ShakB(Lethal) variant. These gap junctions are asymmetrically voltage-gated and exhibit rectification, transmitting depolarization signals predominantly in one direction - from the ShakB(N+16)-expressing cell to the ShakB(Lethal)-expressing cell. This example suggests that rectifying electrical synapses can provide fast unidirectional signal transfer from sensory interneurons to motor centers. Coupling between LPTCs and downstream DNs and motor neurons could be composed of such rectifying electrical synapses. However, gap junctions between two LPTCs must be bidirectional, and therefore symmetric. This would be in line with the proposed functional role of these electrical synapses in integrating motion responses from different regions of the visual field. The distinct functional roles of gap junctions formed by HS cells suggests that they might be structurally different and hence, differentially affected by our genetic disruption.

In fact, as it was mentioned above, shakB^2 and FlpStopDshakB have a crucial difference in the expression of shakB isoforms. shakB^2 flies express the truncated ShakB-PF variant that can

reduce the formation of functional ShakB channels. Therefore, the remaining isoforms, ShakB-PA(Lethal) and ShakB-PE, can still form electrical synapses in FlpStopDshakB but not in shakB^2 mutant flies. If this is correct, then ShakB-PA(Lethal) or ShakB-PE in HS cells form junctions only with postsynaptic motoneurons. This would explain the differential electrical coupling in ShakB2 and FlpStopD flies.

Even though functional and structural differences between inter-LPTCs electrical synapses and electrical synapses formed with postsynaptic neurons are plausible, a thorough genetic and physiological analysis would be required to unravel exact molecular composition and physiological properties of ShakB electrical synapses in tangential cells.

4.1.3 Gap junctions and electrophysiological properties of HS cells

Electrophysiological analysis shows that the loss of gap junctions affects passive membrane properties of HS cells, but not their overall direction-selective tuning. The resting membrane potential of HS cells in FlpStopDshakB flies exhibits strong fluctuations. These fluctuations occur in a regular manner at a frequency band of 10-30Hz, and therefore can be classified as oscillations. These membrane oscillations seem to be of the same origin as β-oscillations described in shakB^2 flies (Ammer et al., 2022). It suggests that gap junctions formed between HS cells facilitate the dissipation of cell-intrinsic noise that otherwise can interfere with signals arriving from presynaptic cells. Interestingly, in addition to fast β-oscillations, HS cells in shakB^2 flies exhibit ultra-slow waves with a frequency of 0.02–0.2 Hz, that are not observed in FlpStopDshakB mutant. It may suggest that ultra-slow waves occur due to a complete loss of gap junction channels in shakB^2 flies, resulting from the expression of the dominant negative ShakB-PF isoform. We did not observe either the slow or the fast oscillations in DB331-GAL4-mediated inducible mutant flies. It shows that a significant reduction of ShakB protein in tangential cells, detected in these flies, does not result in a loss of gap junction channels, and therefore does not have a pronounced effect on passive membrane properties of HS cells. Similarly to tangential cells in shakB^2 flies, HS cells in FlpStopDshakB flies show slightly higher baseline membrane potential. It suggests that electrical coupling contributes to the maintenance of resting membrane potential, and its loss may alter the properties of voltage-gated channels that operate in these neurons.

HS cells respond with a strong transient depolarization to both light increment (ON) and decrement (OFF). The observation that the amplitude of transient off-responses, and not on-responses, is reduced in mutant flies, points to the distinct role of electrical coupling in ON and OFF channels. The origins of this effect could lie in the early stages of visual processing in lamina, since L1 and L2 neurons, that give rise to ON and OFF channels, were shown to be coupled via ShakB gap-junctions (Joesch et al., 2010).

Importantly, the overall direction selectivity of HS cells, as well as the velocity and contrast tuning of direction-selective responses, are not affected in FlpStopDshakB mutant flies. Gap junctions, therefore, do not seem to mediate motion computation in the fly optic lobe. The most striking change in direction-selective responses of HS cells lacking gap junctions is the increase in the amplitude of hyperpolarization in response to gratings moving in the ND. Interestingly, this effect is not observed when drifting dots are presented instead of gratings. The dynamics of HS responses to these two types of stimuli differs significantly, especially in the null direction. While moving gratings trigger a very strong and immediate hyperpolarizing response, drifting dots induce slowly ramping and sustained hyperpolarization. The strong transient hyperpolarization induced by grating stimuli decays fast, potentially due to the activation of hyperpolarization-activated cation currents. It is possible that the dynamic of opening of these channels is changed in HS cells lacking gap junctions due to changes in the baseline membrane potential and cell input resistance. Interestingly, hyperpolarization-activated cation currents were suggested to be involved in generation of ultra-slow waves in shakB^2 flies, which are characterized by extensive drops in

membrane potential of 15–25mV. Therefore, these channels can play a role in stabilizing membrane potential of tangential cells during strong hyperpolarizing events.

Gap junctions in tangential cells do not seem to solely mediate interaction between neurons, but also refine passive and active membrane properties. Surprisingly, this homeostatic role of electrical synapses in neural circuits is often disregarded despite the fact that gap junctions mediate the flow of ions as well as small molecules and metabolites that are crucial for membrane excitability.

4.1.4 Spatial pattern of HS cell receptive fields

Loss of gap junctions has a prominent effect on the distribution and relative strength of local motion responses in HS cells suggesting that electrical coupling between tangential cells shapes their receptive fields. Since each HS cell has distinct electrical partners, the loss of gap junctions manifests itself differently in the three cells. The most striking effect is observed in HSE cells. In FlpStopNDshakB wild type animals these neurons receive strong contralateral excitatory input for motion in the preferred direction, that is not present in FlpStopDshakB mutant flies. Strong dye-coupling suggests that this input could be arriving from spiking back-to-front-motion-sensitive H2 neurons. This electrical coupling is very prominent, and has also been described in blow flies. Indeed, the HSE-to-H2 connection in FlpStopDshakB mutant flies is disrupted or largely weakened, pointing to the importance of this connection in shaping receptive fields in HSE cells.

The electrical connection between contralateral HSE and H2 neurons is especially important since it mediates binocular integration of horizontal motion cues. This binocular connectivity is thought to be key for accurate interpretation of optic flows that are dominated by horizontal components, such as yaw rotation and translation. Yaw rotation is associated with binocular horizontal motion of the same direction, slip translation - with dominated frontal horizontal motion, and thrust translation - with binocular horizontal motion of the opposite directions. Since these optic flows have extended regions of overlapping vector fields, their faithful interpretation would require integration of motion information from multiple visual areas. Therefore, the loss of binocular integration of horizontal motion, mediated by HSE-to-H2 connection, would restrict the analysis of the optic flow to each single hemisphere. This loss of spatial integration largely limits the ability of the fly visual system to differentiate rotational and translational optic flows, and therefore to instruct adequate steering behaviors.

4.1.5 Electrical coupling arbitrates course control via binocular integration of motion

Results of behavioral studies using a combination of uni- and bilateral rotation stimuli shows that loss of gap junctions in horizontally-sensitive tangential cells impairs the interpretation of global motion cues. This is manifested in a striking reversal in behavior of the animal to front-to-back motion in FlpStopDshakB mutant flies, as well as in overall changes in the dynamic of the response to full-field rotation due to a decrease in so-called anti-saccades. Additionally, we noted that the average turning response to full-field rotation for FlpStopDshakB mutant flies is a simple summation of the unilateral back-to-front and front-to-back responses, which is not the case for FlpStopNDshakB wild type flies.

We observed that FlpStopNDshakB wild type flies turn against unilateral front-to-back motion, and show a gradual decay in their responses to full field rotation. This dynamic suggests the presence of two parallel and competing pathways, one detecting rotation and another translation. Since front-to-back motion is more likely to be generated while walking (forward thrust generated front-to-back motion), it is plausible that this motion is not interpreted as being part of global rotation and as such, does not elicit the classic optomotor turning. Back-to-front motion,

on the other hand, is highly unlikely to be elicited during walking, and is perceived by the fly as rotation. Finally, when rotational motion is displayed only to the left and right quarters of the visual field (with no motion in the frontal region), wild type flies do not respond, while FlpStopDshakB mutant flies turn in the direction of the stimulus (Sup. Figure 5). This might indicate that the motion information from different regions of the visual field are primarily used to extract distinct optic flow cues, namely translation and rotation.

Curiously, the dynamics of the response to full rotation stimulus is shaped by so-called anti-saccades. The anti-saccades seen in the flies are reminiscent of the optokinetic response observed in mammals, and follow exactly the same pattern with smooth tracking in the direction of the stimulus followed by a saccade opposite to the direction of motion. Earlier studies have shown that saccades in the direction of motion are triggered when smooth turning is unable to compensate for the retinal slip. Subsequently, an integrator sums the retinal slip overtime and triggers a saccade when the cumulative retina slip (error) reaches a threshold. The anti-saccades could be triggered by a similar mechanism but the fact that they happen opposite to the direction of motion might suggest that this maneuver is meant to reset the gaze of the fly such that it can re-initiate smooth turning, akin to the optokinetic response.

Why do FlpStopDshakB mutant flies show a reduced number of anti-saccades and therefore stronger and more sustained responses to full-field rotation stimulus? Mutant and wild type flies show a similar amount of saccadic turns during free walking. It suggests that the mechanism to elicit saccades is intact in FlpStopDshakB mutant flies. The reduced number of anti-saccades during unilateral front-to-back and bilateral rotations points to only one of aforementioned pathways to be responsible for driving anti-saccades in these visual settings. More precisely, the pathway that detects rotation and provides strong sustained responses seems not to require anti-saccades, contrary to the pathway that detects translation. This can also explain the reduction of anti-saccades in wild type flies in response to rotational stimuli with low contrast. The pathway to detect translation is more active in response to stimuli with high contrast. This activity seems to drive large amounts of anti-saccades that are observed for unilateral back-to-front and full rotation stimuli at high contrast.

To our knowledge, this study is the first that describes turning of the wild-type flies against the unilateral front-to-back motion. Some studies have shown weak turning responses opposite to the direction of motion at higher stimulus contrasts but only for unilateral back-to-front-motion, not front-to-back stimulus. It must be noted that our setup differs from traditional setups for measuring optomotor experiments in some very important ways. First, the fly is freely walking while in most previous studies, flying or walking, the fly is tethered. A freely walking fly might have a significantly different behavior repertoire than a tethered fly due to i. an altered behavioral state and ii. different mechanosensory feedback. The behavioral state is especially important since the strength of the turning response depends on the activity of the animal. Nonetheless, the main conclusions we make are independent of the state of the animal. Second, we are presenting the visual stimulus with a projector setup while the majority of studies in the past have used LED panels. While a projector is very versatile and can be used to show a wide variety of stimuli, it introduces a significant lag between the behavior of the animal and update of the stimulus. This delay, which is roughly ~50 ms for our experiments, might significantly alter how the stimulus is perceived. Given the recent popularity and relative ubiquity of projector setups, this has major implications for behavioral experiments similar to ours. However, we are unaware of any previous study that has found any difference in behavior between LED panels and projectors. Finally and most importantly, we are presenting the visual stimulus from the top, which means that we are targeting the dorsal part of the visual field of the animal. As far as we know, we were the first to use such a setup. This makes it difficult to extrapolate our behavior results to other experimental settings. It is possible that the effects we see in this study cannot be seen if the stimulus is presented in a different manner, e.g., on a cylindrical drum or on a spherical screen with a tethered animal or

on the floor of the arena with a freely walking fly. This, nonetheless, indicates that the location of motion stimulus is crucial for its accurate interpretation by the animal.

Distinct ways in which flies respond to matching motion cues that occur in different regions of the visual field suggest that extraction of optic flow patterns evolves in parallel with animal behavioral repertoire. In other words, the visual circuits do not naively accord one sensory pattern with one behavioral output, but incorporate prior assumptions about animal environment and its self-motion in order to elicit only relevant responses. Our analysis of *shakB* mutant flies suggests that stereotyped electrical coupling between horizontal-motion-sensitive neurons can be important to disambiguate between translational and rotational components of the optic flow. This way, integration of motion cues from different visual areas via electrical synapses enable the LPTC network to instruct responses, maximally relevant in concrete environmental and behavioral settings.

4.2 Combinatorial approach for mapping neural substrates of fly course control: genetic mosaic tools for manipulation of neuronal activity

4.2.1 Stochastic optogenetic manipulation of HS cells

Novel genetic mosaic techniques offer new possibilities for efficient mapping of neuronal substrates of behaviors in *Drosophila*. A preliminary characterization and analysis of sparse optogenetic stimulation of tangential cells suggests that this method could prove to be extremely effective in discovering the full behavioral repertoire instructed by the LPTC network.

One of the great advantages of using the genetic SPARC-mediated approach for targeting neurons is that we can excite the optogenetic proteins non-invasively unlike prior studies that used objective lenses to target the lobula plate in a head-fixed fly. However, the same fact also introduces a new caveat in the experiment. Since we are shining the optogenetic stimulation in a non-targeted fashion, any off-target expression of the driver line can lead to the excitation of non-LPTC neurons which will make the interpretation of results challenging. We are not aware to what extent this is also a consideration for experiments that target the beam of light onto specific regions in the fly brain using objective, since the scattering of light can also potentially lead to excitation of off-target neurons. An obvious solution to the problem of off-target expression is the use of very specific split-GAL4 driver lines. We showed that HS- and HS/VS-specific split-GAL4 lines can induce stochastic expression of SPARC2-D-CsChrimson via UAS-mediated expression of PhiC31 recombinase. However, we observed that the use of split-GAL4 results in lower efficiency of excision on average. This could be addressed by a boost of PhiC31 recombinase expression using alternative promoters, such as strong pan-neuronal promoter element nSyb. nSyb-PhiC31 variant of recombinase can be also used in combination with the Opto-switch construct, if 100% of labelling is a requirement. The Opto-switch construct poses an additional challenge - the unbiased expression of the two effectors. We observed a significant difference in the ratio of expression CsChrimson/GtACR1 when using different driver lines. While the overall bias towards the excision of stop sequence and subsequent induction of CsChrimson can be explained by the shorter distance between PhiC31 integrase binding sites, the origin of driver line-dependent bias is rather puzzling. Nevertheless, all the stated points require a thorough analysis of a driver line before using it in the behavioral assays.

In addition to the technical aspects related to the control of reporter excision, optogenetic stimulation requires strict control of conditions for the optostimulation. Since direct measurement of neuronal activity upon optogenetic stimulation is only possible after cuticle removal, this light titration cannot be interpolated to behavioral assays in freely walking animals. Therefore, one way to titrate the lightning conditions for optogenetic activation is to express CsChrimson using several driver lines that are known to drive consistent behavioral responses. Then, the intensity of light can be adjusted in respect to its ability to drive those stereotyped responses. In any case, several lightning conditions can be applied in experiments if different levels of neuronal activation are expected to drive distinct behavioral outcomes. The titration of lightning conditions for the Opto-switch technique can be more challenging due to the difference in the absorption peaks: 590nm for CsChrimson and 515 nm for GtACR1. Since far-red light has a better ability to penetrate the tissue, it is expected that GtACR1 can require higher intensity of activating light. Similar to the choice of expression conditions, lightning conditions also require a fine titration for a robust activation of optogenetic effectors.

After the experimental conditions are tested, the combinatorial behavioral assay can be very fast and robust. Any parameters of behavioral responses can be considered for further analysis. For example, for HS cells just a simple assessment of the velocity was sufficient to detect differences in responses induced by HSN versus HSE or HSS cells. We hypothesize that these

differences most probably result from the fact that HS neurons get visual inputs from different regions of the visual field that have different ethological significance. HSN looks towards the sky, HSE looks towards the front and horizon and HSS looks towards the ground. As such, it is not surprising that motion from ground would be interpreted differently that motion from the sky. In fact, some previous studies have hinted at this (Hausen, 1981). The stochastic expression method provides an opportunity to test this hypothesis directly, for the first time. However, the locomotion of the fly is extremely complicated and involves the precise control of their wings and limbs. As such, more comprehensive analysis is required to detect finer behavioral changes that might not seem significant in our behavioral arenas but are nonetheless, extremely relevant in the wild. This can be done by annotating and tracking the limbs and wings of the fly in the videos using machine learning tools such as DeepLabCut and LEAP. Analyzing the minute effects of excitation and inhibition of LPTCs on limb coordination and gait parameters could provide a clearer and richer picture of the role of LPTCs in behavior (DeAngelis et al., 2019; Mendes et al., 2013).

Even though it is associated with technical challenges, sparse optogenetic activation using genetic mosaic technique opens unique opportunities for mapping neuronal substrates of fly behavior in non-invasive conditions. In the LPTC network, this method provides a functional approach to identification of individual subnetworks that are responsible for distinct optic flow-mediated steering responses.

4.2.2 SPARC for sparse genetic neuronal ablation

While optogenetics accounts for most of the recent progress in identifying neural mechanisms that instruct fly behavior, this technique cannot be easily applied in combination with visual stimulations. Therefore, the method of choice for visual neurons are effectors for chronic neuronal silencing, such as Kir2.1 and TNT. The SPARC toolkit permits sparse expression of different effectors using the LexA-LexAop expression system. This, however, requires an introduction of additional transgene, which increases the time for obtaining the final flies for the assays. In addition, unlike the UAS/GAL4 system, LexA-LexAop offers a rather limited choice of driver lines. These complications motivated us to create new transgenic animals that carry *20xUAS-SPARC2-I-Kir2.1::eGFP* and *20xUAS-SPARC2-D-Kir2.1::eGFP* cassettes. These constructs can be used in combination with PhiC31 integrase and specific driver lines in order to induce sparse neuronal silencing.

SPARC2-I-Kir2.1 worked well with the HS-specific split-GAL4 driver line. Similarly to optogenetic mosaic tools, SPARC2-Kir2.1 cassettes can require an optimization of driver lines used in the experiment. Sparse stochastic ablation of HS cells resulted in differences in the strength and directional bias of optomotor responses in mosaic flies.

Assessing the meaningful variability in behavioral responses is however not an easy task. Flies, even grown in identical conditions, can exhibit a strong variability in their visually-induced responses. Therefore, an additional control can be introduced in order to estimate an average variability in visual responses of flies without any neuronal ablations.

Finally, we also studied the locomotion of the fly in the absence of any visual stimulations. It is known that LPTCs receive mechanical feedback from the limbs via ascending neurons. As such, silencing a random subset of these neurons might introduce inconsistencies in the walking of the animal even in the absence of any visual stimuli. In addition, the choice of visual stimuli is very important. Before applying the visual stimulus for combinatorial assay, its effect has to be studied in detail in wild-type animals to avoid difficulties with the interpretation. Overall, the choice of controls for behavioral analysis as well as finely adjusted experimental conditions and the choice of visual stimuli are key for a successful functional assessment of sparse neuronal silencing in visual neurons.

Importantly, SPARC2-Kir2.1 cassette is versatile and can be easily used to address the functional effect of sparse neuronal ablation in a wide range of circuits.

4.3 Understanding circuits in their complexity

The studies of the LPTC network presented here demonstrate that the analysis of distinct patterns of optic flow are performed by a coordinated activity of different subsets of tangential neurons. This coordination is established via stereotyped lateral synaptic interactions between individual neurons. The loss of these synaptic interactions does not abolish motion-guided responses per se, but rather challenges the extraction of essential motion cues that are crucial for the interpretation of global optic flow patterns. Therefore, accurate interpretation of panoramic motion cues in the LPTC network can be achieved only via integration of wide-field visual information arriving from multiple tangential neurons.

The example of the LPTC network demonstrates that the instruction of behavioral commands can be performed by specific patterns of population activity. In neural circuits where various behavioral responses are instructed by various patterns of neuronal activity, each neuron has to be considered in relation to others. More precisely, the properties of an individual neuron have direct influence on the response properties and the activity of other neurons connected to it. For example, as was discussed for horizontal motion-sensitive cells, the H2 neuron via electrical coupling shapes to a large extent the spatial distribution of motion sensitivity in the HSE cell. This connection has direct behavioral implications. Adequate compensatory responses to horizontal optic flow can be instructed only by the combined activity of these two types of neurons. This logic of circuit function is fundamentally different from a single neuron or a whole population of neurons driving defined behavioral responses, and therefore requires different experimental paradigms. More precisely, classical approaches to manipulate neuronal activity would not be informative due to the rigidity of their spatial control. Instead, experimental approaches that focus on synaptic connectivity and spatial control of neuronal activity have to be considered.

The described properties of the LPTC network demonstrate that sensory neural circuits adapt to corresponding stimuli throughout the evolutionary history of an animal. Since selection acts on a circuit as a whole, the approach of dissecting individual structural elements of neural circuits can be not the most effective. Instead, efforts have to be put to approach neural circuits from the perspective of their adaptation to the environment as a whole.

References

Abdelfattah, A. S., Kawashima, T., Singh, A., Novak, O., Liu, H., Shuai, Y., Huang, Y.-C., Campagnola, L., Seeman, S. C., Yu, J., Zheng, J., Grimm, J. B., Patel, R., Friedrich, J., Mensh, B. D., Paninski, L., Macklin, J. J., Murphy, G. J., Podgorski, K., … Schreiter, E. R. (2019). Bright and photostable chemigenetic indicators for extended in vivo voltage imaging. *Science*, *365*(6454), 699–704.

Ache, J. M., Namiki, S., Lee, A., Branson, K., & Card, G. M. (2019). State-dependent decoupling of sensory and motor circuits underlies behavioral flexibility in Drosophila. *Nature Neuroscience*, *22*(7), 1132–1139.

Adams, M. D., Celniker, S. E., Holt, R. A., Evans, C. A., Gocayne, J. D., Amanatides, P. G., Scherer, S. E., Li, P. W., Hoskins, R. A., Galle, R. F., George, R. A., Lewis, S. E., Richards, S., Ashburner, M., Henderson, S. N., Sutton, G. G., Wortman, J. R., Yandell, M. D., Zhang, Q., Venter, J. C. (2000). The genome sequence of Drosophila melanogaster. *Science*, *287*(5461), 2185–2195.

Adesnik, H., & Abdeladim, L. (2021). Probing neural codes with two-photon holographic optogenetics. *Nature Neuroscience*, *24*(10), 1356–1366.

Akin O., Bajar B. T., Keles M. F., Frye M. A., Zipursky S. L. (2019) Cell-type-Specific Patterned Stimulus-Independent Neuronal Activity in the Drosophila Visual System during Synapse Formation. *Neuron*. 101(5):894-904.

Alcamí, P., & Pereda, A. E. (2019). Beyond plasticity: the dynamic impact of electrical synapses on neural circuits. *Nature Reviews. Neuroscience*, *20*(5), 253–271.

Ammer, G., Vieira, R. M., Fendl, S., & Borst, A. (2022). Anatomical distribution and functional roles of electrical synapses in Drosophila. *Current Biology: CB*, *32*(9), 2022–2036.e4.

Arenz, A., Drews, M. S., Richter, F. G., Ammer, G., & Borst, A. (2017). The Temporal Tuning of the Drosophila Motion Detectors Is Determined by the Dynamics of Their Input Elements. *Current Biology: CB*, *27*(7), 929–944.

Bahl, A., Ammer, G., Schilling, T., & Borst, A. (2013). Object tracking in motion-blind flies. *Nature Neuroscience*, *16*(6), 730–738.

Baines, R. A., Uhler, J. P., Thompson, A., Sweeney, S. T., & Bate, M. (2001). Altered electrical properties in Drosophila neurons developing without synaptic transmission. *The Journal of Neuroscience: The Official Journal of the Society for Neuroscience*, *21*(5), 1523–1531.

Baker, M. W., & Macagno, E. R. (2014). Control of neuronal morphology and connectivity: emerging developmental roles for gap junctional proteins. *FEBS Letters*, *588*(8), 1470–1479.

Barbara, G. S., Zube, C., Rybak, J., Gauthier M., Grunewald B. (2005). Acetylcholine, GABA and glutamate induce ionic currents in cultured antennal lobe neurons of the honeybee, *Apis mellifera*. *J Comp Physiol A* 191, 823–836

Barlow, H. B., & Levick, W. R. (1965). The mechanism of directionally selective units in rabbit's retina. *The Journal of Physiology*, *178*(3), 477–504.

Barnhart, E. L., Wang, I. E., Wei, H., Desplan, C., Clandinin, T. R. Sequential nonlinear filtering of local motion cues by global motion circuits. *Neuron,* 100 (1), 229-243; 2018.

Bartussek, J., & Lehmann, F.-O. (2016). Proprioceptive feedback determines visuomotor gain in Drosophila. *Royal Society Open Science*, *3*(1), 150562.

Bauer, R., Löer, B., Ostrowski, K., Martini, J., Weimbs, A., Lechner, H., & Hoch, M. (2005). Intercellular communication: the Drosophila innexin multiprotein family of gap junction proteins. *Chemistry & Biology*, *12*(5), 515–526.

Beatus, T., Guckenheimer, J. M., & Cohen, I. (2015). Controlling roll perturbations in fruit flies. *Journal of the Royal Society, Interface / the Royal Society*, *12*(105). https://doi.org/10.1098/rsif.2015.0075

Behnia, R., Clark, D. A., Carter, A. G., Clandinin, T. R., & Desplan, C. (2014). Processing properties of ON and OFF pathways for Drosophila motion detection. *Nature*, *512*(7515), 427–430.

Biswas, T., Lee, C. (2017) Visual Motion: Cellular Implementation of a Hybrid Motion Detector. *Current Biology,* 27: R274-R276.

Blagburn, J. M., Alexopoulos, H., Davies, J. A., & Bacon, J. P. (1999). Null mutation in shaking-B eliminates electrical, but not chemical, synapses in the Drosophila giant fiber system: a structural study. *The Journal of Comparative Neurology*, *404*(4), 449–458.

Blaj, G., & van Hateren, J. H. (2004). Saccadic head and thorax movements in freely walking blowflies. *Journal of Comparative Physiology. A, Neuroethology, Sensory, Neural, and Behavioral Physiology*, *190*(11), 861–868.

Blondeau, J. (1981). Electrically evoked course control in the fly *Calliphora erythrocephala*. *The Journal of Experimental Biology*, *92*(1), 143–153.

Boergens, K. M., Kapfer, C., Helmstaedter, M., Denk, W., & Borst, A. (2018). Full reconstruction of large lobula plate tangential cells in Drosophila from a 3D EM dataset. *PloS One*, *13*(11), e0207828.

Borst, A. (2018). A biophysical mechanism for preferred direction enhancement in fly motion vision. *PLoS Computational Biology*, *14*(6), e1006240.

Borst, A., & Egelhaaf, M. (1989). Principles of visual motion detection. *Trends in Neurosciences*, *12*(8), 297–306.

Borst, A., & Haag, J. (2002). Neural networks in the cockpit of the fly. *Journal of Comparative Physiology. A, Neuroethology, Sensory, Neural, and Behavioral Physiology*, *188*(6), 419–437.

Borst, A., Haag, J., & Reiff, D. F. (2010). Fly motion vision. *Annual Review of Neuroscience*, *33*, 49–70.

Brainard, D. H. (1997). The Psychophysics Toolbox. *Spatial Vision*, *10*(4), 433–436.

Brand, A. H., & Perrimon, N. (1993). Targeted gene expression as a means of altering cell fates and generating dominant phenotypes. *Development*, *118*(2), 401–415.

Brembs, B., & Heisenberg, M. (2001). Conditioning with compound stimuli in Drosophila melanogaster in the flight simulator. *The Journal of Experimental Biology*, *204*(Pt 16), 2849–2859.

Briggman, K. L., & Bock, D. D. (2012). Volume electron microscopy for neuronal circuit reconstruction. *Current Opinion in Neurobiology*, *22*(1), 154–161.

Britt, J. P., McDevitt, R. A., & Bonci, A. (2012). Use of channelrhodopsin for activation of CNS neurons. *Current Protocols in Neuroscience,* Chapter 2, Unit 2.16.

Brooks, J. X., & Cullen, K. E. (2019). Predictive Sensing: The Role of Motor Signals in Sensory Processing. *Biological Psychiatry. Cognitive Neuroscience and Neuroimaging*, *4*(9), 842–850.

Buschbeck, E. K., & Strausfeld, N. J. (1997). The relevance of neural architecture to visual performance: phylogenetic conservation and variation in Dipteran visual systems. *The Journal of Comparative Neurology*, *383*(3), 282–304.

Busch, C., Borst, A., & Mauss, A. S. (2018). Bi-directional Control of Walking Behavior by Horizontal Optic Flow Sensors. *Current Biology: CB*, *28*(24), 4037–4045.e5.

Capito, L., Ozguner, U., & Redmill, K. (2020). Optical Flow based Visual Potential Field for Autonomous Driving. *2020 IEEE Intelligent Vehicles Symposium (IV)*, 885–891.

Chen, T.-W., Wardill, T. J., Sun, Y., Pulver, S. R., Renninger, S. L., Baohan, A., Schreiter, E. R., Kerr, R. A., Orger, M. B., Jayaraman, V., Looger, L. L., Svoboda, K., & Kim, D. S. (2013). Ultrasensitive fluorescent proteins for imaging neuronal activity. *Nature*, *499*(7458), 295–300.

Chiappe, M. E., Seelig, J. D., Reiser, M. B., & Jayaraman, V. (2010). Walking modulates speed sensitivity in Drosophila motion vision. *Current Biology: CB*, *20*(16), 1470–1475.

Chow, D. M., Theobald, J. C., & Frye, M. A. (2011). An olfactory circuit increases the fidelity of visual behavior. *The Journal of Neuroscience: The Official Journal of the Society for Neuroscience*, *31*(42), 15035–15047.

Clark, D. A., Bursztyn, L., Horowitz, M. A., Schnitzer, M. J., & Clandinin, T. R. (2011). Defining the computational structure of the motion detector in Drosophila. *Neuron*, *70*(6), 1165–1177.

Colomb, J., & Brembs, B. (2014). Sub-strains of Drosophila Canton-S differ markedly in their locomotor behavior. *F1000Research*, *3*, 176.

Corrales, M., Cocanougher, B. T., Kohn, A. B., Wittenbach, J. D., Long, X. S., Lemire, A., Cardona, A., Singer, R. H., Moroz, L. L., & Zlatic, M. (2022). A single-cell transcriptomic atlas of complete insect nervous systems across multiple life stages. *Neural Development*, *17*(1), 8.

Cruz, T., Fujiwara, T., Varela, N., Mohammad, F., Claridge-Chang, A., & Eugenia Chiappe, M. (2019). Motor context coordinates visually guided walking in Drosophila. In *bioRxiv* (p. 572792).

Cruz, T. L., Pérez, S. M., & Chiappe, M. E. (2021). Fast tuning of posture control by visual feedback underlies gaze stabilization in walking Drosophila. *Current Biology: CB*, *31*(20), 4596–4607.e5.

Cuntz, H., Haag, J., Forstner, F., Segev, I., & Borst, A. (2007). Robust coding of flow-field parameters by axo-axonal gap junctions between fly visual interneurons. *Proceedings of the National Academy of Sciences of the United States of America*, *104*(24), 10229–10233.

Curtin, K. D., Zhang, Z., & Wyman, R. J. (2002). Gap junction proteins expressed during development are required for adult neural function in the Drosophila optic lamina. *The Journal of Neuroscience: The Official Journal of the Society for Neuroscience*, *22*(16), 7088–7096.

Dana, H., Mohar, B., Sun, Y., Narayan, S., Gordus, A., Hasseman, J. P., Tsegaye, G., Holt, G. T., Hu, A., Walpita, D., Patel, R., Macklin, J. J., Bargmann, C. I., Ahrens, M. B., Schreiter, E. R., Jayaraman, V., Looger, L. L., Svoboda, K., & Kim, D. S. (2016). Sensitive red protein calcium indicators for imaging neural activity. *eLife*, *5*.

Davie, K., Janssens, J., Koldere, D., De Waegeneer, M., Pech, U., Kreft, Ł., Aibar, S., Makhzami, S., Christiaens, V., Bravo González-Blas, C., Poovathingal, S., Hulselmans, G., Spanier, K. I., Moerman, T., Vanspauwen, B., Geurs, S., Voet, T., Lammertyn, J., Thienpont, B., … Aerts, S. (2018). A Single-Cell Transcriptome Atlas of the Aging Drosophila Brain. *Cell*, *174*(4), 982–998.e20.

Davies, M. N., & Green, P. R. (1990). Optic flow-field variables trigger landing in hawk but not in pigeons. *Die Naturwissenschaften*, *77*(3), 142–144.

Davis, F. P., Nern, A., Picard, S., Reiser, M. B., Rubin, G. M., Eddy, S. R., & Henry, G. L. (2020). A genetic, genomic, and computational resource for exploring neural circuit function. *eLife*, *9*.

Dawydow, A., Gueta, R., Ljaschenko, D., Ullrich, S., Hermann, M., Ehmann, N., Gao, S., Fiala, A., Langenhan, T., Nagel, G., & Kittel, R. J. (2014). Channelrhodopsin-2-XXL, a powerful optogenetic tool for low-light applications. *Proceedings of the National Academy of Sciences of the United States of America*, *111*(38), 13972–13977.

DeAngelis, B. D., Zavatone-Veth, J. A., & Clark, D. A. (2019). The manifold structure of limb coordination in walking Drosophila. *eLife*, *8*.

de Belle, J. S., & Heisenberg, M. (1996). Expression of Drosophila mushroom body mutations in alternative genetic backgrounds: a case study of the mushroom body miniature gene (mbm). *Proceedings of the National Academy of Sciences of the United States of America*, *93*(18), 9875–9880.

de Bruyne, M., Clyne, P. J., & Carlson, J. R. (1999). Odor coding in a model olfactory organ: the Drosophila maxillary palp. *The Journal of Neuroscience: The Official Journal of the Society for Neuroscience*, *19*(11), 4520–4532.

Deisseroth, K. (2015). Optogenetics: 10 years of microbial opsins in neuroscience. *Nature Neuroscience*, *18*(9), 1213–1225.

Denk, W., Strickler, J. H., & Webb, W. W. (1990). Two-photon laser scanning fluorescence microscopy. *Science*, *248*(4951), 73–76.

Dickinson, M. H., & Muijres, F. T. (2016). The aerodynamics and control of free flight manoeuvres in Drosophila. *Philosophical Transactions of the Royal Society of London. Series B, Biological Sciences*, *371*(1704).

Dietzl, G., Chen, D., Schnorrer, F., Su, K.-C., Barinova, Y., Fellner, M., Gasser, B., Kinsey, K., Oppel, S., Scheiblauer, S., Couto, A., Marra, V., Keleman, K., & Dickson, B. J. (2007). A genome-wide transgenic RNAi library for conditional gene inactivation in Drosophila. *Nature*, *448*(7150), 151–156.

Dionne, H., Hibbard, K. L., Cavallaro, A., Kao, J.-C., & Rubin, G. M. (2018). Genetic Reagents for Making Split-GAL4 Lines in Drosophila. *Genetics*, *209*(1), 31–35.

Douglass, J.K., Strausfeld, N.J. (2007) Diverse speed response properties of motion sensitive neurons in the fly's optic lobe. *J Comp Physiol A,* 193, 233–247.

Drews, M. S., Leonhardt, A., Pirogova, N., Richter, F. G., Schuetzenberger, A., Braun, L., Serbe, E., & Borst, A. (2020). Dynamic Signal Compression for Robust Motion Vision in Flies. *Current Biology: CB*, *30*(2), 209–221.e8.

Duistermars, B. J., Care, R. A., & Frye, M. A. (2012). Binocular interactions underlying the classic optomotor responses of flying flies. *Frontiers in Behavioral Neuroscience*, *6*, 6.

Duistermars, B. J., Chow, D. M., Condro, M., & Frye, M. A. (2007). The spatial, temporal and contrast properties of expansion and rotation flight optomotor responses in Drosophila. *The Journal of Experimental Biology*, *210*(Pt 18), 3218–3227.

Eckert, H. (1980). Functional properties of the H1-neurone in the third optic Ganglion of the Blowfly, Phaenicia. *Journal of Comparative Physiology*, *135*(1), 29–39.

Eckert, H., & Dvorak, D. R. (1983). The centrifugal horizontal cells in the lobula plate of the blowfly, Phaenicia sericata. *Journal of Insect Physiology*, *29*(7), 547–560.

Eckert, M. P., & Zeil, J. (2001). Towards an Ecology of Motion Vision. In J. M. Zanker & J. Zeil (Eds.), *Motion Vision: Computational, Neural, and Ecological Constraints* (pp. 333–369). Springer Berlin Heidelberg.

Efros, Berg, Mori, & Malik. (2003). Recognizing action at a distance. *Proceedings Ninth IEEE International Conference on Computer Vision*, 726–733 vol.2.

Egelhaaf, M. (1985). On the neuronal basis of figure-ground discrimination by relative motion in the visual system of the fly. *Biological Cybernetics*, *52*(3), 195–209.

Egelhaaf, M., & Borst, A. (1989). Transient and steady-state response properties of movement detectors. *Journal of the Optical Society of America. A, Optics and Image Science*, *6*(1), 116–127.

Egelhaaf, M., Hausen, K., Reichardt, W., & Wehrhahn, C. (1988). Visual course control in flies relies on neuronal computation of object and background motion. *Trends in Neurosciences*, *11*(8), 351–358.

Eichner, H., Joesch, M., Schnell, B., Reiff, D. F., & Borst, A. (2011). Internal structure of the fly elementary motion detector. *Neuron*, *70*(6), 1155–1164.

Elyada, Y. M., Haag, J., Borst, A. (2013) Dendritic end inhibition in large-field visual neurons of the fly. *J Neurosci*, 20;33(8):3659-67.

Erickson, R. G., & Thier, P. (1991). A neuronal correlate of spatial stability during periods of self-induced visual motion. *Experimental Brain Research. Experimentelle Hirnforschung. Experimentation Cerebrale*, *86*(3), 608–616.

Estes, P. S., Ho, G. L., Narayanan, R., & Ramaswami, M. (2000). Synaptic localization and restricted diffusion of a Drosophila neuronal synaptobrevin--green fluorescent protein chimera in vivo. *Journal of Neurogenetics*, *13*(4), 233–255.

Farrow, K. (2005). Lateral Interactions and Receptive Field Structure of Lobula Plate Tangential Cells in the Blowfly. *Ludwig-Maximilians-Universität München*.

Farrow, K., Borst, A., & Haag, J. (2005). Sharing receptive fields with your neighbors: tuning the vertical system cells to wide field motion. *The Journal of Neuroscience: The Official Journal of the Society for Neuroscience*, *25*(15), 3985–3993.

Farrow, K., Haag, J., & Borst, A. (2006). Nonlinear, binocular interactions underlying flow field selectivity of a motion-sensitive neuron. *Nature Neuroscience*, *9*(10), 1312–1320.

Feinberg, E. H., Vanhoven, M. K., Bendesky, A., Wang, G., Fetter, R. D., Shen, K., & Bargmann, C. I. (2008). GFP Reconstitution Across Synaptic Partners (GRASP) defines cell contacts and synapses in living nervous systems. *Neuron*, *57*(3), 353–363.

Fenk, L. M., Avritzer, S. C., Weisman, J. L., Nair, A., Randt, L. D., Mohren, T. L., Siwanowicz, I., & Maimon, G. (2022). Muscles that move the retina augment compound eye vision in Drosophila. *Nature*, 1–7.

Fennema, C. L., & Thompson, W. B. (1979). Velocity determination in scenes containing several moving objects. *Computer Graphics and Image Processing*, *9*(4), 301–315.

Ferreira, C. H., & Moita, M. A. (2020). Behavioral and neuronal underpinnings of safety in numbers in fruit flies. *Nature Communications*, *11*(1), 4182.

Fischbach, K.-F., & Dittrich, A. P. M. (1989). The optic lobe of Drosophila melanogaster. I. A Golgi analysis of wild-type structure. *Cell and Tissue Research*, *258*(3), 441–475.
Fischer, P. J., & Schnell, B. (2022). Multiple mechanisms mediate the suppression of motion vision during escape maneuvers in flying Drosophila. *iScience*, *25*(10), 105143.
Fisher, Y. E., Lu, J., D'Alessandro, I., & Wilson, R. I. (2019). Sensorimotor experience remaps visual input to a heading-direction network. *Nature*, *576*(7785), 121–125.
Fisher, Y. E., Yang, H. H., Isaacman-Beck, J., Xie, M., Gohl, D. M., & Clandinin, T. R. (2017). FlpStop, a tool for conditional gene control in Drosophila. *eLife*, *6*.
Flood, T. F., Gorczyca, M., White, B. H., Ito, K., & Yoshihara, M. (2013). A large-scale behavioral screen to identify neurons controlling motor programs in the Drosophila brain. *G3*, *3*(10), 1629–1637.
Franz, M. O., & Krapp, H. G. (2000). Wide-field, motion-sensitive neurons and matched filters for optic flow fields. *Biological Cybernetics*, *83*(3), 185–197.
Fritsches, K. A., & Marshall, N. J. (2002). Independent and conjugate eye movements during optokinesis in teleost fish. *The Journal of Experimental Biology*, *205*(Pt 9), 1241–1252.
Fujiwara, T., Brotas, M., & Chiappe, M. E. (2022). Walking strides direct rapid and flexible recruitment of visual circuits for course control in Drosophila. *Neuron*, *110*(13), 2124–2138.e8.
Fujiwara, T., Cruz, T. L., Bohnslav, J. P., & Chiappe, M. E. (2017). A faithful internal representation of walking movements in the Drosophila visual system. *Nature Neuroscience*, *20*(1), 72–81.
Fu, Q., & Yue, S. (2020). Modelling Drosophila motion vision pathways for decoding the direction of translating objects against cluttered moving backgrounds. *Biological Cybernetics*, *114*(4-5), 443–460.
Ganetzky, B., & Wu, C. F. (1986). Neurogenetics of membrane excitability in Drosophila. *Annual Review of Genetics*, *20*, 13–44.
Geiger, G., & Nässel, D. R. (1981). Visual orientation behaviour of flies after selective laser beam ablation of interneurones. *Nature*, *293*(5831), 398–399.
Gibson, J. J. (1950). The perception of the visual world. *Houghton Mifflin.*
Gong, X., Mendoza-Halliday, D., Ting, J. T., Kaiser, T., Sun, X., Bastos, A. M., Wimmer, R. D., Guo, B., Chen, Q., Zhou, Y., Pruner, M., Wu, C. W.-H., Park, D., Deisseroth, K., Barak, B., Boyden, E. S., Miller, E. K., Halassa, M. M., Fu, Z., … Feng, G. (2020). An Ultra-Sensitive Step-Function Opsin for Minimally Invasive Optogenetic Stimulation in Mice and Macaques. *Neuron*, *107*(1), 38–51.e8.
Götz, K. G. (1968). Flight control in Drosophila by visual perception of motion. *Kybernetik*, *4*(6), 199–208.
Götz, K. G. (1975). The optomotor equilibrium of the Drosophila navigation system. *Journal of Comparative Physiology*, *99*(3), 187–210.
Götz, K. G. (1980). Visual guidance in Drosophila. *Basic Life Sciences*, *16*, 391–407.
Govorunova, E. G., Sineshchekov, O. A., Janz, R., Liu, X., & Spudich, J. L. (2015). NEUROSCIENCE. Natural light-gated anion channels: A family of microbial rhodopsins for advanced optogenetics. *Science*, *349*(6248), 647–650.
Green, J., Vijayan, V., Mussells Pires, P., Adachi, A., & Maimon, G. (2019). A neural heading estimate is compared with an internal goal to guide oriented navigation. *Nature Neuroscience*, *22*(9), 1460–1468.
Gruntman, E., Romani, S., & Reiser, M. B. (2018). Simple integration of fast excitation and offset, delayed inhibition computes directional selectivity in Drosophila. *Nature Neuroscience*, *21*(2), 250–257.
Gu, Y., Angelaki, D. E., & Deangelis, G. C. (2008). Neural correlates of multisensory cue integration in macaque MSTd. *Nature Neuroscience*, *11*(10), 1201–1210.
Gu, Y., Watkins, P. V., Angelaki, D. E., & DeAngelis, G. C. (2006). Visual and nonvisual contributions to three-dimensional heading selectivity in the medial superior temporal area. *The Journal of Neuroscience: The Official Journal of the Society for Neuroscience*, *26*(1), 73–85.

Güiza J., Barría I., Sáez J. C., Vega J. L. (2018). Innexins: Expression, Regulation, and Functions. Front Physiol, 11;9:1414.

Haag, J., Arenz, A., Serbe, E., Gabbiani, F., & Borst, A. (2016). Complementary mechanisms create direction selectivity in the fly. *eLife*, *5*.

Haag, J., & Borst, A. (2001). Recurrent network interactions underlying flow-field selectivity of visual interneurons. *The Journal of Neuroscience: The Official Journal of the Society for Neuroscience*, *21*(15), 5685–5692.

Haag, J., & Borst, A. (2002). Dendro-dendritic interactions between motion-sensitive large-field neurons in the fly. *The Journal of Neuroscience: The Official Journal of the Society for Neuroscience*, *22*(8), 3227–3233.

Haag, J., & Borst, A. (2003). Orientation tuning of motion-sensitive neurons shaped by vertical-horizontal network interactions. *Journal of Comparative Physiology. A, Neuroethology, Sensory, Neural, and Behavioral Physiology*, *189*(5), 363–370.

Haag, J., & Borst, A. (2004). Neural mechanism underlying complex receptive field properties of motion-sensitive interneurons. *Nature Neuroscience*, *7*(6), 628–634.

Haag, J., & Borst, A. (2008). Electrical coupling of lobula plate tangential cells to a heterolateral motion-sensitive neuron in the fly. *The Journal of Neuroscience: The Official Journal of the Society for Neuroscience*, *28*(53), 14435–14442.

Haag, J., Mishra, A., & Borst, A. (2017). A common directional tuning mechanism of Drosophila motion-sensing neurons in the ON and in the OFF pathway. *eLife*, *6*.

Haag, J., Wertz, A., & Borst, A. (2007). Integration of lobula plate output signals by DNOVS1, an identified premotor descending neuron. *The Journal of Neuroscience: The Official Journal of the Society for Neuroscience*, *27*(8), 1992–2000.

Haag, J., Wertz, A., & Borst, A. (2010). Central gating of fly optomotor response. *Proceedings of the National Academy of Sciences of the United States of America*, *107*(46), 20104–20109.

Hadjieconomou, D., Rotkopf, S., Alexandre, C., Bell, D. M., Dickson, B. J., & Salecker, I. (2011). Flybow: genetic multicolor cell labeling for neural circuit analysis in Drosophila melanogaster. *Nature Methods*, *8*(3), 260–266.

Haikala, V., Joesch, M., Borst, A., & Mauss, A. S. (2013). Optogenetic control of fly optomotor responses. *The Journal of Neuroscience: The Official Journal of the Society for Neuroscience*, *33*(34), 13927–13934.

Hamada, F. N., Rosenzweig, M., Kang, K., Pulver, S. R., Ghezzi, A., Jegla, T. J., & Garrity, P. A. (2008). An internal thermal sensor controlling temperature preference in Drosophila. *Nature*, *454*(7201), 217–220.

Hammond, S., & O'Shea, M. (2007). Escape flight initiation in the fly. *Journal of Comparative Physiology. A, Neuroethology, Sensory, Neural, and Behavioral Physiology*, *193*(4), 471–476.

Hansen, S. B. (2015) Lipid agonism: The PIP2 paradigm of ligand-gated ion channels. *Biochim. Biophys. Acta - Mol. Cell Biol. Lipids*. 1851(5), 620-628.

Hardie, R. C. (1985). Functional Organization of the Fly Retina. In *Progress in Sensory Physiology* (pp. 1–79). Springer Berlin Heidelberg.

Hassenstein, B. (1951). Ommatidienraster und afferente Bewegungsintegration. *Zeitschrift Fur Vergleichende Physiologie*, *33*(4), 301–326.

Hassenstein, B., & Reichardt, W. (1956). Systemtheoretische Analyse der Zeit-, Reihenfolgen- und Vorzeichenauswertung bei der Bewegungsperzeption des Rüsselkäfers Chlorophanus. *Zeitschrift Für Naturforschung B*, *11*(9-10), 513–524.

Hausen, K. (1981). Monocular and binocular computation of motion in the lobula plate of the fly. *Verh. Dtsch.* Zool. *Ges.* 1981, 49-70.

Hausen, K. (1984). The Lobula-Complex of the Fly: Structure, Function and Significance in Visual Behaviour. In M. A. Ali (Ed.), *Photoreception and Vision in Invertebrates* (pp. 523–559). Springer US.

Hausen, K., Wehrhahn, C., & Boycott, B. B. (1983). Microsurgical lesion of horizontal cells changes optomotor yaw responses in the blowfly Calliphora erythrocephala. *Proceedings of the Royal Society of London. Series B. Biological Sciences*, *219*(1215), 211–216.

Heisenberg, M. (1972). Comparative behavioral studies on two visual mutants of Drosophila. *Journal of Comparative Physiology*, *80*(2), 119–136.

Heisenberg, M., & Wolf, R. (1979). On the fine structure of yaw torque in visual flight orientation of Drosophila melanogaster. *Journal of Comparative Physiology*, *130*(2), 113–130.

Heisenberg, M., Wonneberger, R., & Wolf, R. (1978). Optomotor-blindH31—a Drosophila mutant of the lobula plate giant neurons. *Journal of Comparative Physiology*, *124*(4), 287–296.

Helmchen, F. (2009). Two-photon functional imaging of neuronal activity. *In Vivo Optical Imaging of Brain Function*, 428.

Hindmarsh Sten, T., Li, R., Otopalik, A., & Ruta, V. (2021). Sexual arousal gates visual processing during Drosophila courtship. *Nature*, *595*(7868), 549–553.

Honegger, K., & de Bivort, B. (2018). Stochasticity, individuality and behavior. *Current Biology: CB*, *28*(1), R8–R12.

Hotta, Y., & Benzer, S. (1969). Abnormal electroretinograms in visual mutants of Drosophila. *Nature*, *222*(5191), 354–356.

Hou, H., Zheng, Q., Zhao, Y., Pouget, A., & Gu, Y. (2019). Neural Correlates of Optimal Multisensory Decision Making under Time-Varying Reliabilities with an Invariant Linear Probabilistic Population Code. *Neuron*, *104*(5), 1010–1021.e10.

Hu, A., Zhang, W., & Wang, Z. (2010). Functional feedback from mushroom bodies to antennal lobes in the Drosophila olfactory pathway. *Proceedings of the National Academy of Sciences of the United States of America*, *107*(22), 10262–10267.

Hürkey S., Niemeyer N., Schleimer J-H., Ryglewski S., Schreiber S., Duch C. (2022). Insect asynchronous flight requires neural circuit de-synchronization by electrical synapses. In *bioRxiv* (p. 478622).

Huston, S. J., & Krapp, H. G. (2008). Visuomotor transformation in the fly gaze stabilization system. *PLoS Biology*, *6*(7), e173.

Hwang, R. Y., Zhong, L., Xu, Y., Johnson, T., Zhang, F., Deisseroth, K., & Tracey, W. D. (2007). Nociceptive neurons protect Drosophila larvae from parasitoid wasps. *Current Biology: CB*, *17*(24), 2105–2116.

Isaacman-Beck, J., Paik, K. C., Wienecke, C. F. R., Yang, H. H., Fisher, Y. E., Wang, I. E., Ishida, I. G., Maimon, G., Wilson, R. I., & Clandinin, T. R. (2020). SPARC enables genetic manipulation of precise proportions of cells. *Nature Neuroscience*, *23*(9), 1168–1175.

Jan, L. Y., & Jan, Y. N. (1976). Properties of the larval neuromuscular junction in Drosophila melanogaster. *The Journal of Physiology*, *262*(1), 189–214.

Jayaraman, V., & Laurent, G. (2007). Evaluating a genetically encoded optical sensor of neural activity using electrophysiology in intact adult fruit flies. *Frontiers in Neural Circuits*, *1*, 3.

Jenett, A., Rubin, G. M., Ngo, T.-T. B., Shepherd, D., Murphy, C., Dionne, H., Pfeiffer, B. D., Cavallaro, A., Hall, D., Jeter, J., Iyer, N., Fetter, D., Hausenfluck, J. H., Peng, H., Trautman, E. T., Svirskas, R. R., Myers, E. W., Iwinski, Z. R., Aso, Y., … Zugates, C. T. (2012). A GAL4-driver line resource for Drosophila neurobiology. *Cell Reports*, *2*(4), 991–1001.

Jia, Y., Xu, R.-G., Ren, X., Ewen-Campen, B., Rajakumar, R., Zirin, J., Yang-Zhou, D., Zhu, R., Wang, F., Mao, D., Peng, P., Qiao, H.-H., Wang, X., Liu, L.-P., Xu, B., Ji, J.-Y., Liu, Q., Sun, J., Perrimon, N., & Ni, J.-Q. (2018). Next-generation CRISPR/Cas9 transcriptional activation in *Drosophila* using flySAM. *Proceedings of the National Academy of Sciences of the United States of America*, *115*(18), 4719–4724.

Joesch, M., Plett, J., Borst, A., & Reiff, D. F. (2008). Response properties of motion-sensitive visual interneurons in the lobula plate of Drosophila melanogaster. *Current Biology: CB*, *18*(5), 368–374.

Joesch, M., Schnell, B., Raghu, S. V., Reiff, D. F., & Borst, A. (2010). ON and OFF pathways in Drosophila motion vision. *Nature*, *468*(7321), 300–304.

Joesch, M., Weber, F., Eichner, H., & Borst, A. (2013). Functional specialization of parallel motion detection circuits in the fly. *The Journal of Neuroscience: The Official Journal of the Society for Neuroscience*, *33*(3), 902–905.

Juusola, M., Dau, A., Song, Z., Solanki, N., Rien, D., Jaciuch, D., Dongre, S. A., Blanchard, F., de Polavieja, G. G., Hardie, R. C., & Takalo, J. (2017). Microsaccadic sampling of moving image information provides Drosophila hyperacute vision. *eLife*, *6*. https://doi.org/10.7554/eLife.26117

Kaiser, M. K., & Mowafy, L. (1993). Optical specification of time-to-passage: observers' sensitivity to global tau. *Journal of Experimental Psychology. Human Perception and Performance*, *19*(5), 1028–1040.

Kaplan, W. D., & Trout, W. E., 3rd. (1969). The behavior of four neurological mutants of Drosophila. *Genetics*, *61*(2), 399–409.

Kathman, N. D., & Fox, J. L. (2019). Representation of Haltere Oscillations and Integration with Visual Inputs in the Fly Central Complex. *The Journal of Neuroscience: The Official Journal of the Society for Neuroscience*, *39*(21), 4100–4112.

Kim, A. J., Fenk, L. M., Lyu, C., & Maimon, G. (2017). Quantitative Predictions Orchestrate Visual Signaling in Drosophila. *Cell*, *168*(1-2), 280–294.e12.

Kim, A. J., Fitzgerald, J. K., & Maimon, G. (2015). Cellular evidence for efference copy in Drosophila visuomotor processing. *Nature Neuroscience*, *18*(9), 1247–1255.

Kim, S. S., Rouault, H., Druckmann, S., & Jayaraman, V. (2017). Ring attractor dynamics in the Drosophila central brain. *Science*, *356*(6340), 849–853.

Kirk, M. J., Benlian, B. R., Han, Y., Gold, A., Ravi, A., Deal, P. E., Molina, R. S., Drobizhev, M., Dickman, D., Scott, K., & Miller, E. W. (2021). Voltage Imaging in Drosophila Using a Hybrid Chemical-Genetic Rhodamine Voltage Reporter. *Frontiers in Neuroscience*, *15*, 754027.

Kitamoto, T. (2001). Conditional modification of behavior in Drosophila by targeted expression of a temperature-sensitive shibire allele in defined neurons. *Journal of Neurobiology*, *47*(2), 81–92.

Klapoetke, N. C., Murata, Y., Kim, S. S., Pulver, S. R., Birdsey-Benson, A., Cho, Y. K., Morimoto, T. K., Chuong, A. S., Carpenter, E. J., Tian, Z., Wang, J., Xie, Y., Yan, Z., Zhang, Y., Chow, B. Y., Surek, B., Melkonian, M., Jayaraman, V., Constantine-Paton, M., … Boyden, E. S. (2014). Independent optical excitation of distinct neural populations. *Nature Methods*, *11*(3), 338–346.

Kleinlogel, S., Feldbauer, K., Dempski, R. E., Fotis, H., Wood, P. G., Bamann, C., & Bamberg, E. (2011). Ultralight-sensitive and fast neuronal activation with the Ca^2+-permeable channelrhodopsin CatCh. *Nature Neuroscience*, *14*(4), 513–518.

Klibaite, U., & Shaevitz, J. W. (2020). Paired fruit flies synchronize behavior: Uncovering social interactions in Drosophila melanogaster. *PLoS Computational Biology*, *16*(10), e1008230.

Knowles-Barley, S., Longair, M., & Armstrong, J. D. (2010). BrainTrap: a database of 3D protein expression patterns in the Drosophila brain. *Database: The Journal of Biological Databases and Curation*, *2010*, baq005.

Koenderink, J. J. (1986). Optic flow. *Vision Research*, *26*(1), 161–179.

Komatsuzaki, A., Harris, H. E., Alpert, J., & Cohen, B. (1969). Horizontal nystagmus of rhesus monkeys. *Acta Oto-Laryngologica*, *67*(5), 535–551.

Krapp, H. G. (2000). Neuronal Matched Filters for Optic Flow Processing in Flying Insects. In M. Lappe (Ed.), *International Review of Neurobiology* (Vol. 44, pp. 93–120). Academic Press.

Krapp, H. G., Hengstenberg, B., & Hengstenberg, R. (1998). Dendritic structure and receptive-field organization of optic flow processing interneurons in the fly. *Journal of Neurophysiology*, *79*(4), 1902–1917.

Krapp, H. G., & Hengstenberg, R. (1996). Estimation of self-motion by optic flow processing in single visual interneurons. *Nature*, *384*(6608), 463–466.

Kurmangaliyev, Y. Z., Yoo, J., Valdes-Aleman, J., Sanfilippo, P., & Zipursky, S. L. (2020). Transcriptional Programs of Circuit Assembly in the Drosophila Visual System. *Neuron*, *108*(6), 1045–1057.e6.

Kurtz, R., Warzecha, A. K., & Egelhaaf, M. (2001). Transfer of visual motion information via graded synapses operates linearly in the natural activity range. *The Journal of Neuroscience: The Official Journal of the Society for Neuroscience*, *21*(17), 6957–6966.

Lai, S.-L., & Lee, T. (2006). Genetic mosaic with dual binary transcriptional systems in Drosophila. *Nature Neuroscience*, *9*(5), 703–709.

LaJeunesse, D. R., Buckner, S. M., Lake, J., Na, C., Pirt, A., & Fromson, K. (2004). Three new Drosophila markers of intracellular membranes. *BioTechniques*, *36*(5), 784–788, 790.

Land, M. F. (1999). Motion and vision: why animals move their eyes. *Journal of Comparative Physiology. A, Sensory, Neural, and Behavioral Physiology*, *185*(4), 341–352.

Land, M. F. (2015). Eye movements of vertebrates and their relation to eye form and function. *Journal of Comparative Physiology. A, Neuroethology, Sensory, Neural, and Behavioral Physiology*, *201*(2), 195–214.

Larsen, C. W., Hirst, E., Alexandre, C., & Vincent, J.-P. (2003). Segment boundary formation in Drosophila embryos. *Development*, *130*(23), 5625–5635.

Lee, D. N., Lishman, J. R., & Thomson, J. A. (1982). Regulation of gait in long jumping. *Journal of Experimental Psychology. Human Perception and Performance*, *8*(3), 448–459.

Lee, D. N., & Reddish, P. E. (1981). Plummeting gannets: a paradigm of ecological optics. *Nature*, *293*(5830), 293–294.

Lee, T., & Luo, L. (1999). Mosaic analysis with a repressible cell marker for studies of gene function in neuronal morphogenesis. *Neuron*, *22*(3), 451–461.

Lehmann, F.-O., Schützner, P., & Wang, H. (2012). Visual motion sensing and flight path control in flies. In F. G. Barth, J. A. C. Humphrey, & M. V. Srinivasan (Eds.), *Frontiers in Sensing: From Biology to Engineering* (pp. 129–141). Springer Vienna.

Lehrer, M., Srinivasan, M. V., Zhang, S. W., & Horridge, G. A. (1988). Motion cues provide the bee's visual world with a third dimension. *Nature*, *332*(6162), 356–357.

Lima, S. Q., & Miesenböck, G. (2005). Remote control of behavior through genetically targeted photostimulation of neurons. *Cell*, *121*(1), 141–152.

Limb, J. O., & Murphy, J. A. (1975). Estimating the Velocity of Moving Images in Television Signals. *Computer Graphics and Image Processing*, *4*(4), 311–327.

Lin, J. Y. (2011). A user's guide to channelrhodopsin variants: features, limitations and future developments. *Experimental Physiology*, *96*(1), 19–25.

Lin, J. Y., Knutsen, P. M., Muller, A., Kleinfeld, D., & Tsien, R. Y. (2013). ReaChR: a red-shifted variant of channelrhodopsin enables deep transcranial optogenetic excitation. *Nature Neuroscience*, *16*(10), 1499–1508.

Liu, S., Lin, C., Xu, Y., Luo, H., Peng, L., Zeng, X., Zheng, H., Chen, P. R., & Zou, P. (2021). A far-red hybrid voltage indicator enabled by bioorthogonal engineering of rhodopsin on live neurons. *Nature Chemistry*, *13*(5), 472–479.

Longden, K. D., & Krapp, H. G. (2009). State-dependent performance of optic-flow processing interneurons. *Journal of Neurophysiology*, *102*(6), 3606–3618.

Longden, K. D., Muzzu, T., Cook, D. J., Schultz, S. R., & Krapp, H. G. (2014). Nutritional state modulates the neural processing of visual motion. *Current Biology: CB*, *24*(8), 890–895.

Luan, H., Peabody, N. C., Vinson, C. R., & White, B. H. (2006). Refined spatial manipulation of neuronal function by combinatorial restriction of transgene expression. *Neuron*, *52*(3), 425–436.

Mahn, M., Gibor, L., Patil, P., Cohen-Kashi Malina, K., Oring, S., Printz, Y., Levy, R., Lampl, I., & Yizhar, O. (2018). High-efficiency optogenetic silencing with soma-targeted anion-conducting channelrhodopsins. *Nature Communications*, *9*(1), 4125.

Maimon, G., Straw, A. D., & Dickinson, M. H. (2008). A simple vision-based algorithm for decision making in flying Drosophila. *Current Biology: CB*, *18*(6), 464–470.

Maimon, G., Straw, A. D., & Dickinson, M. H. (2010). Active flight increases the gain of visual motion processing in Drosophila. *Nature Neuroscience*, *13*(3), 393–399.

Maisak, M. S., Haag, J., Ammer, G., Serbe, E., Meier, M., Leonhardt, A., Schilling, T., Bahl, A., Rubin, G. M., Nern, A., Dickson, B. J., Reiff, D. F., Hopp, E., & Borst, A. (2013). A directional tuning map of Drosophila elementary motion detectors. *Nature*, *500*(7461), 212–216.

Ma, J., & Ptashne, M. (1987). The carboxy-terminal 30 amino acids of GAL4 are recognized by GAL80. *Cell*, *50*(1), 137–142.

Mangleburg, C. G., Wu, T., Yalamanchili, H. K., Guo, C., Hsieh, Y.-C., Duong, D. M., Dammer, E. B., De Jager, P. L., Seyfried, N. T., Liu, Z., & Shulman, J. M. (2020). Integrated analysis of the aging brain transcriptome and proteome in tauopathy. *Molecular Neurodegeneration*, *15*(1), 56.

Martín, F., & Alcorta, E. (2017). Novel genetic approaches to behavior in Drosophila. *Journal of Neurogenetics*, *31*(4), 288–299.

Matin, E. (1974). Saccadic suppression: a review and an analysis. *Psychological Bulletin*, *81*(12), 899–917.

Matsunaga T., Kohsaka H., Nose A. (2017). Gap Junction-Mediated Signaling from Motor Neurons Regulates Motor Generation in the Central Circuits of Larval *Drosophila*. *J Neurosci*, 22;37(8):2045-2060

Mauss, A. S., Busch, C., & Borst, A. (2017). Optogenetic Neuronal Silencing in Drosophila during Visual Processing. *Scientific Reports*, *7*(1), 13823.

Mauss, A. S., Pankova, K., Arenz, A., Nern, A., Rubin, G. M., & Borst, A. (2015). Neural Circuit to Integrate Opposing Motions in the Visual Field. *Cell*, *162*(2), 351–362.

Mamiya, A., Straw, A.D., Tómasson, E., Dickinson, M.H. (2011). Active and Passive Antennal Movements during Visually Guided Steering in Flying *Drosophila*. *The Journal of Neuroscience: The Official Journal of the Society for Neuroscience*, *31*(18), 6900–6914.

McCann, G. D., & MacGinitie, G. F. (1965). Optomotor response studies of insect vision. *Proceedings of the Royal Society of London. Series B, Containing Papers of a Biological Character. Royal Society*, *163*(992), 369–401.

McEwen, R. S. (1918). The reactions to light and to gravity in Drosophila and its mutants. *The Journal of Experimental Zoology*, *25*(1), 49–106.

McGuire, S. E., Mao, Z., & Davis, R. L. (2004). Spatiotemporal gene expression targeting with the TARGET and gene-switch systems in Drosophila. *Science's STKE: Signal Transduction Knowledge Environment*, *2004*(220), l6.

Meier, M., & Borst, A. (2019). Extreme Compartmentalization in a Drosophila Amacrine Cell. *Current Biology: CB*, *29*(9), 1545–1550.e2.

Mendes, C. S., Bartos, I., Akay, T., Márka, S., & Mann, R. S. (2013). Quantification of gait parameters in freely walking wild type and sensory deprived Drosophila melanogaster. *eLife*, *2*, e00231.

Milde, J. J., & Strausfeld, N. J. (1986). Visuo-motor pathways in arthropods. *Die Naturwissenschaften*, *73*(3), 151–154.

Milde, M. B., Bertrand, O. J. N., Benosmanz, R., Egelhaaf, M., & Chicca, E. (2015). Bioinspired event-driven collision avoidance algorithm based on optic flow. *2015 International Conference on Event-Based Control, Communication, and Signal Processing (EBCCSP)*, 1–7.

Mimura, K. (1982). Discrimination of some visual patterns inDrosophila melanogaster. *Journal of Comparative Physiology*, *146*(2), 229–233.

Mohamed, G. A., Cheng, R.-K., Ho, J., Krishnan, S., Mohammad, F., Claridge-Chang, A., & Jesuthasan, S. (2017). Optical inhibition of larval zebrafish behaviour with anion channelrhodopsins. *BMC Biology*, *15*(1), 103.

Mohammad, F., Stewart, J. C., Ott, S., Chlebikova, K., Chua, J. Y., Koh, T.-W., Ho, J., & Claridge-Chang, A. (2017). Optogenetic inhibition of behavior with anion channelrhodopsins. *Nature Methods*, *14*(3), 271–274.

Mollá-Albaladejo, R., & Sánchez-Alcañiz, J. A. (2021). Behavior Individuality: A Focus on Drosophila melanogaster. *Frontiers in Physiology*, *12*, 719038.

Mostany, R., Miquelajauregui, A., Shtrahman, M., & Portera-Cailliau, C. (2015). Two-photon excitation microscopy and its applications in neuroscience. *Methods in Molecular Biology*, *1251*, 25–42.

Murthy, M., Fiete, I., & Laurent, G. (2008). Testing odor response stereotypy in the Drosophila mushroom body. *Neuron*, *59*(6), 1009–1023.

Nakai, J., Ohkura, M., & Imoto, K. (2001). A high signal-to-noise Ca(2+) probe composed of a single green fluorescent protein. *Nature Biotechnology*, *19*(2), 137–141.

Nern, A., Pfeiffer, B. D., & Rubin, G. M. (2015). Optimized tools for multicolor stochastic labeling reveal diverse stereotyped cell arrangements in the fly visual system. *Proceedings of the National Academy of Sciences of the United States of America*, *112*(22), E2967–E2976.

Nitabach, M. N., Wu, Y., Sheeba, V., Lemon, W. C., Strumbos, J., Zelensky, P. K., White, B. H., & Holmes, T. C. (2006). Electrical hyperexcitation of lateral ventral pacemaker neurons desynchronizes downstream circadian oscillators in the fly circadian circuit and induces multiple behavioral periods. *The Journal of Neuroscience: The Official Journal of the Society for Neuroscience*, *26*(2), 479–489.

Nityananda, V., & Read, J. C. A. (2017). Stereopsis in animals: evolution, function and mechanisms. *The Journal of Experimental Biology*, *220*(Pt 14), 2502–2512.

Ohradzansky, M., Alvarez, H. E., Keshavan, J., Ranganathan, B. N., & Humbert, J. S. (2018). Autonomous Bio-Inspired Small-Object Detection and Avoidance. *2018 IEEE International Conference on Robotics and Automation (ICRA)*, 3442–3447.

Orlandi, N. (2013). Embedded Seeing: Vision in the Natural World. *Noûs*, *47*(4), 727–747.

Pak, W. L., Grossfield, J., & White, N. V. (1969). Nonphototactic mutants in a study of vision of Drosophila. *Nature*, *222*(5191), 351–354.

Palacios-Prado, N., Huetteroth, W., & Pereda, A. E. (2014). Hemichannel composition and electrical synaptic transmission: molecular diversity and its implications for electrical rectification. *Frontiers in Cellular Neuroscience*, *8*, 324.

Pan, C., Deng, H., Yin, X. F., & Liu, J. G. (2011). An optical flow-based integrated navigation system inspired by insect vision. *Biological Cybernetics*, *105*(3-4), 239–252.

Patro, R., Duggal, G., Love, M. I., Irizarry, R. A., & Kingsford, C. (2017). Salmon provides fast and bias-aware quantification of transcript expression. *Nature Methods*, *14*(4), 417–419.

Peirce, J., Gray, J. R., Simpson, S., MacAskill, M., Höchenberger, R., Sogo, H., Kastman, E., & Lindeløv, J. K. (2019). PsychoPy2: Experiments in behavior made easy. *Behavior Research Methods*, *51*(1), 195–203.

Pézier, A. P., Jezzini, S. H., Bacon, J. P., & Blagburn, J. M. (2016). Shaking B Mediates Synaptic Coupling between Auditory Sensory Neurons and the Giant Fiber of Drosophila melanogaster. *PloS One*, *11*(4), e0152211.

Pfeiffer, B. D., Ngo, T.-T. B., Hibbard, K. L., Murphy, C., Jenett, A., Truman, J. W., & Rubin, G. M. (2010). Refinement of tools for targeted gene expression in Drosophila. *Genetics*, *186*(2), 735–755.

Pflugfelder, G. O., Roth, H., Poeck, B., Kerscher, S., Schwarz, H., Jonschker, B., & Heisenberg, M. (1992). The lethal(1)optomotor-blind gene of Drosophila melanogaster is a major organizer of optic lobe development: isolation and characterization of the gene. *Proceedings of the National Academy of Sciences of the United States of America*, *89*(4), 1199–1203.

Phelan, P. (2005) Innexins: members of an evolutionarily conserved family of gap-junction proteins. *Biochim Biophys Acta Biomembr,* 1711(2), 225-245.

Phelan, P., Bacon, J. P., Davies, J. A., Stebbings, L. A., Todman, M. G., Avery, L., Baines, R. A., Barnes, T. M., Ford, C., Hekimi, S., Lee, R., Shaw, J. E., Starich, T. A., Curtin, K. D., Sun, Y. A., & Wyman, R. J. (1998). Innexins: a family of invertebrate gap-junction proteins. *Trends in Genetics: TIG*, *14*(9), 348–349.

Phelan, P., Goulding, L. A., Tam, J. L. Y., Allen, M. J., Dawber, R. J., Davies, J. A., & Bacon, J. P. (2008). Molecular mechanism of rectification at identified electrical synapses in the Drosophila giant fiber system. *Current Biology: CB*, *18*(24), 1955–1960.

Phelan, P., Nakagawa, M., Wilkin, M. B., Moffat, K. G., O'Kane, C. J., Davies, J. A., & Bacon, J. P. (1996). Mutations in shaking-B prevent electrical synapse formation in the Drosophila giant fiber system. *The Journal of Neuroscience: The Official Journal of the Society for Neuroscience*, *16*(3), 1101–1113.

Phelan, P., Stebbings, L. A., Baines, R. A., Bacon, J. P., Davies, J. A., & Ford, C. (1998). Drosophila Shaking-B protein forms gap junctions in paired Xenopus oocytes. *Nature*, *391*(6663), 181–184.

Platisa, J., Ye, X., Ahrens, A. M., Liu, C., Chen, I. A., Davison, I. G., Tian, L., Pieribone, V. A., & Chen, J. L. (2021). High-Speed Low-Light In Vivo Two-Photon Voltage Imaging of Large Neuronal Populations. In *bioRxiv* (p. 2021.12.07.471668).

Portugues, R., & Engert, F. (2009). The neural basis of visual behaviors in the larval zebrafish. *Current Opinion in Neurobiology*, *19*(6), 644–647.

Potter, C. J., Tasic, B., Russler, E. V., Liang, L., & Luo, L. (2010). The Q system: a repressible binary system for transgene expression, lineage tracing, and mosaic analysis. *Cell*, *141*(3), 536–548.

Pratt, D. W. (1982). Saccadic eye movements are coordinated with head movements in walking chickens. *The Journal of Experimental Biology*, *97*, 217–223.

Ramakrishnan A., Sheeba V. (2021). Gap junction protein Innexin2 modulates the period of free-running rhythms in *Drosophila melanogaster*. *iScience*, 20;24(9):103011.

Ramdya, P., Lichocki, P., Cruchet, S., Frisch, L., Tse, W., Floreano, D., & Benton, R. (2015). Mechanosensory interactions drive collective behaviour in Drosophila. *Nature*, *519*(7542), 233–236.

Ramon y Cajal S, Sanchez D. (1915). Contribución al conocimiento de los centros nerviosos de los insectos. *Trabajos del Laboratorio de Investigaciones biológicas de la Universidad de Madrid.*

Ramos-Traslosheros, G., Henning, M. & Silies, M. Motion detection: cells, circuits and algorithms. *Neuroforum*, vol. 24, no. 2, 2018, pp. A61-A72.

Raphan, T., Cohen, B., Suzuki, J., & Henn, V. (1983). Nystagmus generated by sinusoidal pitch while rotating. *Brain Research*, *276*(1), 165–172.

Reichardt, W. (1957). Autokorrelations-Auswertung als Funktionsprinzip des Zentralnervensystems. *Zeitschrift Für Naturforschung B*, *12*(7), 448–457.

Riabinina, O., Luginbuhl, D., Marr, E., Liu, S., Wu, M. N., Luo, L., & Potter, C. J. (2015). Improved and expanded Q-system reagents for genetic manipulations. *Nature Methods*, *12*(3), 219–222.

Richter, F. G., Fendl, S., Haag, J., Drews, M. S., & Borst, A. (2018). Glutamate Signaling in the Fly Visual System. In *iScience* (Vol. 7, pp. 85–95).

Robie, A. A., Hirokawa, J., Edwards, A. W., Umayam, L. A., Lee, A., Phillips, M. L., Card, G. M., Korff, W., Rubin, G. M., Simpson, J. H., Reiser, M. B., & Branson, K. (2017). Mapping the Neural Substrates of Behavior. *Cell*, *170*(2), 393–406.e28.

Roman, G., Endo, K., Zong, L., & Davis, R. L. (2001). PSwitch, a system for spatial and temporal control of gene expression in *Drosophila melanogaster*. *Proceedings of the National Academy of Sciences*, *98*(22), 12602–12607.

Rooke, R., Rasool, A., Schneider, J., & Levine, J. D. (2020). Drosophila melanogaster behaviour changes in different social environments based on group size and density. *Communications Biology*, *3*(1), 304.

Rosenzweig, M., Brennan, K. M., Tayler, T. D., Phelps, P. O., Patapoutian, A., & Garrity, P. A. (2005). The Drosophila ortholog of vertebrate TRPA1 regulates thermotaxis. *Genes & Development*, *19*(4), 419–424.

Rovainen, C. M. (1976). Vestibulo-ocular reflexes in the adult sea lamprey. *Journal of Comparative Physiology*, *112*(2), 159–164.

Rubin, G. M., & Spradling, A. C. (1982). Genetic transformation of Drosophila with transposable element vectors. *Science*, *218*(4570), 348–353.

Sandeman, D. C., & Okajima, A. (1973). Statocyst-Induced Eye Movements in the Crab Scylla Serrata: II. The Responses of the Eye Muscles. *The Journal of Experimental Biology*, *58*(1), 197–212.

Scheffer, L. K., Xu, C. S., Januszewski, M., Lu, Z., Takemura, S.-Y., Hayworth, K. J., Huang, G. B., Shinomiya, K., Maitlin-Shepard, J., Berg, S., Clements, J., Hubbard, P. M., Katz, W. T., Umayam, L., Zhao, T., Ackerman, D., Blakely, T., Bogovic, J., Dolafi, T., … Plaza, S. M. (2020). A connectome and analysis of the adult Drosophila central brain. *eLife*, *9*. https://doi.org/10.7554/eLife.57443

Schnell, B., Joesch, M., Forstner, F., Raghu, S. V., Otsuna, H., Ito, K., Borst, A., & Reiff, D. F. (2010). Processing of horizontal optic flow in three visual interneurons of the Drosophila brain. *Journal of Neurophysiology*, *103*(3), 1646–1657.

Schnell, B., Raghu, S. V., Nern, A., & Borst, A. (2012). Columnar cells necessary for motion responses of wide-field visual interneurons in Drosophila. *Journal of Comparative Physiology. A, Neuroethology, Sensory, Neural, and Behavioral Physiology*, *198*(5), 389–395.

Schnell, B., Weir, P. T., Roth, E., Fairhall, A. L., & Dickinson, M. H. (2014). Cellular mechanisms for integral feedback in visually guided behavior. *Proceedings of the National Academy of Sciences of the United States of America*, *111*(15), 5700–5705.

Schroll, C., Riemensperger, T., Bucher, D., Ehmer, J., Völler, T., Erbguth, K., Gerber, B., Hendel, T., Nagel, G., Buchner, E., & Fiala, A. (2006). Light-induced activation of distinct modulatory neurons triggers appetitive or aversive learning in Drosophila larvae. *Current Biology: CB*, *16*(17), 1741–1747.

Seelig, J. D., Chiappe, M. E., Lott, G. K., Dutta, A., Osborne, J. E., Reiser, M. B., & Jayaraman, V. (2010). Two-photon calcium imaging from head-fixed Drosophila during optomotor walking behavior. *Nature Methods*, *7*(7), 535–540.

Serres, J., & Ruffier, F. (2016). Optic flow-based robotics. In *Wiley Encyclopedia of Electrical and Electronics Engineering* (pp. 1–14).

Serres, J. R., & Viollet, S. (2018). Insect-inspired vision for autonomous vehicles. *Current Opinion in Insect Science*, *30*, 46–51.

Shearin, H. K., Macdonald, I. S., Spector, L. P., & Stowers, R. S. (2014). Hexameric GFP and mCherry reporters for the Drosophila GAL4, Q, and LexA transcription systems. *Genetics*, *196*(4), 951–960.

Sheeba, V., Sharma, V. K., Gu, H., Chou, Y.-T., O'Dowd, D. K., & Holmes, T. C. (2008). Pigment dispersing factor-dependent and -independent circadian locomotor behavioral rhythms. *The Journal of Neuroscience: The Official Journal of the Society for Neuroscience*, *28*(1), 217–227.

Shinomiya, K., Huang, G., Lu, Z., Parag, T., Xu, C. S., Aniceto, R., Ansari, N., Cheatham, N., Lauchie, S., Neace, E., Ogundeyi, O., Ordish, C., Peel, D., Shinomiya, A., Smith, C., Takemura, S., Talebi, I., Rivlin, P. K., Nern, A., … Meinertzhagen, I. A. (2019). Comparisons between the ON- and OFF-edge motion pathways in the Drosophila brain. *eLife*, *8*. https://doi.org/10.7554/eLife.40025

Silies, M., Gohl, D. M., Fisher, Y. E., Freifeld, L., Clark, D. A., & Clandinin, T. R. (2013). Modular use of peripheral input channels tunes motion-detecting circuitry. *Neuron*, *79*(1), 111–127.

Smith, L. A., Peixoto, A. A., Kramer, E. M., Villella, A., & Hall, J. C. (1998). Courtship and visual defects of cacophony mutants reveal functional complexity of a calcium-channel alpha1 subunit in Drosophila. *Genetics*, *149*(3), 1407–1426.

Srinivasan, M. V., Lehrer, M., Kirchner, W. H., & Zhang, S. W. (1991). Range perception through apparent image speed in freely flying honeybees. *Visual Neuroscience*, *6*(5), 519–535.

Srinivasan, M. V., Zhang, S., & Chahl, J. S. (2001). Landing strategies in honeybees, and possible applications to autonomous airborne vehicles. *The Biological Bulletin*, *200*(2), 216–221.

Srinivasan, M. V., Zhang, S. W., Chahl, J. S., Barth, E., & Venkatesh, S. (2000). How honeybees make grazing landings on flat surfaces. *Biological Cybernetics*, *83*(3), 171–183.

Srinivasan, M., Zhang, S., Lehrer, M., & Collett, T. (1996). Honeybee navigation en route to the goal: visual flight control and odometry. *The Journal of Experimental Biology*, *199*(Pt 1), 237–244.

Stowers, J. R., Hofbauer, M., Bastien, R., Griessner, J., Higgins, P., Farooqui, S., Fischer, R. M., Nowikovsky, K., Haubensak, W., Couzin, I. D., Tessmar-Raible, K., & Straw, A. D. (2017). Virtual reality for freely moving animals. *Nature Methods*, *14*(10), 995–1002.

Strausfeld, N. J., & Gronenberg, W. (1990). Descending neurons supplying the neck and flight motor of Diptera: organization and neuroanatomical relationships with visual pathways. *The Journal of Comparative Neurology*, *302*(4), 954–972.

Strausfeld, N. J., & Seyan, H. S. (1985). Convergence of visual, haltere, and prosternai inputs at neck motor neurons of Calliphora erythrocephala. *Cell and Tissue Research*, *240*(3), 601–615.

Strauss, R. (2002). The central complex and the genetic dissection of locomotor behaviour. *Current Opinion in Neurobiology*, *12*(6), 633–638.

Strother, J. A., Wu, S.-T., Rogers, E. M., Eliason, J. L. M., Wong, A. M., Nern, A., & Reiser, M. B. (2018). Behavioral state modulates the ON visual motion pathway of *Drosophila*. *Proceedings of the National Academy of Sciences of the United States of America*, *115*(1), E102–E111.

Suver, M. P., Huda, A., Iwasaki, N., Safarik, S., & Dickinson, M. H. (2016). An Array of Descending Visual Interneurons Encoding Self-Motion in Drosophila. *The Journal of Neuroscience: The Official Journal of the Society for Neuroscience*, *36*(46), 11768–11780.

Suver, M. P., Mamiya, A., & Dickinson, M. H. (2012). Octopamine neurons mediate flight-induced modulation of visual processing in Drosophila. *Current Biology: CB*, *22*(24), 2294–2302.

Sweeney, S. T., Broadie, K., Keane, J., Niemann, H., & O'Kane, C. J. (1995). Targeted expression of tetanus toxin light chain in Drosophila specifically eliminates synaptic transmission and causes behavioral defects. *Neuron*, *14*(2), 341–351.

Takemura, S.-Y., Karuppudurai, T., Ting, C.-Y., Lu, Z., Lee, C.-H., & Meinertzhagen, I. A. (2011). Cholinergic circuits integrate neighboring visual signals in a Drosophila motion detection pathway. *Current Biology: CB*, *21*(24), 2077–2084.

Talay, M., Richman, E. B., Snell, N. J., Hartmann, G. G., Fisher, J. D., Sorkaç, A., Santoyo, J. F., Chou-Freed, C., Nair, N., Johnson, M., Szymanski, J. R., & Barnea, G. (2017). Transsynaptic Mapping of Second-Order Taste Neurons in Flies by trans-Tango. *Neuron*, *96*(4), 783–795.e4.

Tammero, L. F., Frye, M. A., & Dickinson, M. H. (2004). Spatial organization of visuomotor reflexes in Drosophila. *The Journal of Experimental Biology*, *207*(Pt 1), 113–122.

Tauber, E. S., & Atkin, A. (1967). Disconjugate eye movement patterns during optokinetic stimulation of the African chameleon, Chameleo melleri. *Nature*, *214*(5092), 1008–1010.

Thévenin, A. F., Kowal, T. J., Fong, J. T., Kells, R. M., Fisher, C. G., & Falk, M. M. (2013). Proteins and mechanisms regulating gap-junction assembly, internalization, and degradation. *Physiology*, *28*(2), 93–116.

Thum, A. S., Knapek, S., Rister, J., Dierichs-Schmitt, E., Heisenberg, M., & Tanimoto, H. (2006). Differential potencies of effector genes in adult Drosophila. *The Journal of Comparative Neurology*, *498*(2), 194–203.

Tinbergen, N. (1951). The study of instinct. *Oxford University Press*.

Tirian, L., & Dickson, B. J. (2017). The VT GAL4, LexA, and split-GAL4 driver line collections for targeted expression in the Drosophila nervous system. In *bioRxiv* (p. 198648). https://doi.org/10.1101/198648

Todd, K. L., Kristan, W. B., Jr, & French, K. A. (2010). Gap junction expression is required for normal chemical synapse formation. *The Journal of Neuroscience: The Official Journal of the Society for Neuroscience*, *30*(45), 15277–15285.

Torre, V., Poggio, T., & Boycott, B. B. (1978). A synaptic mechanism possibly underlying directional selectivity to motion. *Proceedings of the Royal Society of London. Series B. Biological Sciences*, *202*(1148), 409–416.

Troup M., Yap M. H., Rohrscheib C., Grabowska M. J., Ertekin D., Randeniya R., Kottler B., Larkin A., Munro K., Shaw P. J., van Swinderen B. (2018). Acute control of the sleep switch in *Drosophila* reveals a role for gap junctions in regulating behavioral responsiveness. *Elife*, 15;7:e37105.

Turner-Evans, D., Wegener, S., Rouault, H., Franconville, R., Wolff, T., Seelig, J. D., Druckmann, S., & Jayaraman, V. (2017). Angular velocity integration in a fly heading circuit. *eLife*, *6*. https://doi.org/10.7554/eLife.23496

Turner, G. C., Bazhenov, M., & Laurent, G. (2008). Olfactory representations by Drosophila mushroom body neurons. *Journal of Neurophysiology*, *99*(2), 734–746.

Tuthill, J. C., Nern, A., Rubin, G. M., & Reiser, M. B. (2014). Wide-field feedback neurons dynamically tune early visual processing. *Neuron*, *82*(4), 887–895.

Valette, F., Ruffier, F., Viollet, S., & Seidl, T. (2010). Biomimetic optic flow sensing applied to a lunar landing scenario. *2010 IEEE International Conference on Robotics and Automation*, 2253–2260.

van Santen, J. P., & Sperling, G. (1984). Temporal covariance model of human motion perception. *Journal of the Optical Society of America. A, Optics and Image Science*, *1*(5), 451–473.

van Santen, J. P., & Sperling, G. (1985). Elaborated Reichardt detectors. *Journal of the Optical Society of America. A, Optics and Image Science*, *2*(2), 300–321.

Vega-Zuniga, T., Trost, D., Schicker, K., Bogner, E. M., & Luksch, H. (2018). The Medial Ventrothalamic Circuitry: Cells Implicated in a Bimodal Network. *Frontiers in Neural Circuits*, *12*, 9.

Venken, K. J. T., He, Y., Hoskins, R. A., & Bellen, H. J. (2006). P[acman]: a BAC transgenic platform for targeted insertion of large DNA fragments in D. melanogaster. *Science*, *314*(5806), 1747–1751.

Venken, K. J. T., Schulze, K. L., Haelterman, N. A., Pan, H., He, Y., Evans-Holm, M., Carlson, J. W., Levis, R. W., Spradling, A. C., Hoskins, R. A., & Bellen, H. J. (2011). MiMIC: a highly versatile transposon insertion resource for engineering Drosophila melanogaster genes. *Nature Methods*, *8*(9), 737–743.

Venken, K. J. T., Simpson, J. H., & Bellen, H. J. (2011). Genetic manipulation of genes and cells in the nervous system of the fruit fly. *Neuron*, *72*(2), 202–230.

Villette, V., Chavarha, M., Dimov, I. K., Bradley, J., Pradhan, L., Mathieu, B., Evans, S. W., Chamberland, S., Shi, D., Yang, R., Kim, B. B., Ayon, A., Jalil, A., St-Pierre, F., Schnitzer, M. J., Bi, G., Toth, K., Ding, J., Dieudonné, S., & Lin, M. Z. (2019). Ultrafast Two-Photon Imaging of a High-Gain Voltage Indicator in Awake Behaving Mice. *Cell*, *179*(7), 1590–1608.e23.

Viswanathan, S., Williams, M. E., Bloss, E. B., Stasevich, T. J., Speer, C. M., Nern, A., Pfeiffer, B. D., Hooks, B. M., Li, W.-P., English, B. P., Tian, T., Henry, G. L., Macklin, J. J., Patel, R., Gerfen, C. R., Zhuang, X., Wang, Y., Rubin, G. M., & Looger, L. L. (2015). High-performance probes for light and electron microscopy. *Nature Methods*, *12*(6), 568–576.

von Holst, E., & Mittelstaedt, H. (1950). Das Reafferenzprinzip. *Die Naturwissenschaften*, *37*(20), 464–476.

Wang, S., Borst, A., Zaslavsky, N., Tishby, N., & Segev, I. (2017). Efficient encoding of motion is mediated by gap junctions in the fly visual system. *PLoS Computational Biology*, *13*(12): e1005846.

Wang, S., Segev, I. Borst, A., & Palmer, S. (2021). Maximally efficient prediction in the early fly visual system may support evasive flight maneuvers. *PLoS Computational Biology*, 17(5): e1008965.

Warren, W. H. (2021). Information Is Where You Find It: Perception as an Ecologically Well-Posed Problem. *I-Perception*, *12*(2), 20416695211000366.

Warren, W. H., Jr. (1998). Visually Controlled Locomotion: 40 years Later. *Ecological Psychology: A Publication of the International Society for Ecological Psychology*, *10*(3-4), 177–219.

Warzecha, A.-K., Kurtz, R., & Egelhaaf, M. (2003). Synaptic transfer of dynamic motion information between identified neurons in the visual system of the blowfly. *Neuroscience*, *119*(4), 1103–1112.

Wasserman, S. M., Aptekar, J. W., Lu, P., Nguyen, J., Wang, A. L., Keles, M. F., Grygoruk, A., Krantz, D. E., Larsen, C., & Frye, M. A. (2015). Olfactory neuromodulation of motion vision circuitry in Drosophila. *Current Biology: CB*, *25*(4), 467–472.

Watanabe T., Kankel, D. R. (1992). The l(1)ogre gene of Drosophila melanogaster is expressed in postembryonic neuroblasts. *Developmental Biology*, 152(1), 172-183

Weber, F., Machens, C. K., & Borst, A. (2012). Disentangling the functional consequences of the connectivity between optic-flow processing neurons. *Nature Neuroscience*, *15*(3), 441–448, S1–S2.

Wehner, R. (1972). Spontaneous pattern preferences of Drosophila melanogaster to black areas in various parts of the visual field. *Journal of Insect Physiology*, *18*(8), 1531–1543.

Wehner, R. (1981). Spatial Vision in Arthropods. In *Comparative Physiology and Evolution of Vision in Invertebrates* (pp. 287–616). Springer Berlin Heidelberg.

Wehner, R. (1987). "Matched filters" — neural models of the external world. *Journal of Comparative Physiology A*, *161*(4), 511–531.

Wei, H., Kyung, H. Y., Kim, P. J., & Desplan, C. (2020). The diversity of lobula plate tangential cells (LPTCs) in the Drosophila motion vision system. *Journal of Comparative Physiology. A, Neuroethology, Sensory, Neural, and Behavioral Physiology*, *206*(2), 139–148.

Werkhoven, Z., Bravin, A., Skutt-Kakaria, K., Reimers, P., Pallares, L. F., Ayroles, J., & de Bivort, B. L. (2021). The structure of behavioral variation within a genotype. *eLife*, *10*. https://doi.org/10.7554/eLife.64988

Wertz, A., Borst, A., & Haag, J. (2008). Nonlinear integration of binocular optic flow by DNOVS2, a descending neuron of the fly. *The Journal of Neuroscience: The Official Journal of the Society for Neuroscience*, *28*(12), 3131–3140.

Wertz, A., Haag, J., & Borst, A. (2012). Integration of binocular optic flow in cervical neck motor neurons of the fly. *Journal of Comparative Physiology. A, Neuroethology, Sensory, Neural, and Behavioral Physiology*, *198*(9), 655–668.

Wheatstone, C. (1838). XVIII. Contributions to the physiology of vision. —Part the first. On some remarkable, and hitherto unobserved, phenomena of binocular vision. *Philosophical Transactions of the Royal Society of London*, *128*, 371–394.

Wiegert, J. S., Mahn, M., Prigge, M., Printz, Y., & Yizhar, O. (2017). Silencing Neurons: Tools, Applications, and Experimental Constraints. *Neuron*, *95*(3), 504–529.

Wilson, R. I., Turner, G. C., & Laurent, G. (2004). Transformation of olfactory representations in the Drosophila antennal lobe. *Science*, *303*(5656), 366–370.

Wolf, R., & Heisenberg, M. (1990). Visual control of straight flight in Drosophila melanogaster. *Journal of Comparative Physiology. A, Sensory, Neural, and Behavioral Physiology*, *167*(2), 269–283.

Wu, C.-L., Shih, M.-F. M., Lai, J. S.-Y., Yang, H.-T., Turner, G. C., Chen, L., & Chiang, A.-S. (2011). Heterotypic gap junctions between two neurons in the drosophila brain are critical for memory. *Current Biology: CB*, *21*(10), 848–854.

Wylie, D. R., Gutiérrez-Ibáñez, C., Gaede, A. H., Altshuler, D. L., & Iwaniuk, A. N. (2018). Visual-Cerebellar Pathways and Their Roles in the Control of Avian Flight. *Frontiers in Neuroscience*, *12*, 223.

Xue, Z., Wu, M., Wen, K., Ren, M., Long, L., Zhang, X., & Gao, G. (2014). CRISPR/Cas9 mediates efficient conditional mutagenesis in Drosophila. *G3* , *4*(11), 2167–2173.

Yaksi, E., & Wilson, R. I. (2010). Electrical coupling between olfactory glomeruli. *Neuron*, *67*(6), 1034–1047.

Yarbus, A. L. (2013). *Eye Movements and Vision*. Springer.

Zhang, T., Heuer, H. W., & Britten, K. H. (2004). Parietal area VIP neuronal responses to heading stimuli are encoded in head-centered coordinates. *Neuron*, *42*(6), 993–1001.

Zhang, Y. Q., Rodesch, C. K., & Broadie, K. (2002). Living synaptic vesicle marker: synaptotagmin-GFP. *Genesis*, *34*(1-2), 142–145.

Zheng, Z., Lauritzen, J. S., Perlman, E., Robinson, C. G., Nichols, M., Milkie, D., Torrens, O., Price, J., Fisher, C. B., Sharifi, N., Calle-Schuler, S. A., Kmecova, L., Ali, I. J., Karsh, B., Trautman, E. T., Bogovic, J. A., Hanslovsky, P., Jefferis, G. S. X. E., Kazhdan, M., … Bock, D. D. (2018). A Complete Electron Microscopy Volume of the Brain of Adult Drosophila melanogaster. *Cell*, *174*(3), 730–743.e22.